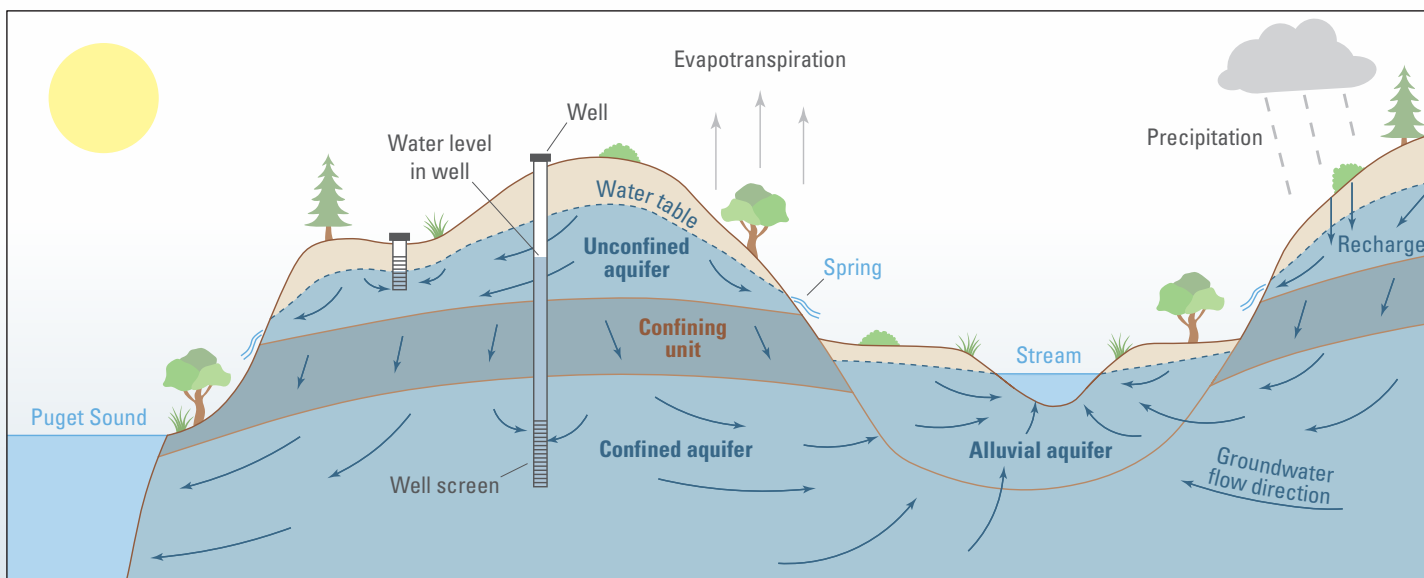


Prepared in cooperation with the Cities of Auburn, Milton, Puyallup, Sumner, and Tacoma; Pierce Conservation District; Pierce County Public Works; Washington State Department of Health; Washington State Department of Ecology; Thurston County Public Utility District; Cascade Water Alliance; Lakehaven Utility District; Lakewood Water District; Firgrove Mutual Water Company; Fruitland Mutual Water Company; Spanaway Water Company; Summit Water & Supply Company; and Mt. View-Edgewood Water Company

Numerical Model of the Groundwater-Flow System Near the Southeastern Part of Puget Sound, Washington, volume 2

Chapters D–E of
Characterization of Groundwater Resources Near the Southeastern Part of Puget Sound, Washington



Scientific Investigations Report 2024–5026–D–E

Cover. Cross-section sketch of typical groundwater-flow system showing hydrostratigraphic layers, water levels in wells, and discharge to streams. Groundwater flows from high to low elevation and discharges to water bodies. Wells can be drilled in confined (pressurized) or unconfined aquifers. Sketch is shown with large vertical exaggeration for illustration purposes.

Numerical Model of the Groundwater-Flow System Near the Southeastern Part of Puget Sound, Washington, volume 2

By Andrew J. Long, Elise E. Wright, Leland T. Fuhrig, and Valerie A.L. Bright

Chapter D

Numerical Model Construction and Calibration

Chapter E

Numerical Model Results

Prepared in cooperation with the Cities of Auburn, Milton, Puyallup, Sumner, and Tacoma; Pierce Conservation District; Pierce County Public Works; Washington State Department of Health; Washington State Department of Ecology; Thurston County Public Utility District; Cascade Water Alliance; Lakehaven Utility District; Lakewood Water District; Firgrove Mutual Water Company; Fruitland Mutual Water Company; Spanaway Water Company; Summit Water & Supply Company; and Mt. View-Edgewood Water Company

Scientific Investigations Report 2024–5026–D–E

U.S. Department of the Interior
U.S. Geological Survey

U.S. Geological Survey, Reston, Virginia: 2024

For more information on the USGS—the Federal source for science about the Earth, its natural and living resources, natural hazards, and the environment—visit <https://www.usgs.gov> or call 1–888–ASK–USGS.

For an overview of USGS information products, including maps, imagery, and publications, visit <https://store.usgs.gov/>.

Any use of trade, firm, or product names is for descriptive purposes only and does not imply endorsement by the U.S. Government.

Although this information product, for the most part, is in the public domain, it also may contain copyrighted materials as noted in the text. Permission to reproduce copyrighted items must be secured from the copyright owner.

Suggested citation:

Long, A.J., Wright, E.E., Fuhrig, L.T., and Bright, V.A.L., 2024, Numerical model of the groundwater-flow system near the southeastern part of Puget Sound, Washington, v. 2 of Welch, W.B., and Long, A.J., eds., Characterization of groundwater resources near the southeastern part of Puget Sound, Washington, 2 chap. (D–E): U.S. Geological Survey Scientific Investigations Report 2024–5026–D–E, [variously paged; 103 p.], <https://doi.org/10.3133/sir20245026v2>.

Associated data for this publication:

McLean, J.E., Welch, W.B., and Long, A.J., 2024, Spatial data in support of the characterization of water resources near the southeastern part of Puget Sound, Washington: U.S. Geological Survey data release, <https://doi.org/10.5066/P9JFKLMG>.

Wright, E.E., Long, A.J., and Fuhrig, L.T., 2023, MODFLOW-NWT model to simulate the groundwater flow system near Puget Sound, Pierce and King Counties, Washington: U.S. Geological Survey data release, <https://doi.org/10.5066/P9LU1PMQ>.

Related report:

Welch, W.B., Bright, V.A.L., Gendaszek, A.S., Dunn, S.B., Headman, A.O., and Fasser, E.T., 2024, Conceptual hydrogeologic framework and groundwater budget near the southeastern part of Puget Sound, Washington, v. 1 of Welch, W.B., and Long, A.J., eds., Characterization of groundwater resources near the southeastern part of Puget Sound, Washington, 3 chap. (A–C): U.S. Geological Survey Scientific Investigations Report 2024–5026–A–C, [variously paged; 71 p.], 1 pl., <https://doi.org/10.3133/sir20245026v1>.

Preface

This is the second of two reports in a multichapter volume characterizing groundwater resources near the southeastern part of Puget Sound, Washington. Chapters A, B, and C (Welch and others, 2024) provide an overall introduction to the multichapter volume (Chapter A), the conceptual hydrogeologic framework (Chapter B), and the groundwater budget (Chapter C). Chapters D and E (this report) describe numerical groundwater-flow model construction and calibration (Chapter D) and the numerical model results (Chapter E). Collectively, these two reports present a characterization and simulation tool for groundwater resources near the southeastern part of Puget Sound, Washington.

Acknowledgments

The conceptual hydrogeologic framework and groundwater budget described in this report were developed by the U.S. Geological Survey (USGS) with the assistance of a large team of technical experts and advisors from the hydrogeologic community. This technical team consisted of representatives of the following organizations: the Cities of Auburn, Milton, Puyallup, Sumner, and Tacoma; Pierce Conservation District; Pierce County Public Works; Washington State Department of Health; Washington State Department of Ecology; Thurston County Public Utility District; Cascade Water Alliance; Lakehaven Utility District; Lakewood Water District; Firgrove Mutual Water Company; Fruitland Mutual Water Company; Spanaway Water Company; Summit Water & Supply Company; and Mt. View-Edgewood Water Company. Special appreciation is acknowledged to the following technical team members for providing in-depth courtesy reviews of the draft report manuscript and numerical groundwater model: Joe Becker, Burt Clothier, Shuhui Dun, Andy Dunn, and Peter Schwartzman. We thank USGS peer reviewers Stephen Hundt and Adel (Eddie) Haj for their thorough reviews of the manuscript and model, and we thank Andrew Gendaszek for estimating the depths and wetted top widths of stream channels that were applied to modeling.

Contents

Preface	iii
Acknowledgments	iv
Executive Summary	1
Introduction to Chapters D and E	2
Glossary	2
Chapter D. Numerical Model Construction and Calibration	D1
Introduction	D1
Design and Construction	D1
Horizontal Discretization and Vertical Layering	D1
Model Boundary Conditions	D8
Precipitation Recharge	D8
Rejected Recharge, Small Springs, and Seeps	D9
Streams and Large Springs	D9
Streams Entering the Active Model Area (AMA)	D12
Stream Diversions	D12
Externally Drained Lakes	D12
Internally Drained Lakes	D15
Puget Sound	D15
Groundwater Use and Return Flow	D16
Alluvial Valley Margins	D16
Boundary of Active Model Area (AMA)	D17
Initial Conditions	D17
Hydraulic Properties	D17
Model Calibration and Sensitivity	D20
Calibration Targets	D20
Calibration Parameters for Steady State	D22
Calibration Target Weights	D26
Calibration Constraints	D28
Transient Calibration	D28
Assessment of Model Fit	D28
Sensitivity Analysis	D35
References Cited	D36
Chapter E. Numerical Model Results	E1
Introduction	E1
Groundwater Budgets	E1
Scenario Simulations	E2
Scenario 1 Suite—Drought	E3
Scenario 2 Suite—Elimination of Groundwater Use	E8
Scenario 3 Suite—Cyclic Equilibrium with Increased Groundwater Use	E8
Model Limitations and Potential Refinements	E25
References Cited	E27
Appendix 1. Supplementary Tables	3
Appendix 2. Estimation of Base Flow for Points of Inflow to the Active Model Area (AMA)	5
Appendix 3. Supplementary Figures	7

Figures

D1.	Map showing areal extent and selected features for the numerical groundwater-flow model, near the southeastern part of Puget Sound, Washington....	D2
D2.	Map showing distribution of General-Head Boundary Package cells, Drain Package cells, and grid rows and columns in the numerical model, near the southeastern part of Puget Sound, Washington	D7
D3.	Example of model cell adjustment for the mudflow bypass method showing a profile of the original hydrogeologic framework at the margin of the White River valley and the same profile after adjustments	D17
D4.	Scatterplots showing measured and simulated hydraulic-head values for the steady-state model version grouped by hydrogeologic unit and estimated and simulated vertical hydraulic-head differences between model layers, near the southeastern part of Puget Sound, Washington	D29
D5.	Histogram showing hydraulic-head residuals for the steady-state model version, near the southeastern part of Puget Sound, Washington	D30
D6.	Map showing potentiometric surface for hydrogeologic unit A3 simulated by the steady-state model version, near the southeastern part of Puget Sound, Washington.....	D31
D7.	Bar graphs showing estimated and simulated base flow for station locations for the steady-state model version, near the southeastern part of Puget Sound, Washington.....	D32
D8.	Bar graph showing model sensitivity for the steady-state model version by parameter group, as represented by the sensitivity metric, τ , near the southeastern part of Puget Sound, Washington	D35
E1.	Map showing change in simulated hydraulic head for hydrogeologic unit A3 resulting from scenario 2, near the southeastern part of Puget Sound, Washington ...	E9

Tables

D1.	U.S. Geological Survey streamflow measurement stations listed in the order of station ID, in the active model area, near the southeastern part of Puget Sound, Washington.....	D3
D2.	Description of model layers, near the southeastern part of Puget Sound, Washington.....	D8
D3.	Lakes and Puget Sound simulated in numerical modeling, near the southeastern part of Puget Sound, Washington	D10
D4.	Specified flows and diversions for the Streamflow-Routing Package for the steady-state model version, near the southeastern part of Puget Sound, Washington.....	D13
D5.	Hydraulic conductivity zones, near the southeastern part of Puget Sound, Washington.....	D18
D6.	Calibrated hydraulic conductivity values summarized by hydrogeologic unit, near the southeastern part of Puget Sound, Washington	D19
D7.	Calibrated specific yield and specific storage values summarized by hydrogeologic unit, near the southeastern part of Puget Sound, Washington.....	D21
D8.	Parameter groups for the steady-state model version, near the southeastern part of Puget Sound, Washington	D23

D9.	Calibration target groups and weights for steady-state model version, near the southeastern part of Puget Sound, Washington	D27
D10.	Model-calibration fitting metrics, near the southeastern part of Puget Sound, Washington.....	D34
E1.	Simulated groundwater budget for the steady-state model version, near the southeastern part of Puget Sound, Washington	E1
E2.	Estimated groundwater budget from Welch and others (2024, Chapter C, table C6) compared to that for the steady-state model version, near the southeastern part of Puget Sound, Washington	E2
E3.	Changes in simulated steady-state base flow in the active model area for scenarios 1a, 1b, and 1c compared to the calibrated steady-state model version, near the southeastern part of Puget Sound, Washington.....	E3
E4.	Change in simulated August base flow and precipitation recharge for scenario 1d for station locations compared to the calibrated transient model version, near the southeastern part of Puget Sound, Washington	E4
E5.	Change in simulated August base flow and precipitation recharge in the active model area for scenario 1d compared to the calibrated transient model version, near the southeastern part of Puget Sound, Washington	E7
E6.	Changes in simulated steady-state base flow for station locations for scenario 2 compared to the calibrated steady-state model, near the southeastern part of Puget Sound, Washington.....	E10
E7.	Change in simulated steady-state base flow in the active model area for scenario 2 compared to the calibrated steady-state model, near the southeastern part of Puget Sound, Washington	E11
E8.	Changes in simulated monthly base flow resulting from scenario 3b, near the southeastern part of Puget Sound, Washington	E12
E9.	Changes in simulated monthly base flow resulting from scenario 3c, near the southeastern part of Puget Sound, Washington	E15
E10.	Changes in simulated monthly base flow resulting from scenario 3d, near the southeastern part of Puget Sound, Washington	E18
E11.	Changes in simulated monthly base flow resulting from scenario 3e, near the southeastern part of Puget Sound, Washington	E22
E12.	Changes in August base flow resulting from scenarios 3b–3e in the active model area, near the southeastern part of Puget Sound, Washington.....	E25

Conversion Factors

U.S. customary units to International System of Units

Multiply	By	To obtain
	Length	
inch (in.)	2.54	centimeter (cm)
inch (in.)	25.4	millimeter (mm)
foot (ft)	0.3048	meter (m)
mile (mi)	1.609	kilometer (km)

Multiply	By	To obtain
Area		
acre	4,047	square meter (m ²)
acre	0.4047	hectare (ha)
acre	0.4047	square hectometer (hm ²)
acre	0.004047	square kilometer (km ²)
square foot (ft ²)	929.0	square centimeter (cm ²)
square foot (ft ²)	0.09290	square meter (m ²)
square inch (in ²)	6.452	square centimeter (cm ²)
Volume		
acre-foot (acre-ft)	1,233	cubic meter (m ³)
acre-foot (acre-ft)	0.001233	cubic hectometer (hm ³)
Flow rate		
acre-foot per year (acre-ft/yr)	0.001233	cubic hectometer per year (hm ³ /yr)
foot per second (ft/s)	0.3048	meter per second (m/s)
foot per day (ft/d)	0.3048	meter per day (m/d)
foot squared per day (ft ² /d)	0.0929	meter squared per day (m ² /d)
cubic foot per second (ft ³ /s)	0.02832	cubic meter per second (m ³ /s)
cubic foot per day (ft ³ /d)	0.02832	cubic meter per day (m ³ /d)
Hydraulic conductivity		
foot per day (ft/d)	0.3048	meter per day (m/d)
Transmissivity		
foot squared per day (ft ² /d)	0.09290	meter squared per day (m ² /d)

Datums and Coordinate System

Vertical coordinate information is referenced to the North American Vertical Datum of 1988 (NAVD 88).

Horizontal coordinate information is referenced to the North American Datum of 1983 (NAD 83).

Altitude, as used in this report, refers to distance above the vertical datum.

Following is the reference coordinate system used for the development of the hydrogeologic framework and numerical model:

Category	Description
Coordinate system	NAD_1983_StatePlane_Washington_South_FIPS_4602_Feet
Study Projection	Lambert Conformal Conic
Linear unit	Feet, US
False easting	1640416.667
False northing	0
Central meridian	-120.5
Standard parallel 1	45.83333333
Standard parallel 2	47.33333333
Latitude of origin	45.33333333

Well-Numbering System

Wells in the State of Washington are assigned a local well number that identifies each well based on its location in a township, range, section, and 40-acre tract. For example, local well number 20N/04E-14B01 indicates that the well is in township 20 north of the Willamette Base Line, and range 4 east of the Willamette Meridian. The numbers immediately following the hyphen indicate the section (14) in the township. Most range-townships in Washington are divided into 36 equal sections of 1 square mile (640 acres) numbered from 1 to 36. However, the Washington Territory Donation Land Claims of 1852–55 predate the Public Lands Survey and appear on maps as irregularly sized and shaped sections with assigned section numbers greater than 36. The letter following the section (B) gives the 40-acre tract of the section. The two-digit sequence number (01) following the letter is used to distinguish individual wells in the same 40-acre tract. A “D” following the sequence number indicates a well that has been deepened. In the plates of this report, wells are identified using only the section and 40-acre tract, such as 14B01; the township and range are shown on the map borders.

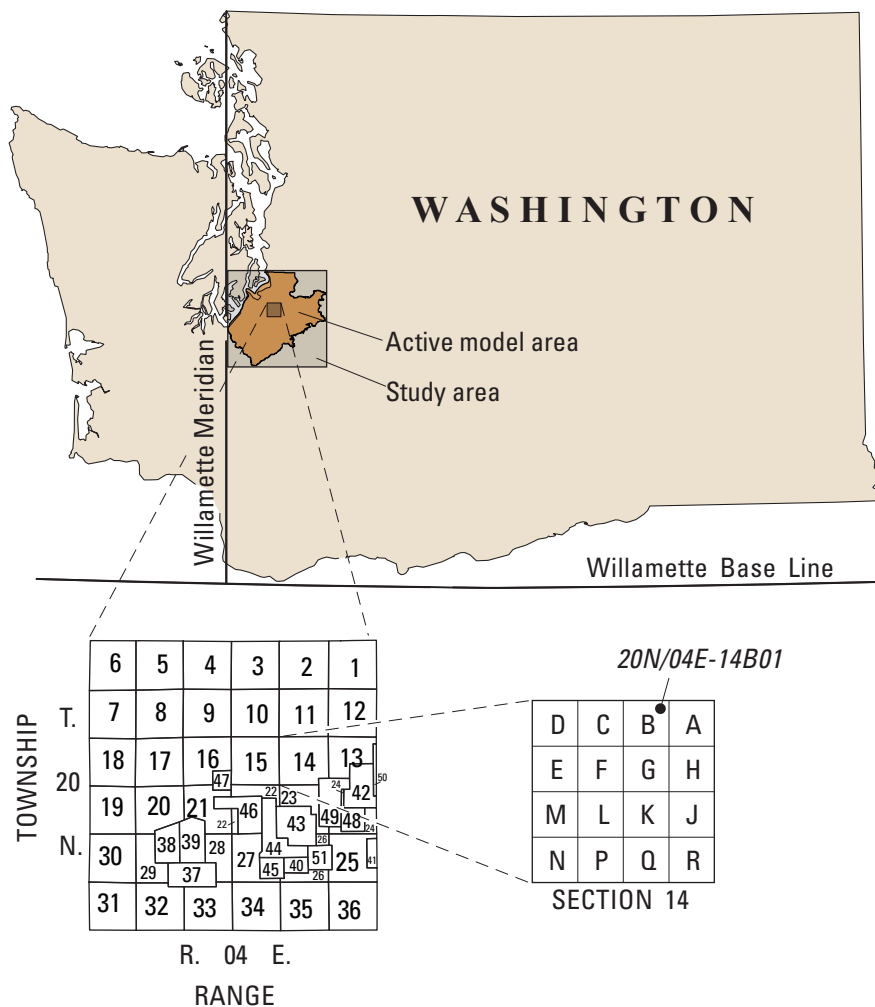


Diagram showing well-numbering system used in Washington.

Abbreviations

AMA	active model area
GHB	General-Head Boundary
HGU	hydrogeologic unit
HYSEP	automated hydrograph separation program
Kh	horizontal hydraulic conductivity, in dimensions of foot per day
Kh/Kv	ratio of horizontal to vertical hydraulic conductivity, dimensionless
Kv	vertical hydraulic conductivity , in dimensions of foot per day
MFLU	upland mudflow confining unit MFLU
MFLV	valley mudflow confining unit MFLV
NWIS	U.S. Geological Survey National Water Information System
PEST	Model-Independent Parameter Estimation
R _p	precipitation recharge
Ss	specific storage, in dimensions of length ⁻¹
SFR	Streamflow-Routing
SWB	Soil-Water-Balance (model)
Sy	specific yield, dimensionless
S-zone	storage parameter zone
USGS	U.S. Geological Survey

Numerical Model of the Groundwater-Flow System Near the Southeastern Part of Puget Sound, Washington

Edited by Andrew J. Long

Executive Summary

Groundwater flow in the active model area (AMA) was simulated using a groundwater-flow model. A steady-state model version of the model simulates equilibrium conditions, and a transient model version simulates monthly variability. The model corresponds to the physical and temporal dimensions of the conceptual model and groundwater budget. The steady-state model version represents average conditions for an 11-year period (January 1, 2005–December 31, 2015), and the transient model represents monthly hydrologic variability within that period. The 13-layer model was constructed using MODFLOW-NWT with a uniformly spaced grid consisting of 416 rows, 433 columns, and cells with a horizontal dimension of 500 feet (ft) on a side.

The model was calibrated to measured values of water levels in wells and lakes and estimated base flow for selected streamflow measurement stations, commonly referred to as streamgages. Model calibration was accomplished using a combination of manual and automatic methods, including the Model-Independent Parameter Estimation (PEST) program that adjusted model input parameters with the aim of minimizing the difference between estimated and model-simulated values of hydraulic head and base flow.

Model boundary conditions consist of all simulated groundwater inflow to and outflow from the AMA. For example, a stream reach that simulates a gain from or loss to groundwater is a boundary condition that allows water to exit or enter, respectively, the groundwater system. Other boundary conditions include springs, seeps, precipitation recharge, groundwater exchange with lakes and Puget Sound, and groundwater pumping. A comparison of the estimated groundwater budget to that simulated by the steady-state model version indicates that the relative percentages of total inflow or total outflow for six major categories of boundary conditions are similar for the two budgets.

The model was used to simulate three suites of scenarios of potential drought and water-use changes. Scenario 1 suite consisted of the steady-state model version that was run with 0, 15, 20, and 25 percent reduction of precipitation

recharge to assess the corresponding reductions in base flow with decreasing recharge. The last simulation for the scenario 1 suite consisted of the transient model version simulating 3 years of consecutive seasonal drought, defined by the months of May through September, to assess the corresponding base-flow reductions. Scenario 2 suite consisted of the steady-state model version with all simulated groundwater use removed, compared with a simulation that includes current groundwater use to evaluate changes to potentiometric surfaces and base flows. Scenario 3 suite consisted of a transient model version of the model that simulated pumping increases for four different categories of water-supply wells (compared to no pumping increases) to evaluate resulting reductions in base flow. Although, these scenarios provide examples of model applications and useful insights, many other scenarios could be simulated. A description of how to download the model is described in the body of this report.

Uncertainty is associated with most model inputs. Groundwater levels, lake levels, and land-surface altitudes are relatively certain; other model inputs are far less certain, including precipitation recharge, base flow, hydraulic properties, water use, and the three-dimensional structure of subsurface hydrogeologic units. Models are useful not because of high levels of accuracy of all model inputs, but because they combine the best information and estimates available, thereby providing the best predictions available related to physical processes.

The model described in this report simulates groundwater flow on a regional scale, which has inherent limitations for simulating hydrologic scenarios at local scales. Model structures and inputs were generalized to be consistent with this regional scale. For example, the actual groundwater system has much greater heterogeneity of hydraulic conductivity than is possible within the model's degrees of freedom. Variations in hydraulic gradients over distances less than 500 ft cannot be simulated. The distances between model features, such as a pumping well and a stream, must be placed at 500-ft intervals and are co-located if both features are within the same model cell.

Introduction to Chapters D and E

Chapter A of Welch and others (2024) provides an extensive introduction to this multichapter volume of reports, consisting of the purpose and scope of the volume; previous investigations; and a description of the study area, including physiography, drainage features, land use, climate, population, and geologic setting. Construction of the numerical groundwater flow model described in this report draws upon the extensive work described in Welch and others (2024).

Glossary

active model area (AMA) The part (887 square miles) of the study area that includes the conceptual hydrogeologic framework, estimated water-budget, and numerical groundwater-flow model.

base flow The component of streamflow that results from groundwater inflow to the stream.

conceptual hydrogeologic framework A spatially continuous, three-dimensional representation of hydrogeologic units, maps of the extents and thicknesses of major water-bearing units, groundwater levels, potentiometric surfaces, groundwater flow directions, and generalized groundwater/surface-water interactions.

discharge Flow rate, as a volume per time.

hydraulic conductivity Rate of groundwater flow per unit area under a unit hydraulic gradient (unit: length/time).

large spring A spring that has been identified and generally named and has larger discharge than a seep.

potentiometric surface A surface representing the static head of groundwater in tightly cased wells that tap a water-bearing rock unit (aquifer) or, in the case of unconfined aquifers, the water table (see <https://doi.org/10.3133/wsp1988>).

precipitation recharge Groundwater recharge from precipitation on the land surface.

reach Defined for numerical modeling as the stream segment within one model cell.

rejected recharge Potential groundwater infiltration of precipitation recharge that does not infiltrate because of saturated soil conditions.

seep Small spring located along the bluffs of river valleys and Puget Sound with less discharge than a large spring.

segment Defined for numerical modeling as a group of connected reaches.

station A location at which data are collected, such as streamflow.

stream Rivers, their tributaries, and other streams and creeks.

streamgage Station at which hydrologic data are collected.

Chapter D. Numerical Model Construction and Calibration

By Andrew J. Long, Elise E. Wright, Leland T. Fuhrig, and Valerie A.L. Bright

Introduction

The open-source software used to build the model was MODFLOW-NWT (Niswonger and others, 2011), a three-dimensional, finite-difference modeling code for simulating groundwater flow. Two versions of a numerical groundwater-flow model (model) were constructed: steady-state and transient model versions. The purpose of the model was to (1) test and refine the assumptions and estimates developed for the conceptual hydrogeologic framework (Chapter B of Welch and others, 2024; hereinafter referred to as “Chapter B”) and estimated groundwater budget components (Chapter C of Welch and others, 2024; hereinafter referred to as “Chapter C”), (2) simulate hydrologic scenarios of potential interest to water-resources managers, and (3) provide a tool that can be adapted for additional hydrologic scenarios and research endeavors.

The steady-state model version was constructed to simulate the groundwater-flow system for average conditions for 2005–15, with the assumption that all inflows and outflows occur at steady rates. This model version serves two purposes. First, the steady-state model version provides the ability to calibrate hundreds of parameters because of its quick run time. Second, the steady-state model version provides a means to quickly simulate simple scenarios of long-term (equilibrium) responses to changes in recharge or pumping rates. For example, reducing the recharge input to the steady-state model version can be used to simulate a scenario of a long-term decrease in average recharge for a new equilibrium condition. This simulation would result in lowered hydraulic-head values and decreased base flows in comparison to the calibrated steady-state model. The difference in the groundwater budget between the scenario simulation (new equilibrium) and the calibrated model (current conditions) would provide the long-term change in groundwater storage for this scenario.

The steady-state model version was then modified to a transient model version that simulates monthly temporal variability for 2005–15. The transient model version represents monthly hydrologic variability within that period (132 monthly stress periods) and is applicable for more complex scenarios where temporal variability is of interest.

Both model versions correspond to the physical and temporal dimensions of the framework and water budget. The active model area (AMA) (fig. D1) is the area simulated

and also the area corresponding to the estimated groundwater budget described in Chapter C. Additional datasets used in model construction to define conditions during this period are described in appendix 1 (app. 1, tables 1.1–1.14). Table D1 includes base-flow values averaged from the monthly values from (McLean and others, 2024), with the exception of the three seasonal streamflow measurement stations (see comments column of the table). Model input, output, executable application, and source code for the model, including additional simulations of hydrologic scenarios, are available from Wright and others (2023).

Design and Construction

Horizontal Discretization and Vertical Layering

In the horizontal plane, the model grid is aligned with the Washington State Plane coordinate system (fig. D1) and has uniformly spaced cells that are 500-by-500 feet (ft) wide. The grid is 433-cells wide in the east-west direction and 416-cells wide in the north-south direction (416 rows and 433 columns). The AMA is defined as the area within the rectangular model grid that contains active model cells (fig. D2). All model cells outside this area are inactive, and some cells within this area are inactive. The three-dimensional grid has 13 layers of variable thickness and continuity that correspond to the 14 units of the hydrogeologic framework, as described in Chapter B. Layers 1–12 each represent a single hydrogeologic unit (HGU), and layer 13 represents two HGUs (table D2). Within layer 13, HGU G is present in the northwestern 63 percent of the AMA (Chapter B, fig. B12), and HGU Bedrock occupies the eastern part of layer 13. All model inputs and outputs are in consistent units of feet and days.

Table D2 describes each HGU as an aquifer, a confining unit, or undifferentiated deposits. In this report, individual HGUs are referred by the HGU name only. For example, the first and second HGUs in table D2 are referred to as “HGU MFLU” and “HGU AL1,” respectively.

All model cells outside the AMA were set to inactive, leaving 879,476 active cells. Model cells with altitudes above the land surface are inactive. For example, layer 1 has active cells only where HGU MFLU is present, with the remainder

D2 Numerical Model of the Groundwater-Flow System Near the Southeastern Part of Puget Sound, Washington

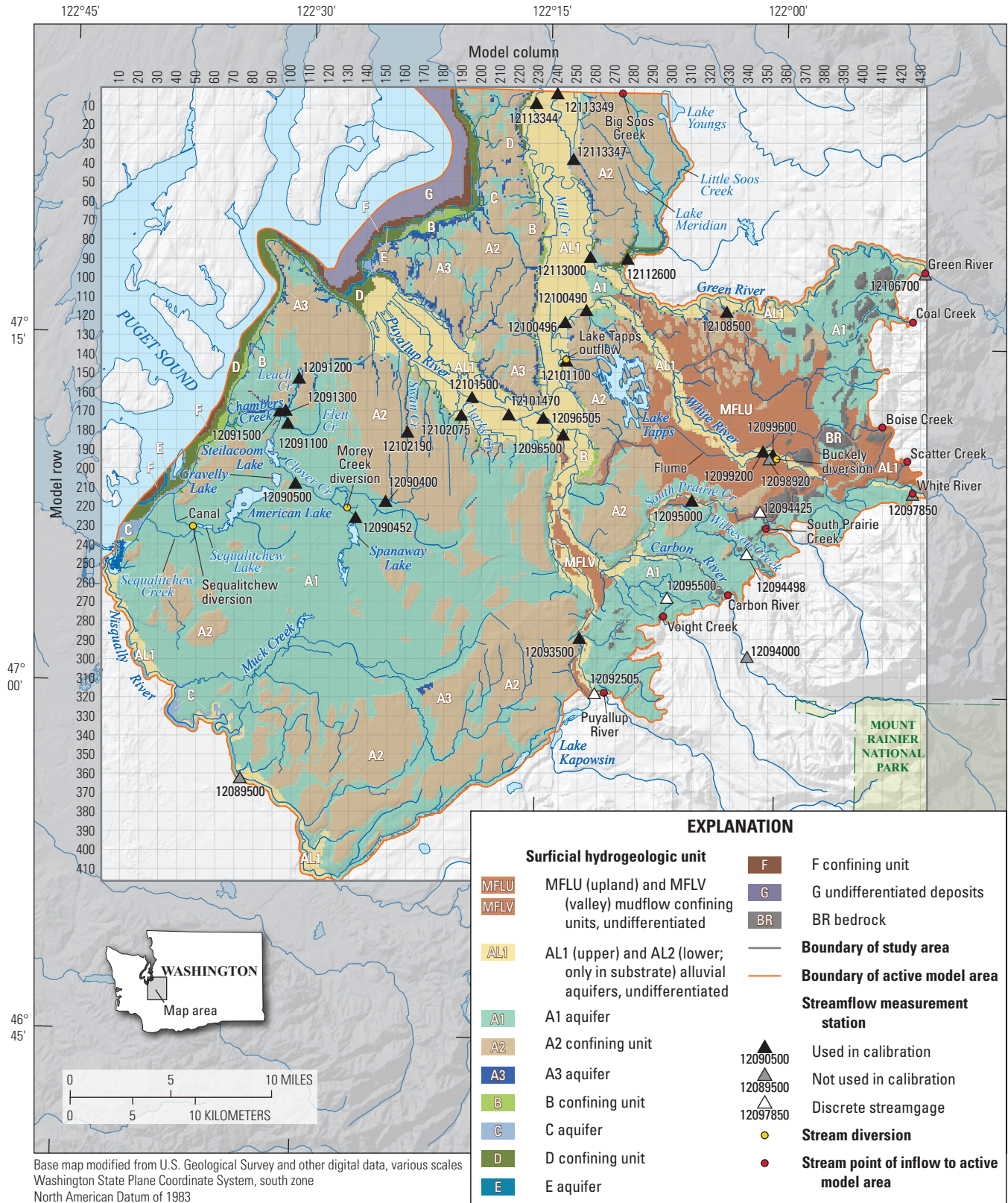


Figure D1. Areal extent and selected features for the numerical groundwater-flow model, near the southeastern part of Puget Sound, Washington.

Table D1. U.S. Geological Survey streamflow measurement stations listed in the order of station ID, in the active model area, near the southeastern part of Puget Sound, Washington.

[Estimated average base-flow values (2005–15) are from Welch and others (2024, Chapter C, table C9), except for the three seasonal stations, which are described in section, “Model Calibration and Sensitivity.” **Abbreviations:** BL, below; CR, Creek; E, East; ID, identifier; LK, Lake; NA, not applicable; NR, near; ST, Street; WA, Washington; ft³/s, cubic foot per second]

Station ID	Station name	Short name	Estimated average base flow (ft ³ /s)	Used in model calibration	Calibration target name	Affected by streamflow from outside active model area	Factors affecting base-flow estimates	Comments
12090400	NORTH FORK CLOVER CREEK NEAR PARKLAND, WA	NForkCloverCrkParkland	5.1	Yes	o4691	No	NA	
12090452	SPANAWAY CR AT SPANAWAY LK OUTLET NR SPANAWAY, WA	SpanawayCrSpanLkOutlet	15.1	Yes	o4698	No	NA	
12090500	CLOVER CREEK NEAR TILlicum, WA	CloverCrTillicum	33.7	Yes	o4680	No	NA	
12091100	FLETT CREEK AT TACOMA, WA	FlettCrTacoma	12.6	Yes	o4681	No	NA	
12091200	LEACH CREEK NEAR FIRCREST, WA	LeachCrFirecrest	3.5	Yes	o4685	No	NA	
12091300	LEACH CREEK NEAR STEILACOOM, WA	LeachCrSteilacoom	8.7	Yes	o4686	No	NA	
12091500	CHAMBERS CREEK BL LEACH CREEK NEAR STEILACOOM, WA	ChambersCrBlLeach	101.8	Yes	o4678	No	NA	
12102075	CLARKS CREEK AT TACOMA ROAD NEAR PUYALLUP, WA	ClarksCrTacoma	57.0	Yes	o4679	No	NA	
12102190	SWAN CREEK AT 80TH ST EAST NEAR TACOMA, WA	SwanCr80thSt	2.0	Yes	o4699	No	NA	Seasonal station ¹

Table D1. U.S. Geological Survey streamflow measurement stations listed in the order of station ID, in the active model area, near the southeastern part of Puget Sound, Washington.—Continued

[Estimated average base-flow values (2005–15) are from Welch and others (2024, Chapter C, table C9), except for the three seasonal stations, which are described in section, “Model Calibration and Sensitivity.” **Abbreviations:** BL, below; CR, Creek; E, East; ID, identifier; LK, Lake; NA, not applicable; NR, near; ST, Street; WA, Washington; ft³/s, cubic foot per second]

Station ID	Station name	Short name	Estimated average base flow (ft ³ /s)	Used in model calibration	Calibration target name	Affected by streamflow from outside active model area	Factors affecting base-flow estimates	Comments
12095000	SOUTH PRAIRIE CREEK AT SOUTH PRAIRIE, WA	SPrairieCrSPrairie	173.9	Yes	o4697	Yes	Snowmelt	
12094000	CARBON RIVER NEAR FAIRFAX	CarbonRvFairfax	334.7	No	NA	Yes	Glacier, snowmelt	Outside of model area
12093500	PUYALLUP RIVER NEAR ORTING, WA	PuyallupRvOrting	602.5	Yes	o4696	Yes	Glacier, snowmelt	
12096500	PUYALLUP RIVER AT ALDERTON, WA	PuyallupRvAlderton	1,272	Yes	o4693	Yes	Glacier, snowmelt	
12096505	PUYALLUP RIVER AT E MAIN BRIDGE AT PUYALLUP, WA	PuyallupRvMainBrdg	1,337	Yes	o4694	Yes	Glacier, snowmelt	Seasonal station ¹
12101470	PUYALLUP RIVER AT 5TH ST BRIDGE AT PUYALLUP, WA	PuyallupRv5thStBrdg	2,625	Yes	o4692	Yes	Glacier, snowmelt	Seasonal station ¹
12101500	PUYALLUP RIVER AT PUYALLUP, WA	PuyallupRvPuyallup	2,681	Yes	o4695	Yes	Glacier, snowmelt	
12099600	BOISE CREEK AT BUCKLEY, WA	BoiseCrBuckley	29.2	Yes	o4677	Yes	NA	
12097850	WHITE RIVER BELOW CLEARWATER RIVER NR BUCKLEY, WA	WhiteRvBIClearwater	1,169	No	o4702	Yes	Glacier, snowmelt	Model inflow point
12099200	WHITE RIVER ABOVE BOISE CREEK AT BUCKLEY, WA	WhiteRvAbBoiseCr	1,108	Yes	o4700	Yes	Glacier, snowmelt	

Table D1. U.S. Geological Survey streamflow measurement stations listed in the order of station ID, in the active model area, near the southeastern part of Puget Sound, Washington.—Continued

[Estimated average base-flow values (2005–15) are from Welch and others (2024, Chapter C, table C9), except for the three seasonal stations, which are described in section, “Model Calibration and Sensitivity.” **Abbreviations:** BL, below; CR, Creek; E, East; ID, identifier; LK, Lake; NA, not applicable; NR, near; ST, Street; WA, Washington; ft³/s, cubic foot per second]

Station ID	Station name	Short name	Estimated average base flow (ft ³ /s)	Used in model calibration	Calibration target name	Affected by streamflow from outside active model area	Factors affecting base-flow estimates	Comments
12100490	WHITE RIVER AT R STREET NEAR AUBURN, WA	WhiteRvRStrAuburn	1,267	Yes	o4701	Yes	Glacier, snowmelt	
12100496	WHITE RIVER NEAR AUBURN, WA	WhiteRvAuburn	1,317	Yes	o4703	Yes	Glacier, snowmelt	
12108500	NEWAUKUM CREEK NEAR BLACK DIAMOND, WA	NewaukumCrBlackDia	49.7	Yes	o4689	No	NA	
12112600	BIG SOOS CREEK ABOVE HATCHERY NEAR AUBURN, WA	BigSoosCrAbHatch	119.8	Yes	o4676	Yes	NA	
12106700	GREEN RIVER AT PURIFICATION PLANT NEAR PALMER, WA	GreenRvPurif	734.9	No	o4683	Yes	Regulated, snowmelt	Model inflow point
12113000	GREEN RIVER NEAR AUBURN, WA	GreenRvAuburn	1,081	Yes	o4684	Yes	Regulated, snowmelt	Base flow adjusted for basin area outside of model
12113344	GREEN RIVER AT 200TH STREET AT KENT, WA	GreenRv200th	1,185	Yes	o4682	Yes	Regulated, snowmelt	Base flow adjusted for basin area outside of model
12113347	MILL CREEK AT EARTHWORKS PARK AT KENT, WA	MillCrEarthworks	2.7	Yes	o4687	No	NA	

Table D1. U.S. Geological Survey streamflow measurement stations listed in the order of station ID, in the active model area, near the southeastern part of Puget Sound, Washington.—Continued

[Estimated average base-flow values (2005–15) are from Welch and others (2024, Chapter C, table C9), except for the three seasonal stations, which are described in section, “Model Calibration and Sensitivity.” **Abbreviations:** BL, below; CR, Creek; E, East; ID, identifier; LK, Lake; NA, not applicable; NR, near; ST, Street; WA, Washington; ft³/s, cubic foot per second]

Station ID	Station name	Short name	Estimated average base flow (ft ³ /s)	Used in model calibration	Calibration target name	Affected by streamflow from outside active model area	Factors affecting base-flow estimates	Comments
12113349	MILL CREEK NEAR MOUTH AT ORILLIA, WA	MillCrMouthOrilla	10.4	Yes	o4688	No	NA	
12089500	NISQUALLY RIVER AT MCKENNA, WA	NisquallyMckenna	1,114	No	o4690	Yes	Regulated	Contributing flow from outside of model area not estimated

Estimation of average base flow for seasonal stations is described in section, “Model Calibration and Sensitivity.”

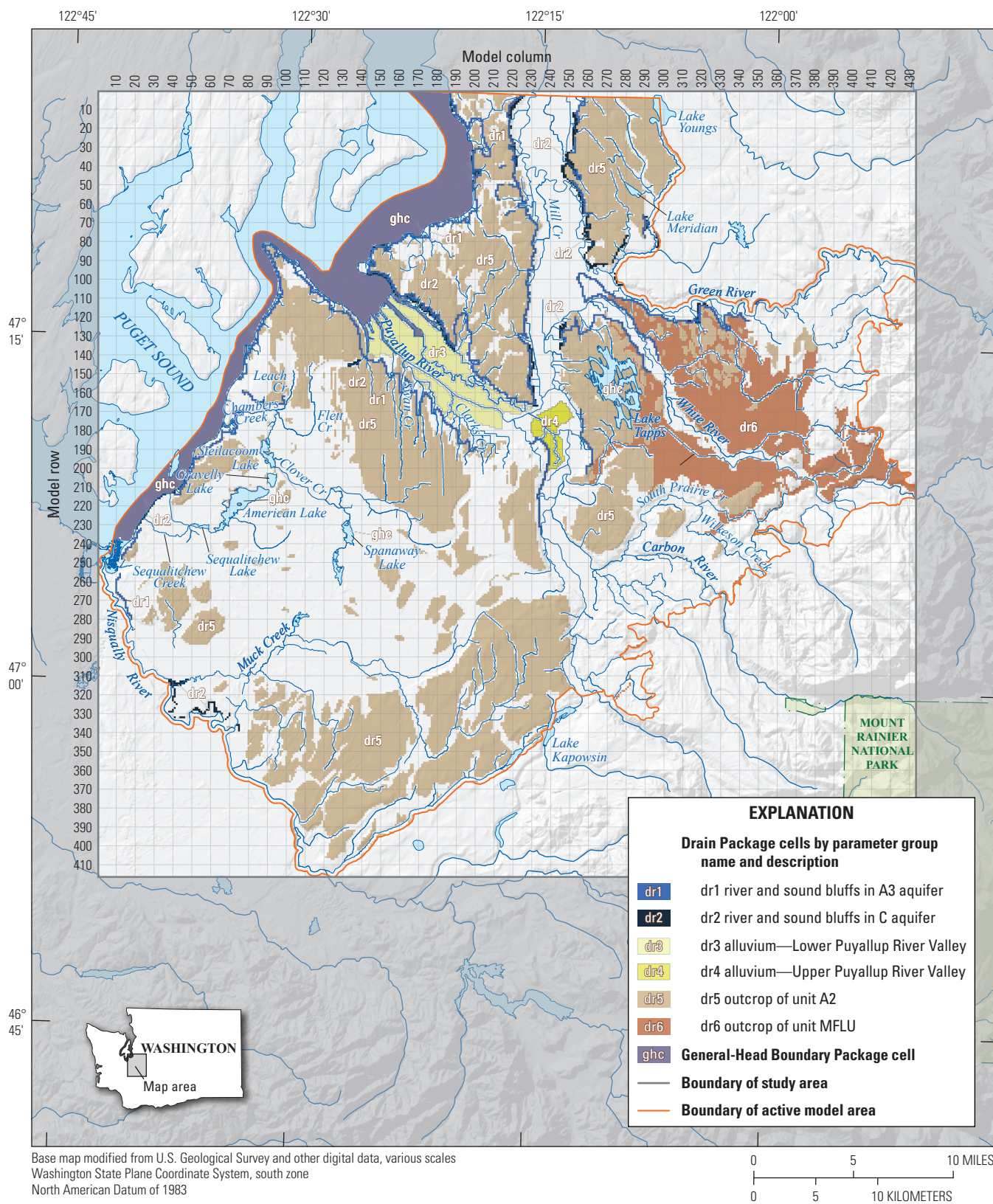


Figure D2. Distribution of General-Head Boundary Package cells, Drain Package cells, and grid rows and columns in the numerical model, near the southeastern part of Puget Sound, Washington.

Table D2. Description of model layers, near the southeastern part of Puget Sound, Washington.

[See figure D1 for the outcrop locations of hydrogeologic units. **Layer type:** A convertible layer indicates variable transmissivity that is dependent on the simulated saturated thickness. A confined layer indicates a constant transmissivity as though the layer is fully saturated at all times.]

Model layer	Hydrogeologic unit name	Description	Layer type
1	MFLU	Upland mudflow confining unit	Convertible
2	AL1	Upper alluvial aquifer	Convertible
3	MFLV	Valley-fill mudflow confining unit	Convertible
4	AL2	Lower alluvial aquifer	Convertible
5	A1	Aquifer	Convertible
6	A2	Confining unit	Convertible
7	A3	Aquifer	Convertible
8	B	Confining unit	Convertible
9	C	Aquifer	Convertible
10	D	Confining unit	Convertible
11	E	Aquifer	Confined
12	F	Confining unit	Confined
13	G (northwestern part)	Undifferentiated deposits	Confined
13	Bedrock (eastern part)	Confining unit	Confined

being inactive cells above the uppermost active model cells. The same is true for layers 2–5 in regard to HGU AL1, MFLV, AL2, and A1, respectively.

Within the AMA, HGUs are discontinuous, as described in Chapter B. Except for layer 13, each model layer represents a single HGU. When constructing a groundwater-flow model using MODFLOW-NWT, cells within model layers where HGUs are absent must remain active if vertical flow is to pass through each layer. For example, layer 8 represents HGU B, which is absent in parts of the Clover Creek area, and cells in this area were made active to allow hydraulic connection between the overlying and underlying layers (HGUs A3 and C in layers 7 and 9, respectively). Model layers 2–12 each contain some of these active cells whose only purpose is to allow vertical flow to pass through. These cells were given a small thickness of 0.2 ft (so that the volume in the model would be negligible) and were assigned a uniform vertical hydraulic conductivity of 2,000 feet per day (ft/d) to allow for unimpeded vertical flow. Horizontal hydraulic conductivity had a value of 200 ft/d.

Model Boundary Conditions

Boundary conditions of the model include all simulated groundwater inflow to and outflow from the AMA; these are categorized as flow boundaries. For example, a gaining stream is a boundary condition that allows groundwater to exit the AMA. No-flow boundaries are those that do not allow flow to cross. Horizontal no-flow boundaries consist of model cells along the outer boundaries of the AMA that do not allow horizontal flow into or out of this area. The bottom

of the lowest model layer (layer 13) is a vertical no-flow boundary because vertical flow cannot enter or exit the AMA through this boundary. A conceptual overview of hydrologic and hydrogeologic features associated with flow boundaries (streams, springs, seeps, lakes, Puget Sound, and precipitation recharge) and their connections to specific HGUs is described in Chapters B and C.

Precipitation Recharge

Precipitation recharge (R_p) is groundwater recharge originating from precipitation on the land surface that infiltrates below the soil zone. An estimate of R_p was obtained from the application of the Soil-Water-Balance (SWB) model (Westenbroek and others, 2010) described in Chapter C. The SWB Model accounts for daily storage change within the soil zone, with outputs that include R_p , evapotranspiration, interception, surface runoff. SWB Model output, including the sum of daily infiltration by month and the overall average for the 11-year model period, is available from Gendaszek (2023).

The SWB Model estimate of R_p was used as input for the Recharge Package (Harbaugh, 2005) in MODFLOW-NWT to simulate R_p for the steady-state and transient model versions. Recharge was applied to all cells in the model that represent the land surface. The Recharge Package applies recharge directly to the saturated component of groundwater; therefore, storage of groundwater below the soil zone and above the groundwater table is neglected in the temporal sense. Consequently, the lag time resulting from this storage is assumed to be zero in the transient model version. The Recharge Package is a specified-flux boundary condition because the recharge rate is specified in the model input.

The SWB Model simulates varying degrees of soil saturation, and infiltration continues until the soil is fully saturated. The SWB Model assumes that the groundwater table is below the soil zone and does not interfere with infiltration. However, if the water table rises to the land surface, which saturates the soil and prevents further infiltration, the infiltration estimated by the SWB Model should not be used as groundwater recharge but instead should be accounted for as surface runoff. This incongruity between infiltration estimated by the SWB Model and R_p in MODFLOW was adjusted for by imposing other boundary conditions that simulate runoff during the wettest months, as described in the next section, “Rejected Recharge, Small Springs, and Seeps.”

As described in Chapter C, 10 lakes were determined to have no outlet stream and were classified as internally drained (table D3). Water enters these lakes through direct precipitation and is removed by evaporation, as simulated by the SWB Model (Chapter C). If precipitation exceeds evaporation, then groundwater recharge is positive, and the model simulates the lake recharging groundwater; if the opposite occurs, then recharge is negative, and the model simulates groundwater flow into the lake that is removed by evaporation. Therefore, the Recharge Package was used to account for groundwater flow to or from these lakes and is referred to as the “lake-recharge estimation method.”

Rejected Recharge, Small Springs, and Seeps

The Drain Package (Harbaugh, 2005) was used to simulate runoff when the simulated water table rises to the land surface, particularly in areas of low permeability such as till. We use the term, “rejected recharge,” to describe runoff simulated in this way. The Drain Package commonly is used to simulate springs or agricultural drains. When the simulated hydraulic head in a drain cell exceeds the specified drain altitude, the Drain Package simulates a groundwater flux out of the cell that is calculated by Darcian flow. The flow rate is dependent on the difference between the groundwater hydraulic head and the drain altitude and the conductance of the intervening porous medium (Harbaugh, 2005). The Drain Package is a head-dependent boundary type that allows outflow from the groundwater system. To simulate rejected recharge, drain cells were assigned to all outcrop areas of HGUs A2 and MFLU (layers 1 and 6; figure D2). Drain cells also were applied to HGU AL1 (layer 2) to simulate rejected recharge for some areas of the Puyallup River valley floodplain, primarily to account for urban drainage channels (fig. D2). Drain altitudes for layers 1, 2, and 6 were set to the average land-surface altitude for each drain cell, also equal to the top of the cell. These drains flow only in areas where hydraulic head exceeds the land surface and were assumed to contribute to runoff.

As described in Chapter B, small springs and seeps flow from outcrops of HGUs A3 and C (layers 7 and 9) along the bluffs sloping toward river valleys and Puget Sound (fig. D2). These were simulated with the Drain Package. Altitudes of these drains were set to the midpoint between the top and bottom of the model cell because these cells represent HGUs that were cut into by sloping bluffs, with springflow exiting horizontally from these HGUs. Flow from these features was assumed to be small in comparison to large springs that are described in section, “Streams and Large Springs.” During summer, groundwater discharge from all drain cells in the model was assumed to be taken up by evapotranspiration. During winter, when evapotranspiration is small, discharge might flow into streams, contributing to stream base flow. Because we assume that this discharge is small and seasonal, it was not used for purposes of accounting for simulated base flow.

Streams and Large Springs

The interaction of groundwater with streams and large springs was simulated with the Streamflow-Routing (SFR) Package. This package simulates a head-dependent boundary condition in which groundwater flow into or out of the stream is determined by the hydraulic head in the model cell, the stream stage, and the conductance of the streambed material (Prudic and others, 2004). The SFR Package also simulates downstream surface-water flow within the channel, which is available as model output for any point in the stream network, such as at the location of a station. The stream stage is a function of flow in the channel.

The SFR Package was used to simulate the interaction of groundwater with streams and was applied to simulate the base-flow component of streamflow only. The package was applied to all model cells that intersect the stream network shown on figure D1. The term “stream” in this report includes rivers, creeks, and their tributaries. The SFR Package also was used to simulate about 200 large springs. As described in Chapter B, these springs are referred to as large springs because they have been specifically identified and often named (documented springs in McLean and others, 2024) and because this term distinguishes them from small springs and seeps, which have not been individually identified as points of groundwater discharge. However, like small springs and seeps, large springs are common along the bluffs that slope toward river valleys or Puget Sound. Large springs commonly are located at stream headwaters or other points along stream channels and contribute base flow directly to streams (fig. D1). Therefore, these springs were simulated by the SFR Package as part of the stream network. If the spring is located at the headwater of the stream, no upstream flow is available to enter the HGU.

D10 Numerical Model of the Groundwater-Flow System Near the Southeastern Part of Puget Sound, Washington

Table D3. Lakes and Puget Sound simulated in numerical modeling , near the southeastern part of Puget Sound, Washington.

[Abbreviations: GHB, General-Head Boundary; K, horizontal hydraulic conductivity; NA, not applicable]

Name of surface-water feature	Area (acres)	Model boundary condition	Description of boundary condition	Inflow and outflow category	Model layer with GHB cells
Puget Sound	NA	GHB Package	Chapter D	Stream inflow	2, 8–13
Lake Tapps	2,444	GHB Package	Chapter D	Stream inflow and outflow	6
American Lake	1,092	GHB Package	Chapter D	Stream inflow and outflow	6, 7
Lake Youngs	685.2	GHB Package	Chapter D	Stream inflow and outflow	6
Lake Kapowsin	496.5	GHB Package	Chapter D	Stream inflow and outflow	2
Steilacoom Lake	306.1	GHB Package	Chapter D	Stream inflow and outflow	6
Spanaway Lake	248.6	GHB Package	Chapter D	Stream inflow and outflow	5
Lake Meridian	149.5	GHB Package	Chapter D	Stream inflow and outflow	6
Gravelly Lake	147.5	Lake-recharge estimation method; high-K pass-through method	Chapters C and D	Internally drained	Lake water represented by layer 6
Lake Louise	38.1	Lake-recharge estimation method	Chapter C	Internally drained	NA
Fivemile Lake	35.4	Lake-recharge estimation method	Chapter C	Internally drained	NA
Waughop Lake	30.1	Lake-recharge estimation method	Chapter C	Internally drained	NA
Little Wapato Lake	26.5	Lake-recharge estimation method	Chapter C	Internally drained	NA
Mirror Lake	17.7	Lake-recharge estimation method	Chapter C	Internally drained	NA
Wright Marsh	16.2	Lake-recharge estimation method	Chapter C	Internally drained	NA
Old Fort Lake	15.4	Lake-recharge estimation method	Chapter C	Internally drained	NA
Hyde Lake	7.8	Lake-recharge estimation method	Chapter C	Internally drained	NA
Mud Lake ¹	2.7	Lake-recharge estimation method	Chapter C	Internally drained	NA

¹Located 6 miles northwest of Lake Tapps.

The term “reach” is defined in the SFR Package as the reach of stream contained within one model cell. In the SFR Package, streambed conductance (C) is a term defined for each reach as

$$C = (K_b w L) / m \quad (\text{D1})$$

where

- K_b is the vertical hydraulic conductivity of the streambed, in units of length per time;
- w is the width of a stream reach, in units of length;
- L is the length of a stream reach, in units of length; and
- m is the thickness of streambed deposits in a stream reach, in units of length.

Equation D1 is calculated internally in the SFR Package, and K_b , w , L , and m are specified as model inputs. Model specifications for the SFR Package are detailed in [appendix 1 \(table 1.1\)](#).

The term “segment” is defined in the SFR Package as a group of connected reaches, and flow is routed from each reach to the next downstream reach and from each segment to the next downstream segment ([app. 1, table 1.1](#)). The width of each SFR segment was assumed to be uniform. This was estimated by a method developed by Magirl and Olsen (2009) for Washington State that relates the width at the top of the wetted channel (W_i) to mean annual discharge (Q):

$$W_i = 4.85 Q^{0.45} \quad (\text{D2})$$

Stream widths were calculated for each SFR segment from [equation D2](#) and used as the stream width in [equation D1](#). Mean annual discharge (Q) was available from the National Hydrography Dataset Plus (NHDPlus) version 2 (U.S. Environmental Protection Agency, 2020). The widths of SFR stream segments were limited to a minimum of 5 ft because the statistical relation developed by Magirl and Olsen (2009) was not well constrained for small streams.

The vertical hydraulic conductivity of the streambed in [equation D1](#) was estimated through model calibration, as described in the section, “[Model Calibration and Sensitivity](#)” ([app. 1, table 1.1](#)). The reach length (L) was determined by overlaying the model grid with the linear trace of the stream

network and calculating the length of stream within a model cell. Because the thickness of all streambeds within the model would be difficult to determine, m was specified as 1.0 ft for all reaches, which is assumed to be much less than actual streambed thicknesses in many cases. Therefore, the calibrated values of K_b do not represent the actual properties of the streambed. If the streambed thicknesses were known, better estimates of K_b could be obtained by multiplying the calibrated values of K_b by bed thicknesses.

Streambed altitudes were estimated by first obtaining water-surface altitudes from the Puget Sound Lidar Supermosaic (Puget Sound Lidar Consortium, 2011) for many points along streams. Water-surface altitudes were assigned to each SFR reach by means of linear interpolation between points, and streambed altitudes then were determined by estimating stream depths ([app. 1, table 1.1](#)). The water depth (D) of each SFR segment was estimated as function of the mean annual discharge (Q) by the method of Magirl and Olsen (2009), as described by

$$D = 0.23 Q^{0.37} \quad (\text{D3})$$

The SFR Package can be set to allow for variable water depths calculated on the basis of simulated stream discharges and channel geometries, or the depths can be specified as constant values. For the steady-state model, constant depths were applied to all streams because nothing varies in steady state. For the transient model, constant depths were applied to the three major rivers: the Green, White, and Puyallup Rivers, which are perennial. These rivers are surrounded by steep groundwater gradients, and the height of groundwater levels surrounding the major rivers is much greater than the potential variability in river stage. Therefore, the effects of variations in the stages of major rivers on the surrounding groundwater gradients are negligible.

All other streams, many of which are either intermittent or ephemeral, were set to calculate variable depths. Variable depth for ephemeral streams improves model stability during transitions between a flowing stream and a dry channel. The variable depth allows smooth transitions from flowing to dry because, by design of the model code, the calculated stream depth asymptotically approaches zero as the stream becomes dry; the transition from dry to flowing also is smooth for similar reasons. The MODFLOW-NWT variable, ICALC, can be set to 0 or 1 to specify the stream depth as constant or variable, respectively ([app. 1, table 1.1](#)). All stream segments were specified to have rectangular channels.

Streams Entering the Active Model Area (AMA)

Many streams in the model accumulate base flow before entering the AMA. Stream base flow that accumulates outside the AMA enters the model at 10 points of inflow (fig. D1), for which base flow must be specified as model input in the SFR Package. Downstream from these locations, simulated base flow is increased, and in some cases reduced, because of groundwater interaction. Most of these points of inflow are on the eastern model boundary, where streams originate from the Cascade Range (fig. D1). Average monthly base-flow estimates at the points of inflow for Coal, Boise, and Scatter Creeks were assumed to be equivalent to precipitation recharge rates for these three watersheds, which were estimated by Gendaszek (2023). These base-flow rates were applied to the steady-state and transient model versions (app. 1, table 1.2). Average monthly base-flow rates for the other seven points of inflow (Green, White, Carbon, and Puyallup Rivers and Big Soos, South Prairie, and Voight Creeks) were estimated by methods described in appendix 2 and are available in appendix 1, table 1.3. The description in appendix 2 is lengthy and detailed and, therefore, was separated from this section to avoid detracting from an otherwise concise description of boundary conditions. The averages of the monthly base-flow values from appendix 1, tables 1.2 and 1.3, are combined in table D4, which were applied to the steady-state model version as specified flow rates for the SFR Package.

Stream Diversions

Flow entering Lake Tapps was estimated using station 12098920, which measures the discharge diverted at the Buckley Diversion from the White River into a canal that discharges into Lake Tapps (fig. D1; table D4). This station has daily data for August 2010–December 2015, and monthly averages were calculated from the daily data (app. 1, table 1.3). To estimate the flows prior to August 2010, the mean daily flows were calculated to get a long-term average for each day of the year. Monthly averages were then calculated from the mean daily values and used as the monthly estimates for the period of missing data (app. 1, table 1.3). Simulated streamflow in the White River as large as the value specified in table 1.3 for each stress period was diverted into the canal.

Flow exiting Lake Tapps discharges into the White River and was estimated using U.S. Geological Survey (USGS) station 12101100 (fig. D1; table D4). Daily streamflow data were available for May 2005–December 2015 for this station, and monthly averages were calculated from the daily data. To estimate the flow data for the missing period, the same method as that used for the lake inflow was applied (app. 1, table 1.3). These diversion rates were applied as specified flows in the SFR Package.

Spanaway Lake empties into Spanaway Creek, where about 13 percent of the streamflow is diverted into Morey Creek to the west (fig. D1; table D4; Pierce County, 2017), and the SFR Package was set accordingly. Outflow from the west end of Sequelitchew Lake flows into Sequelitchew Creek, where it is partly is diverted into the Sequelitchew diversion canal to the north. Measurements taken at the diversion canal weir indicate a diversion rate of about 6–7 ft³/s (Aspect Consulting, LLC, 2009). The SFR Package was set to divert all flow from Sequelitchew Creek by as much as 6.5 ft³/s into the diversion canal.

Externally Drained Lakes

Groundwater interaction with eight lakes that drain into streams (as described in Chapter B) was simulated as head-dependent boundaries by applying the General-Head Boundary (GHB) Package (Harbaugh, 2005). This package was applied to Lake Tapps, American Lake, Lake Youngs, Lake Kapowsin, Steilacoom Lake, Spanaway Lake, Lake Meridian, and Puget Sound (fig. D1; table D3). All these lakes have inflow and outflow streams that influence lake levels. The GHB Package simulates Darcian flow into or out of a model cell, calculated from the difference between the hydraulic head for the model cell and the water level in a conceptual external storage tank that is connected by an intervening porous medium. The conductance term for the GHB Package is identical to that described in equation D1, except that the streambed dimensions are generalized to represent the intervening porous medium of the GHB cell, in this case the lakebed or seafloor sediments. The GHB Package was applied to cells that directly underlay lakes and Puget Sound, with the conceptual external tank representing the lake or sound. Groundwater flow to or from a lake changes the flow rate in a stream that drains the lake. Therefore, simulated flow from groundwater into a lake or from a lake into groundwater was accounted for by adding or subtracting, respectively, this groundwater flow to or from the base flow simulated by the SFR Package downstream from the lake. This adjustment was applied by post-processing model output and, therefore, did not affect the computed stream stage downstream from lakes.

Detailed information describing outflow structures and controls for lakes was not available, and the GHB Package was suitable because this information is not required for its application. Monthly average lake-surface altitudes used in modeling were obtained or estimated for January 2005–December 2015 for Lake Tapps and American, Gravelly, Steilacoom, and Spanaway Lakes (app. 1, table 1.4). The remainder of this section describes the methods used to calculate or estimate these monthly values. Data for USGS hydrologic stations were obtained from the USGS National Water Information System (NWIS) database (U.S. Geological Survey, 2020).

Table D4. Specified flows and diversions for the Streamflow-Routing Package (Prudic and others, 2004) for the steady-state model version, near the southeastern part of Puget Sound, Washington.

[Estimated flows are described and presented in Chapter C of Welch and others (2024). IPRIOR defines how the flow is specified in the Streamflow-Routing Package (Prudic and others, 2004). **Abbreviations:** SFR, Streamflow-Routing; SWB, Soil-Water-Balance model; USGS, U.S. Geological Survey; ft³/s, cubic foot per second; ft³/d, cubic foot per day; NA, not applicable]

Feature name	Feature description	Model specification	Basis for flow estimate	IPRIOR	Steady-state base flow (ft ³ /s; tables 1.3 and 1.9)	Model specified base flow (ft ³ /s)	Model specified base flow (ft ³ /d)	SFR segment	Downstream segment	Upstream segment for diversions
Big Soos Creek	Big Soos Creek inflow at model boundary	Specified flow into SFR segment	Station data: USGS 12112600	0	86.3	86.3	7.46 × 10 ⁶	883	885	NA
Green River	Green River inflow at model boundary	Specified flow into SFR segment	Station data: USGS 12106700	0	736.1	736.1	6.36 × 10 ⁷	822	823	NA
Coal Creek	Coal Creek inflow at model boundary	Specified flow into SFR segment	SWB estimated recharge	0	23.4	23.4	2.02 × 10 ⁶	815	816	NA
Boise Creek	Boise Creek inflow at model boundary	Specified flow into SFR segment	SWB estimated recharge	0	14.0	14.0	1.21 × 10 ⁶	312	313	NA
Scatter Creek	Scatter Creek inflow at model boundary	Specified flow into SFR segment	SWB estimated recharge	0	18.8	18.8	1.62 × 10 ⁶	289	290	NA
White River	White River inflow at model boundary	Specified flow into SFR segment	Station data: USGS 12097850 and 12099200	0	1,113	1,113	9.62 × 10 ⁷	293	294	NA
South Prairie Creek	South Prairie Creek inflow at model boundary	Specified flow into SFR segment	Station data: USGS 12095000, 12094425, and 12094498	0	142.3	142.3	1.23 × 10 ⁷	438	439	NA

Table D4. Specified flows and diversions for the Streamflow-Routing Package (Prudic and others, 2004) for the steady-state model version, near the southeastern part of Puget Sound, Washington.—Continued

[Estimated flows are described and presented in Chapter C of Welch and others (2024). IPRIOR defines how the flow is specified in the Streamflow-Routing Package (Prudic and others, 2004). **Abbreviations:** SFR, Streamflow-Routing; SWB, Soil-Water-Balance model; USGS, U.S. Geological Survey; ft³/s, cubic foot per second; ft³/d, cubic foot per day; NA, not applicable]

Feature name	Feature description	Model specification	Basis for flow estimate	IPRIOR	Steady-state base flow (ft ³ /s; tables 1.3 and 1.9)	Model specified base flow (ft ³ /s)	Model specified base flow (ft ³ /d)	SFR segment	Downstream segment	Upstream segment for diversions
Carbon River	Carbon River inflow at model boundary	Specified flow into SFR segment	Station data: USGS 12094000	0	342.6	342.6	2.96 × 10 ⁷	449	452	NA
Voight Creek	Voight Creek inflow at model boundary	Specified flow into SFR segment	Station data: USGS 12095000 and 12095500	0	47.8	47.8	4.13 × 10 ⁶	463	464	NA
Puyallup River	Puyallup River inflow at model boundary	Specified flow into SFR segment	Station data: USGS 12093500 and 12092505	0	576.2	576.2	4.98 × 10 ⁷	497	498	NA
Lake Tapps outflow diversion	Outflow from Lake Tapps into White River	Specified flow into SFR segment	Station data: USGS 12101100	0	71.2	71.2	6.15 × 10 ⁶	383	384	NA
Buckley diversion	Diversion from White River into a canal that flows into Lake Tapps	All streamflow up to the value in table 1.9 is diverted.	Station data: USGS 12098920	0	NA	NA	NA	1,024	NA	310
Morey Creek diversion	Diversion from Spanaway Creek into Morey Creek	Diversion rate specified as 13 percent of upstream flow.	Pierce County (2017)	-2	NA	NA	NA	203	204	199
Sequalitchew diversion canal	Diversion from Sequalitchew Creek into the canal	All streamflow as much as 6.5 ft ³ /s is diverted.	Aspect Consulting, LLC (2009)	0	NA	NA	NA	1,023	NA	163

Lake-surface altitude for Lake Tapps is monitored at station 12101000. Daily station height data were averaged to monthly values and converted from National Geodetic Vertical Datum of 1929 (NGVD 1929) to North American Vertical Datum of 1988 (NAVD 88) using a datum shift of 3.547 ft.

Beginning in May 2000, volunteers measured lake-surface altitudes for American and Gravelly Lakes once or twice per month from May through October and again in December (inconsistently) as part of the Lakewood Lake Monitoring Program through the Pierce Conservation District (app. 1, table 1.5). Linear interpolation was used to estimate daily lake-surface altitude values from monthly observations for the study period. Monthly average values were calculated from these daily values for January 2005–December 2015. The mean water-level altitude for the study period was 231.75 ft above NAVD 88 for American Lake and 211.75 ft above NAVD 88 for Gravelly Lake. Seasonal variability in lake-surface altitude across the model area for the study period was derived by calculating the amount of monthly variation from the average water level for American and Gravelly Lakes.

No lake-surface altitude observations were available for Steilacoom Lake. To estimate lake-surface altitude, a remote water elevation measurement for Steilacoom Lake was obtained from lidar elevation data. Lidar data over Steilacoom Lake were collected on December 8 and 10, 2010, and on January 2 and 4, 2011, and compiled data were downloaded from the Washington Lidar Portal (2011). The remote water level was assigned as the mean monthly value for December 2010, and the seasonal variability derived from American and Gravelly Lakes then was applied to the remaining months in the study period to estimate the monthly lake-surface altitude record.

Lake-surface altitudes for Spanaway Lake were estimated using a combination of continuous lake-surface observations (app. 1, table 1.5) where available and seasonal groundwater fluctuations in a nearby shallow well to derive the remaining values. The Pierce Conservation District provided continuous lake-stage altitude levels measured at the Enchanted Island meteorological station with an electronic data logger from July 2014 to December 2015 (Brown and Caldwell, 2016). Continuous measurements were averaged to create daily average values, and then monthly average values.

To estimate lake-surface altitude for the remainder of the study period for Spanaway Lake, nearby shallow wells with groundwater altitude measurements were identified. One shallow well within 0.5 mile (mi) of Spanaway Lake (station 470721122275101) had recorded monthly water-level measurements for March 2007–September 2008 and April 2010–August 2015. Dates and values for the highest and lowest available water levels for each year were averaged separately to fill gaps in the groundwater-level record for 2005, 2006, 2009, and 2015. Linear regression was applied to relate lake-surface altitude to groundwater level for dates where a groundwater observation and lake-level altitude

observation existed, resulting in the following regression equation: Lake level = $0.3018 \times$ groundwater level + 236.79 ft (coefficient of determination $[R^2] = 0.905$). This correlation is evidence for hydraulic connection between the lake and shallow groundwater and indicates that the groundwater level can be used to estimate lake levels for periods of missing data. The regression equation was applied to the monthly groundwater levels to estimate monthly lake stage for the period of missing data (March 2004–October 2016). Daily values then were estimated by applying linear interpolation between the monthly values, and monthly average values were calculated from the daily values.

Internally Drained Lakes

Ten lakes are classified as internally drained lakes (table D3). The GHB Package was not applied to these lakes because (1) water-level records were not available as GHB Package input and (2) the groundwater exchange could be estimated by other means and applied to the model by the Recharge Package. Because these lakes have no outflow stream, water is removed only by evaporation or by infiltration to groundwater. Both of these possible flows were accounted for by the “lake-recharge estimation method” and simulated by the Recharge Package, as described in section, “Precipitation Recharge.” Gravelly Lake is the largest of the internally drained lakes and, therefore, may have a large component of horizontal groundwater interaction, which is not simulated by the lake-recharge estimation method. This interaction was simulated by what is referred to herein as the “high-K pass-through method” (table D3) in which the water-body volume was represented by model cells with an exceedingly large value of horizontal hydraulic conductivity to approximate flow of open water that fills the lake volume. The lake overlies HGU A3 (layer 7), with horizontal connection to HGU A2 (layer 6). In the area of the lake, model cells in layer 6 were assigned this high-K value, which allowed horizontal connection to HGU A2 and vertical connection to HGU A3. Because of the high-K value, these lake cells resulted in a nearly flat simulated potentiometric surface, which approximates the lake surface.

Puget Sound

Submarine groundwater discharge to Puget Sound is represented by the GHB Package (fig. D1). Model cells directly underlying the sound were set as GHB cells. Seawater is denser than fresh water and, therefore, exerts greater hydrostatic pressure at the sea floor than fresh water. To compensate for this density difference, specified hydraulic-head values for the GHB cells were set higher than sea level according to assumptions described by van Heeswijk and Smith (2002), which are described by equation D4.

$$h'_{st} = h_{st} + H(0.023) \quad (D4) \quad \text{Alluvial Valley Margins}$$

where

- h'_{st} is the adjusted sea-level altitude above North American Vertical Datum of 1988 (NAVD 88) to compensate for the density difference,
- h_{st} is altitude of sea level above NAVD 88, and
- H is the height of the vertical column of seawater above the three-dimensional centroid of the model cell at the sea floor.

H is multiplied by 0.023, which is the difference in specific gravity between saline water in Puget Sound and fresh water (van Heeswijk and Smith, 2002). The mean sea level for a tide station at Tacoma, Washington, is 6.84 ft above the mean lower-low water level, or 4.45 ft above NAVD 88 (National Oceanic and Atmospheric Administration, 2021). A constant sea-level altitude of 4.45 ft above NAVD 88 was used as h_{st} in equation D4, and the adjusted sea-level altitude (h'_{st}) was applied to all Puget Sound GHB cells.

Groundwater Use and Return Flow

Human use of groundwater, including return flows to the groundwater system (such as domestic septic systems and leaking distribution pipes) is described in Chapter C, with estimated values available in McLean and others (2024). The Well Package (Harbaugh, 2005) was used to simulate pumping wells and return flows. The Well Package also was used to simulate water withdrawn from large springs for public supply, as described in Chapter C and in McLean and others (2024). Use of the well package for these springs allowed for known flow rates to be specified for these springs and separated from other springflow that is assumed to contribute to stream base flow. Head-dependent boundary conditions (SFR and Drain Packages) also are present at the locations of these springs to simulate any additional springflow that occurs when groundwater levels exceed land-surface altitudes.

Near the southeastern model boundary where HGU Bedrock was not included in the model, pumping wells withdrawing from bedrock (as estimated by McLean and others, 2024) were not simulated. This omission resulted in a reduction of a total estimated groundwater use of 0.05 percent for the steady-state model version.

MODFLOW-NWT reduces the pumping rate for any simulated well if the saturated thickness of the model cell is less than a set threshold (Niswonger and others, 2011), which was set as 10 percent of the layer thickness. The purpose of simulated pumping reductions is to simulate decreases in well yields that would be expected under these conditions. Therefore, the simulated rate of groundwater use may be less than that estimated. Details and results of these simulated pumping reductions are described in section, “[Calibration Constraints](#).”

At some locations along the margins of alluvial valleys, HGUs A1, A3, C, and E are in horizontal contact with valley fill aquifers (HGUs AL1 and AL2), which have cut downward into the older deposits. Because HGUs A1, A3, C, and E are represented by model layers 5, 7, 9, and 11, a horizontal connection to HGU AL1 (layer 2) is not possible in MODFLOW-NWT. At these locations, HGU MFLV also limits vertical flow into HGU AL1 from below. To address this issue, model cell thickness and HGU representations in cells were adjusted near these locations to allow better connection between HGU AL1 and other HGUs that contact HGU AL1 along its margins.

An example of this situation in alluvial valleys is shown in [figure D3A](#), where HGU C should be hydraulically connected horizontally to HGU AL1 at the interface between columns 229 and 230, which is not possible in MODFLOW-NWT because these are in different model layers. The same problem does not occur for HGU AL2, however, because this HGU is below the confining unit (HGU MFLV) and is vertically connected to HGU C.

To mitigate this issue for HGU AL1, adjustments were made to model cells, which consisted of adjusting cell thicknesses and vertical hydraulic conductivity (K_v) values. To assign K_v values, the model uses the ratio of horizontal to vertical hydraulic conductivity (K_h/K_v). Adjustments are illustrated in [figure D3B](#), where HGUs MFLV and AL2 were effectively eliminated to allow direct vertical contact between HGUs C and AL1 in column 230. HGUs MFLV and AL2 were eliminated in column 230 by making the cells thin (0.2 ft) and assigning a K_h/K_v value of 0.1 ($K_v = 2,000$ ft/d) to allow groundwater to pass through freely. Therefore, these cells are not visible in [figure D3B](#). The cell in layer 2 and column 230 in [figure D3B](#) was assigned a K_h/K_v value of 1 ($K_v = 200$ ft/d) to enhance the vertical connection into layer 2. These adjustments are hereinafter referred to as the “mudflow bypass method.”

At these locations, the mudflow bypass method was applied if the side of a HGU AL1 cell was more than 50 percent in contact with a horizontally adjacent cell that also was in a lower layer. For example, in [figure D3A](#), the left side of the HGU AL1 cell in column 230 is 100 percent in contact with the HGU C cell in column 229; therefore, the mudflow bypass method was applied. To implement this method, the bottom altitude of the AL1 cell was moved to the midpoint between the top of the AL1 cell and the bottom of the AL2 cell. The top altitude of the AL1 cell remained the same. All cells below the AL1 cell and the HGU C cell then were made thin (0.2 ft).

The mudflow bypass method is an imperfect solution to simulating flow across the interface between valley fill and adjacent HGUs. An alternative solution would be the application of an unstructured grid that allows direct horizontal connections between any two cells in the model (Langevin and others, 2017), which also would be an imperfect solution. Unlike the model representation of this

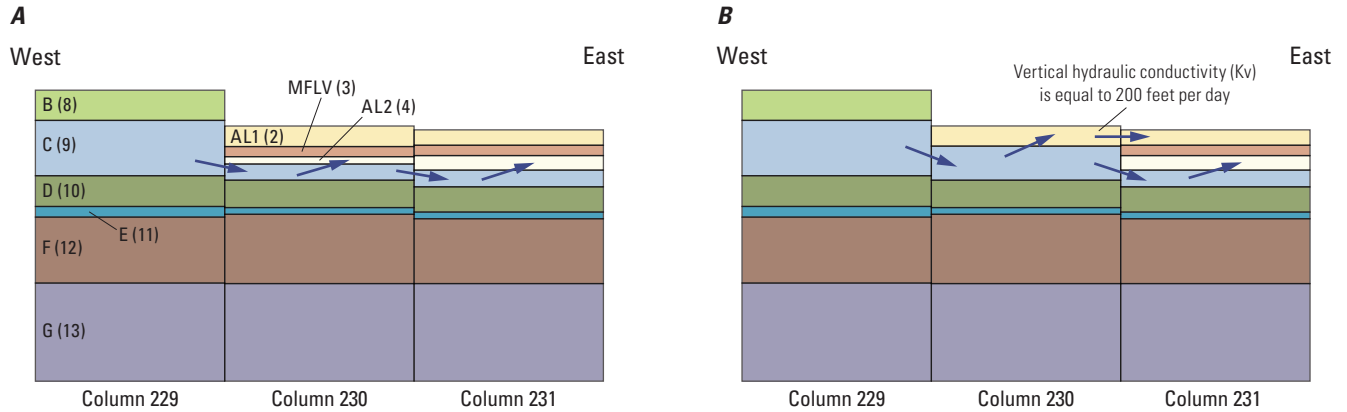


Figure D3. Example of model cell adjustment for the mudflow bypass method showing (A) a profile of the original hydrogeologic framework at the margin of the White River valley (row 137) and (B) the same profile after adjustments. Hydrogeologic units are labeled, with model layers in parentheses. Arrows show how flow is able to move from cell to cell. Very thin model layers are not visible and model cells are shown with large vertical exaggeration.

interface, which is vertical because model cells are vertical (fig. D3A), the actual interface is sloping. Groundwater flow across a sloping interface would be controlled by a combination of horizontal and vertical hydraulic conductivities and gradients. An unstructured grid would allow horizontal flow directly across this interface by connecting cells in two different layers but would neglect the vertical flow component. Furthermore, the unstructured grid approach implies a higher level of certainty in the geometry of the interface than the subsurface data support. An advantage of the mudflow bypass method is that it allows flow across the interface but also is applicable in this simpler structured grid required for MODFLOW-NWT.

Boundary of Active Model Area (AMA)

Boundary conditions at the boundary of the AMA consist of those that simulate Puget Sound, streams, and lakes (fig. D1). The eastern model boundary that is adjacent to mountainous terrain is a no-flow boundary, except where streams are present. At the farthest northern boundary, groundwater was assumed to flow parallel to the boundary, either easterly or westerly toward streams, Puget Sound, or Lake Youngs. Therefore, this is a no-flow boundary, except where surface-water features are present. Puget Sound is represented by the GHB Package (fig. D2). All other boundaries are parallel to streams that are represented by the SFR Package. These streams consist of the Green River and Big and Little Soos Creeks along the northeastern boundary and the Nisqually River and Tanwax Creek along the southern boundary (fig. D1). Stream boundaries also were assumed to be converging groundwater divides; therefore, model cells in layers below SFR cells along these boundaries are no-flow boundaries.

Initial Conditions

Model output for the calibrated steady-state model version was used for the initial hydraulic-head condition for that version. Because model output was used as initial conditions for the same model, generating initial conditions was an iterative process during model calibration. Although the initial conditions do not affect the final conditions in the steady-state model version, these initial conditions allow the numerical solution to close quickly. For the transient model version, hydraulic-head output for December 2008 was used as the initial condition for January 2005 (the first stress period). The reason for this is because the total estimated recharge for the AMA for December 2008 was most similar to that of December 2004 (Chapter C). Like with the steady-state model version, generating initial conditions was an iterative process.

Hydraulic Properties

The model was separated into zones (within which hydraulic conductivity was defined for model calibration) that are referred to as K-zones. Each model layer has one or more K-zones that represent the HGU within that layer (table D5). Layer 13 represents HGU G and bedrock, which are represented by K-zones 13 and 15, respectively. K-zones 14, 18, and 21 represent thin cells whose purpose is to allow vertical flow to pass through, as described in section, “Horizontal Discretization and Vertical Layering.” K-zone 19 consists of cells that implement the mudflow bypass method, and Gravelly Lake is represented by K-zone 20. K-zones 22–29 were added where needed to allow adequate flow to large production wells and springs. Details on the distribution of K-zones are available in Wright and others (2023). Model calibrated values for K_h and K_h/K_v by hydraulic conductivity zone (K-zone) are summarized in table D6.

Table D5. Hydraulic conductivity zones near the southeastern part of Puget Sound, Washington.

[See figure D1 for the location of hydrogeologic units. **Abbreviations:** HGU, hydrogeologic unit; Kh, horizontal hydraulic conductivity; Kv, vertical hydraulic conductivity; NA, not applicable]

Model layer	Hydraulic conductivity zone	HGU	Description	Calibration method
1	1	MFLU	Upland mudflow	Pilot points
2	2	AL1	Upper alluvial aquifer, western area	Pilot points
2	16	AL1	Upper alluvial aquifer, eastern area	Pilot points
3	3	MFLV	Valley-fill mudflow	Pilot points
4	4	AL2	Alluvial aquifer	Pilot points
5	5	A1	Aquifer	Pilot points
6	6	A2	Semiconfining unit	Pilot points
7	7	A3	Aquifer	Pilot points
7	17	A3	Aquifer, larger Kh than elsewhere in A3	Pilot points
8	8	B	Semiconfining unit	Pilot points
9	9	C	Aquifer	Pilot points
10	10	D	Semiconfining unit	Pilot points
11	11	E	Aquifer	Pilot points
12	12	F	Semiconfining unit	Pilot points
13	13	G	Undifferentiated deposits	Pilot points
13	15	Bedrock	Semiconfining unit	Pilot points
2–12	14	NA	Thin cells that allow vertical pass-through flow ¹	Uniform fixed value
9–10	18	NA	Thin cells that allow vertical pass-through flow ¹	Uniform fixed value
5	21	NA	Thin cells that allow vertical pass-through flow ¹	Uniform fixed value
2	19	NA	Mudflow bypass method ²	Uniform fixed value
6	20	NA	Gravelly Lake ³	Uniform fixed value
8	22	B	Parameters adjusted to mitigate pumping reductions	Uniform fixed value
2, 7, 8, 9	23	AL1, A3, B, C	Parameters adjusted to mitigate pumping reductions	Uniform fixed value
9	24	C	Parameters adjusted to mitigate pumping reductions	Uniform fixed value
7, 9, 11	25	A3, C, E	Parameters adjusted to mitigate pumping reductions	Uniform fixed value
6, 9	26	A2, C	Parameters adjusted to mitigate pumping reductions	Uniform fixed value
8	27	B	Parameters adjusted to mitigate pumping reductions	Uniform fixed value
8	28	B	Parameters adjusted to mitigate pumping reductions	Uniform fixed value
5, 7	29	A1, A3	Parameters adjusted to mitigate pumping reductions	Uniform fixed value

¹Thin model cells have a high Kv value in areas where the HGU is not present in that layer.

²This method allows lateral flow into alluvial valley fill from adjacent HGUs.

³Model cells that represent the volume occupied by Gravelly Lake water.

Table D6. Calibrated hydraulic conductivity values summarized by hydrogeologic unit, near the southeastern part of Puget Sound, Washington.[See figure D1 for the location of HGU's. **Abbreviations:** HGU, hydrogeologic unit; Kh, horizontal hydraulic conductivity; Kv, vertical hydraulic conductivity]

Model layer	Hydraulic conductivity zone	HGU	Kh (foot per day)				Kh/Kv (dimensionless)			
			Mean	Standard deviation	Minimum	Maximum	Mean	Standard deviation	Minimum	Maximum
1	1	MFLU	232.7	114.1	50.0	600.0	41.1	161.8	1.00	3,000
2	2, 16, 19, 23	AL1	182.3	73.6	1.03	300.0	0.6	7.6	0.10	3,000
3	3	MFLV	7.6	15.3	2.12	50.0	749.6	1,950	1.00	5,828
4	4	AL2	54.7	68.8	1.41	300.0	8.8	6.2	1.01	25.0
5	5, 29	A1	1,741	2,366	0.011	10,000	15.7	12.6	2.81	55.6
6	6, 26	A2	6.3	9.1	0.002	100.0	975.1	1,406	2.14	9,876
7	7, 17, 23, 25, 29	A3	61.7	146.5	0.003	1,780	11.2	11	1.50	49.8
8	8, 22, 23, 27, 28	B	1.2	11.7	0.001	500.0	549.3	1,175	1.00	9,792
9	9, 23-26	C	52.8	81.2	0.011	533.0	8.4	7.5	1.93	49.3
10	10	D	1.9	2.5	0.001	23.1	391.3	828.9	2.41	9,741
11	11, 25	E	15.9	38.1	0.898	496.0	16.1	12.1	2.00	50.2
12	12	F	2.1	4.1	0.003	49.4	999.9	1,208	3.03	9,776
13	13	G	133.8	234.0	0.086	1,500	801.3	1,618	6.55	10,000
13	15	Bedrock	0.26	0.43	0.015	1.0	7.7	3.9	1.00	10.0

¹Does not include zone 20, representing Gravelly Lake water (Kh = 50,000 ft/d; Kh/Kv = 250,000).

To allow for spatially variable values of K_h and K_h/K_v , parameter values were assigned to pilot points, which are point locations for model parameters (Doherty, 2018). Pilot points were applied to all K-zones that represent HGUs; all other zones contained a uniform parameter value (table D5). Further details on pilot points are described in the section, “Model Calibration and Sensitivity.” Kriging was applied to interpolate between pilot points within each K-zone and was applied separately to each K-zone. The storage parameters, specific yield (S_y) and specific storage (S_s), are summarized in table D7 by HGU. As many as 13 parameter zones (S-zone) are present within a model layer. Storage parameters are spatially uniform within each S-zone and, therefore, pilot points were not used. Details on the distribution of S-zones are available in Wright and others (2023).

Model Calibration and Sensitivity

Calibration Targets

The model was calibrated to measured values of water levels in wells and lakes and estimated base flow for the streamflow stations listed in table D1. These measured and estimated values are referred to as calibration targets. Hydraulic head-calibration targets for the transient and steady-state model versions are available in appendix 1, tables 1.6 and 1.7, respectively. Monthly base-flow values (app. 1, table 1.8) were estimated by methods described in Chapter C and were used as calibration targets for the transient model version, the averages of which were used as steady-state calibration targets for each station app. 1 (table 1.9).

Average monthly hydraulic-head values (2005–15) were calculated for 273 wells; these values were used in calibration of the transient model version (U.S. Geological Survey, 2020) (app. 1, table 1.6). The average of the monthly values for each well was used as a calibration target for the steady-state model version.

Hydraulic-head values for an additional 3,719 wells were used as calibration targets for the steady-state model version, for a total of 3,992 steady-state targets. Many of these 3,719 wells had multiple hydraulic-head measurements, and the average value for each of these wells (2005–15) was calculated according to methods described in Chapter B (app. 1, table 1.7). As described in Chapter B, for wells with time-series records, anomalously low or high water levels could have been the result of pumping the well, measurement errors, or data errors; these values were removed from transient calibration data.

Simulated hydraulic head for the model cells representing the water volume of Gravelly Lake were calibrated to monthly average lake-level measurements for the transient model version (app. 1, table 1.4). The average of monthly values for Gravelly Lake were used as a calibration target for the steady-state model version. The Observation Process

(Harbaugh and Hill, 2009) was used to obtain simulated values from the transient model version for comparison to measured values.

The model also was calibrated to vertical hydraulic gradients. The difference in hydraulic head between two HGUs was estimated for selected locations. Locations were selected where a hydraulic-head target was available for each of two different HGUs in the same general horizontal location, but not necessarily the exact location. Therefore, to estimate a hydraulic-head difference in the exact vertical direction, one of the two targets was selected as one vertical end point, and the other end point was taken from the estimated potentiometric surface (Chapter B) for that location. These vertical hydraulic-head differences were used as calibration targets that are available in app. 1, table 1.10, which consists of 616 targets, including the difference value, location, and upper and lower model layers.

Simulated groundwater flooding occurs when unconfined areas of the model simulate hydraulic heads above the land surface. Some areas of the model were prone to groundwater flooding during preliminary model testing. In these areas, hydraulic-head targets equal to the land-surface altitude were added to help prevent groundwater flooding in the calibrated model (app. 1, table 1.11).

Simulated base-flow values consist of base flow simulated by the SFR Package and estimated base flow entering the AMA. Base-flow gain within the AMA consists only of that simulated by the SFR Package, which was the effective target of calibration because the latter component has fixed values, remaining constant when parameters are adjusted. These simulated values were calibrated in the steady-state and transient model versions to data for 25 stations (table D1). Four additional stations were not used in calibration, as described in table D1 (“Used in model calibration” column). Hydrograph separation, as described in Chapter C, was used to estimate monthly base-flow values that were used as transient calibration targets (McLean and others, 2024). The averages of monthly values for each station were used as steady-state calibration targets, with the exception of three seasonal stations (table D1).

The seasonal stations, two on the Puyallup River (stations 12096505 and 12101470) and one on Swan Creek (station 12102190), were not measured during May–September; therefore, the averages of the measured periods would be seasonally biased. The two stations on the Puyallup River also were not measured prior to 2010. To estimate the steady-state calibration target for station 12096505, the average daily base-flow gain between this station and the next upstream station (12096500) was calculated as 64.1 ft³/s, which was then added to the steady-state target for the upstream station as a surrogate for the steady-state target for station 12096505. A similar approach was taken to estimate the steady-state target for station 12101470, which had an average daily gain of 63.4 ft³/s from this station to the next downstream station (12101500), which then was subtracted from the downstream station.

Table D7. Calibrated specific yield and specific storage values summarized by hydrogeologic unit, near the southeastern part of Puget Sound, Washington.[See figure D1 for the location of hydrogeologic units. **Abbreviations:** HGU, hydrogeologic unit; NA, not applicable; Ss, specific storage; Sy, specific yield]

Layer	HGU	Number of parameter zones	Ss				Sy			
			Mean	Standard deviation	Minimum	Maximum	Mean	Standard deviation	Minimum	Maximum
1	MFLU	3	1.25×10^4	1.25×10^4	1.00×10^7	2.58×10^4	0.18	0.12	0.001	0.30
2	AL1	4	5.30×10^5	9.43×10^5	1.00×10^7	2.58×10^4	0.13	0.08	0.001	0.30
3	MFLV	2	4.03×10^5	8.12×10^5	1.00×10^5	2.58×10^4	0.12	0.07	0.100	0.30
4	AL2	3	4.56×10^5	8.72×10^5	1.00×10^6	2.58×10^4	0.13	0.07	0.020	0.30
5	A1	12	1.31×10^4	1.74×10^4	1.00×10^7	1.00×10^3	0.17	0.11	0.001	0.30
16	A2	13	8.49×10^5	1.68×10^4	1.00×10^7	1.00×10^3	0.10	0.04	0.001	0.30
7	A3	12	1.09×10^4	3.69×10^4	1.00×10^7	5.00×10^3	0.10	0.04	0.001	0.30
8	B	8	2.54×10^5	7.50×10^5	1.00×10^7	5.00×10^3	0.09	0.03	0.001	0.30
9	C	10	8.98×10^5	3.35×10^4	1.00×10^7	5.00×10^3	0.08	0.04	0.001	0.30
10	D	3	2.32×10^6	9.64×10^6	1.00×10^6	2.58×10^4	0.03	0.03	0.020	0.30
11	E	3	1.93×10^6	2.74×10^6	1.00×10^6	1.00×10^5	NA	NA	NA	NA
12	F	3	1.12×10^6	1.04×10^6	1.00×10^6	1.00×10^5	NA	NA	NA	NA
13	G	1	1.11×10^6	5.31×10^6	1.00×10^6	2.58×10^4	NA	NA	NA	NA
13	Bedrock	3	1.20×10^4	1.27×10^4	1.00×10^6	2.58×10^4	NA	NA	NA	NA

¹Does not include layer 6 cells representing Gravelly Lake water (Ss = 0.0179; Sy = 0.95).

The only data available to estimate base flow were daily streamflow records; therefore, the only option available to estimate base flow was hydrograph separation. As described in Chapter C, the method selected was the automated hydrograph separation program HYSEP (Sloto and Crouse, 1996). Hydrograph separation is not an accurate method for base-flow estimation because it completely relies on the shape of the hydrograph of total streamflow to determine the daily proportions of base flow and runoff. Additionally, shallow groundwater in the unsaturated zone that flows downslope toward streams, known as interflow, is not explicitly separated by HYSEP or similar methods. We assume that base flow estimated by HYSEP includes interflow, a flow component that MODFLOW does not simulate. On this basis, base flow simulated by MODFLOW is expected to be less than that estimated by HYSEP because MODFLOW simulates only fully saturated groundwater flow to streams.

The accuracy of hydrograph separation may vary by season, as well as other factors. For summer periods of low streamflow, as much as 100 percent of streamflow is base flow for streams not fed by glaciers. Summer base-flow estimates for these streams are much more accurate than for winter because the runoff component is very small or absent. However, large uncertainty is associated with base-flow estimates for streams fed by glaciers, and in all cases, large uncertainty is associated with winter high-flow periods in this study area.

Base-flow calibration targets were adjusted for two stations on the Green River (12113000 and 12113344) because part of the watershed upstream from these locations is outside the model area. The adjustment was necessary to include these two stations in model calibration. This watershed area is on the north side of the Green River, where the river coincides with the boundary of the AMA, which is not accounted for by specified inflows for the SFR Package (fig. D1). This area is 32 percent of the watershed area upstream from station 12113000 (Green River) and downstream from 12112600 (Big Soos Creek) and 12106700 (Green River at the model inflow point). Watershed areas were determined by StreamStats v4.4.0 (U.S. Geological Survey, 2021). Therefore, the base-flow gain within this area was multiplied by 0.32 and subtracted from the base flow for stations 12113000 and 12113344. McLean and others (2024) contained the estimated monthly base flow for these stations and also the adjusted values used for calibration of the transient model version.

The station on the Nisqually River (station 12089500; figure D1) was not included in model calibration for several reasons. Like the Green River, this river is a model boundary, and the flow contribution from outside the model would need

to be estimated. To do this, an estimate of base flow at the location where the river enters the AMA would be necessary, which would be difficult because a continuous station is not located at or near this model inflow point (southern tip of model), as is the case for the other large rivers. Next, the watershed area outside the AMA that contributes to the river reach between this inflow point and the station would be needed, which would depend on an accurate estimate of streamflow at the inflow point. Finally, because of the location of the station, calibrating the model to the station would affect only a small area at the southern tip of the model. Given these disadvantages, calibrating to this station would not add enough value to justify its inclusion.

Calibration Parameters for Steady State

Model calibration consisted of adjusting model parameters with the aim of reducing the differences, or residuals, between calibration targets and simulated values. The steady-state model version was calibrated by a combination of automatic and manual calibration through numerous trials during the calibration process. Preliminary manual calibration was applied prior to adding pilot points by adjusting uniform values K_h and K_h/K_v values to each layer. After pilot points were added, preliminary automatic calibration with Model-Independent Parameter Estimation (PEST) (Doherty, 2018) was applied. PEST calibration is an iterative process that aims to minimize an objective function: the sum of the squared and weighted residuals (Doherty, 2015). Additional pilot points and other parameters were added as needed. For example, zones of streambed hydraulic conductivity were added as needed to allow more heterogeneity of streambed material. Once the model was adequately parameterized, automatic calibration was re-applied for final calibration.

The steady-state model version contains 1,444 calibrated parameters, consisting of 6 parameters for the Drain Package, 5 for the GHB Package, 1 for the Recharge Package, 1,024 for the SFR Package, and 408 pilot points. Each of the 1,448 parameters was assigned to 1 of 73 groups for purposes of discussion or to treat a group of parameters as one element during model calibration. The group name, description, and number of parameters in each group is shown in table D8. Appendix 1, table 1.12 lists each parameter individually, along with calibration settings for each parameter. Each parameter represents a property that is applied to a model cell or zone. For example, the parameter, $ghc1$, is the vertical conductance for all cells that represent the lakebed for American Lake.

Table D8. Parameter groups for the steady-state model version, near the southeastern part of Puget Sound, Washington.

[See table D2 for description and figure D1 for location of hydrogeologic units (HGU)s. **MODFLOW package:** GHB, General-Head Boundary; SFR, Streamflow-Routing; UPW, Upstream Weighting. **Parameter type:** K, hydraulic conductivity; Kh, horizontal hydraulic conductivity; Kh/Kv, ratio of horizontal to vertical hydraulic conductivity. **Units:** ft²/d, foot per day; ft²/d, foot squared per day. **Description:** R, River, St, Street]

Parameter group	Number of parameters in group	MODFLOW package	Parameter type	Units	Description	Sensitivity metric (τ), equation D-8
dr1	1	Drain Package	Conductance	ft ² /d	River bluffs in HGU A3	1.93
dr2	1	Drain Package	Conductance	ft ² /d	River bluffs in HGU C	3.64
dr3	1	Drain Package	Conductance	ft ² /d	Lower Puyallup River alluvium	0.30
dr4	1	Drain Package	Conductance	ft ² /d	Puyallup River alluvium above main bridge	0.95
dr5	1	Drain Package	Conductance	ft ² /d	Outcrop of HGU A2	0.28
dr6	1	Drain Package	Conductance	ft ² /d	Outcrop of HGU MFLU	0.40
rm0	1	Recharge Package	Recharge multiplier	Dimensionless	Entire model area	194.9
ghc1	1	GHB Package	Conductance	ft ² /d	American Lake	0.24
ghc3	1	GHB Package	Conductance	ft ² /d	Steilacoom Lake	0.41
ghc4	1	GHB Package	Conductance	ft ² /d	Spanaway Lake	0.18
ghc5	1	GHB Package	Conductance	ft ² /d	Lake Tapps	7.02
ghc6	1	GHB Package	Conductance	ft ² /d	Puget Sound	2.92
st159	11	SFR Package	Vertical K	ft/d	American Lake area	0.31
st883	41	SFR Package	Vertical K	ft/d	Big Soos Creek above hatchery	0.51
st312	14	SFR Package	Vertical K	ft/d	Boise Creek near Buckley	1.25
st205	10	SFR Package	Vertical K	ft/d	Chambers Creek below Leach Creek	0.33
st584	27	SFR Package	Vertical K	ft/d	Clarks Creek Tacoma	0.76
st177	24	SFR Package	Vertical K	ft/d	Clover Creek Tillicum	0.76
st1024	1	SFR Package	Vertical K	ft/d	Diversion to Lake Tapps	6.45
st214	3	SFR Package	Vertical K	ft/d	Flett Creek Tacoma	0.46
st924	73	SFR Package	Vertical K	ft/d	Green River 200th St	0.21
st820	41	SFR Package	Vertical K	ft/d	Green River Auburn	5.76
st223	1	SFR Package	Vertical K	ft/d	Leach Creek Steilacoom	0.30
st999	1	SFR Package	Vertical K	ft/d	Mill Creek at Earthworks	0.31
st1000	21	SFR Package	Vertical K	ft/d	Mill Creek near mouth	0.11
st815	29	SFR Package	Vertical K	ft/d	Newaukum Creek at Black Diamond	2.23

Table D8. Parameter groups for the steady-state model version, near the southeastern part of Puget Sound, Washington.—Continued

[See table D2 for description and figure D1 for location of hydrogeologic units (HGU)s. **MODFLOW package:** GHB, General-Head Boundary; SFR, Streamflow-Routing; UPW, Upstream Weighting. **Parameter type:** K, hydraulic conductivity; Kh, horizontal hydraulic conductivity; Kh/Kv, ratio of horizontal to vertical hydraulic conductivity. **Units:** ft/d, foot per day; F²/d, foot squared per day. **Description:** R, River; St, Street]

Parameter group	Number of parameters in group	MODFLOW package	Parameter type	Units	Description	Sensitivity metric (τ), equation D-8
st187	4	SFR Package	Vertical K	ft/d	North Fork Clovers Creek Parkland	0.25
st657	56	SFR Package	Vertical K	ft/d	Puyallup River slope north	0.55
st236	25	SFR Package	Vertical K	ft/d	Puyallup River slope south	1.20
st371	39	SFR Package	Vertical K	ft/d	Puyallup River 5th St bridge 1	0.64
st377	24	SFR Package	Vertical K	ft/d	Puyallup River 5th St bridge 2	1.41
st395	7	SFR Package	Vertical K	ft/d	Puyallup River 5th St bridge 3	0.08
st443	94	SFR Package	Vertical K	ft/d	Puyallup River Alderton 1	1.92
st536	7	SFR Package	Vertical K	ft/d	Puyallup River Alderton 2	1.42
st567	4	SFR Package	Vertical K	ft/d	Puyallup River Alderton 3	0.42
st571	6	SFR Package	Vertical K	ft/d	Puyallup River main bridge	0.92
st583	13	SFR Package	Vertical K	ft/d	Puyallup River at Puyallup	0.28
st156	164	SFR Package	Vertical K	ft/d	Puget Sound outflow	0.44
st1	157	SFR Package	Vertical K	ft/d	Southern model area	2.56
st208	2	SFR Package	Vertical K	ft/d	Spanaway Creek at lake outlet	0.13
st284	41	SFR Package	Vertical K	ft/d	Southeast model area	0.21
st617	1	SFR Package	Vertical K	ft/d	Swan Creek 80th St	0.29
st637	13	SFR Package	Vertical K	ft/d	Wapato Creek	0.36
st287	25	SFR Package	Vertical K	ft/d	White River above Boise Creek	0.88
st326	17	SFR Package	Vertical K	ft/d	White River R St 1	0.52
st328	9	SFR Package	Vertical K	ft/d	White River R St 2	0.71
st352	19	SFR Package	Vertical K	ft/d	White River Auburn	0.15
Kh layer 01	3	UPW Package	Kh pilot point	ft/d	Layer 1—HGU MFLU	2.10
Kh layer 02	9	UPW Package	Kh pilot point	ft/d	Layer 2—HGU AL1	7.27
Kh layer 03	1	UPW Package	Kh pilot point	ft/d	Layer 3—HGU MFLV	1.59
Kh layer 04	3	UPW Package	Kh pilot point	ft/d	Layer 4—HGU AL2	3.89
Kh layer 05	14	UPW Package	Kh pilot point	ft/d	Layer 5—HGU A1	15.17
Kh layer 06	31	UPW Package	Kh pilot point	ft/d	Layer 6—HGU A2	32.97
Kh layer 07	35	UPW Package	Kh pilot point	ft/d	Layer 7—HGU A3	28.92

Table D8. Parameter groups for the steady-state model version, near the southeastern part of Puget Sound, Washington.—Continued

[See table D2 for description and figure D1 for location of hydrogeologic units (HGU)s. **MODFLOW package:** GHB, General-Head Boundary; SFR, Streamflow-Routing; UPW, Upstream Weighting. **Parameter type:** K, hydraulic conductivity; Kh, horizontal hydraulic conductivity; Kh/Kv, ratio of horizontal to vertical hydraulic conductivity. **Units:** ft/d, foot per day; F²/d, foot squared per day. **Description:** R, River; St, Street]

Parameter group	Number of parameters in group	MODFLOW package	Parameter type	Units	Description	Sensitivity metric (τ), equation D-8
Kh layer 08	24	UPW Package	Kh pilot point	ft/d	Layer 8—HGU B	25.53
Kh layer 09	27	UPW Package	Kh pilot point	ft/d	Layer 9—HGU C	32.55
Kh layer 10	18	UPW Package	Kh pilot point	ft/d	Layer 10—HGU D	26.61
Kh layer 11	13	UPW Package	Kh pilot point	ft/d	Layer 11—HGU E	11.05
Kh layer 12	14	UPW Package	Kh pilot point	ft/d	Layer 12—HGU F	15.57
Kh layer 13	16	UPW Package	Kh pilot point	ft/d	Layer 13—HGU G and Bedrock	20.44
Kh/Kv layer 01	3	UPW Package	Kh/Kv pilot point	Dimensionless	Layer 1—HGU MFLU	0.56
Kh/Kv layer 02	4	UPW Package	Kh/Kv pilot point	Dimensionless	Layer 2—HGU AL1	0.48
Kh/Kv layer 03	1	UPW Package	Kh/Kv pilot point	Dimensionless	Layer 3—HGU MFLV	0.76
Kh/Kv layer 04	3	UPW Package	Kh/Kv pilot point	Dimensionless	Layer 4—HGU AL2	1.96
Kh/Kv layer 05	14	UPW Package	Kh/Kv pilot point	Dimensionless	Layer 5—HGU A1	4.06
Kh/Kv layer 06	30	UPW Package	Kh/Kv pilot point	Dimensionless	Layer 6—HGU A2	30.82
Kh/Kv layer 07	33	UPW Package	Kh/Kv pilot point	Dimensionless	Layer 7—HGU A3	7.89
Kh/Kv layer 08	24	UPW Package	Kh/Kv pilot point	Dimensionless	Layer 8—HGU B	25.32
Kh/Kv layer 09	27	UPW Package	Kh/Kv pilot point	Dimensionless	Layer 9—HGU C	2.51
Kh/Kv layer 10	18	UPW Package	Kh/Kv pilot point	Dimensionless	Layer 10—HGU D	25.57
Kh/Kv layer 11	13	UPW Package	Kh/Kv pilot point	Dimensionless	Layer 11—HGU E	1.28
Kh/Kv layer 12	14	UPW Package	Kh/Kv pilot point	Dimensionless	Layer 12—HGU F	14.76
Kh/Kv layer 13	16	UPW Package	Kh/Kv pilot point	Dimensionless	Layer 13—HGU G and Bedrock	1.65

Drain and GHB Package parameters represent the vertical conductance of a spring or lakebed material. The recharge parameter (rm0) is a single multiplier applied to all steady-state and transient recharge arrays generated by the SWB Model. The multiplier was used to adjust for potential error in the SWB Model estimates and was allowed to adjust by plus or minus (\pm) 25 percent during calibration. SFR Package parameters represent the vertical hydraulic conductivity of the streambed, with one parameter assigned to each of the 1,024 SFR segments. Each SFR parameter was assigned to 1 of 35 groups, according to general location in the model area (table D8). There are 208 pilot points for Kh and 200 for Kh/Kv (408 total). Each model layer has one or more K-zones; some zones were parameterized by pilot points and Kriging, whereas others consist of uniform values (table D5). All pilot points were assigned to a parameter group according to model layer (table D8); this group designation is for descriptive purposes only and does not apply to model calibration.

Of the 1,448 parameters for the steady-state model version, 458 were adjusted by automatic calibration (app. 1, table 1.12). Adjustable parameters are those that are specified as “log” for the category “Transformation for calibration (PARTRANS)” in table 1.12, as described by (Doherty, 2018). The adjustable parameters include all parameters for the Drain and Recharge Packages and four of the five parameters for the GHB Package. The fifth parameter for the GHB Package (Lake Tapps) was adjusted manually and set as a fixed value during automatic calibration to constrain the lake’s loss to groundwater to the range estimated by Pacific Groundwater Group (1999). Parameters for the SFR Package were assigned to 35 groups by tying parameters in each group to one parameter in that group. Tied parameters have values that vary together in accordance with one adjustable parameter, which is a way to group multiple parameters that act as a single parameter during automatic calibration (Doherty, 2018). All 412 pilot points were adjustable and, therefore, set to log transformation (app. 1, table 1.12).

Calibration Target Weights

Each calibration target for the steady-state model version was assigned a weight that was applied by PEST to the corresponding residual to compute the value of the objective function. Calibration targets were assigned to calibration groups, and weights were assigned to individual targets within each group (table D9). The collective contribution to the objective function from each group was quantified (table D9) to check that a single group did not dominate the calibration and that each group’s influence on the calibration was proportional to its data quality. Steady-state target values are provided for groups Head1–Head5 (app. 1, table 1.7), Head6 (app. 1, table 1.10), Head7 (app. 1, table 1.11), and Flux (base flow, table D1).

Groups Head1–Head5 are measured water levels in wells and have weights that range from 1 to 10 (table D9). For wells with multiple measurements, the average of all values was used as the target value for that well, as described in Chapter B. Wells with many measurements provide the best representation of the average value for steady-state calibration. Most of the wells with at least 20 measurements were the same wells that were originally selected for the monthly measurement network and have accurate and reliable associated data, including locations, land-surface altitudes, geologic logs, and depths. Therefore, as the number of measurements for a well decreases, the target weight decreases.

Most of the wells in the NWIS database include an initial reported water level measured by the drilling company after well installation. These reported values were found to be inconsistent with the range of values for repeated measurements and, therefore, were not included in the calculation of average water levels for groups Head1–Head4. Group Head5 has the lowest weight because these wells have only one measurement that was reported by the drilling company.

The contribution to the objective function by target group is determined by each target’s weight and the number of targets in the group. This group contribution determines the relative influence that a target group has on the calibration process. Groups Head1–Head5 contributed 70.9 percent to the objective function value (table D9), which means that these targets had a combined relative influence of 70.9 percent on automatic calibration at the end of the calibration process. Target groups Head6, Head7, and Flux represent target categories other than water-level measurements. For these groups, weights were assigned that resulted in a total group contribution that is balanced against groups Head1–Head5 so that all groups are adequately represented in automatic calibration. Target groups Head6, Head7, and Flux contributed 14.6, 3.2, and 11.2 percent, respectively, to the objective function value (table D9). Head6 consists of the vertical hydraulic-head differences, and Head7 consists of the targets to prevent groundwater flooding. The Flux group consists of the base-flow targets, which were given weights that collectively would provide a 30 percent contribution to the objective function for the start of the calibration. As the residuals decreased during model calibration, the group contribution also decreased. Because the magnitudes of base flow in cubic feet per day are orders of magnitude larger than water levels in feet, the weight given to each target in this group was four orders of magnitude smaller than those of the other groups to adjust the total group contribution to the objective function (table D9). The group with the largest influence on the objective function was Head1, accounting for a 42.9 percent contribution to the objective function. The approach of assigning target weights with the aim of balancing the group influence on calibration is described in more detail in Anderson and others (2015).

Table D9. Calibration target groups and weights for steady-state model version, near the southeastern part of Puget Sound, Washington.[Comments: WL, water level. Abbreviation and symbol: NA, not applicable; \geq , greater than or equal to]

Target group name	Number of targets in group	Target type	Description	Weight applied to each target	Number of measurements for a single station	Comments	Group contribution to calibration objective function	Group contribution to objective function, as a percentage	Cumulative group contribution, as a percentage
Head1	278	Hydraulic head	From measured values	10	≥ 20	Excludes WL from driller	2.73×10^7	42.9	42.9
Head2	139	Hydraulic head	From measured values	9	6–10	Excludes WL from driller	4.44×10^6	7.0	49.9
Head3	91	Hydraulic head	From measured values	7	5–9	Excludes WL from driller	8.90×10^5	1.4	51.3
Head4	627	Hydraulic head	From measured values	3	1–4	Excludes WL from driller	7.83×10^6	12.3	63.6
Head5	2,857	Hydraulic head	From measured values	1	1–4	WL from driller	4.67×10^6	7.3	70.9
Head6	616	Hydraulic-head difference	From measured and estimated values	2.5	NA	Estimated values	9.32×10^6	14.6	85.6
Head7	67	Hydraulic head	Set equal to land-surface altitude ¹	15	NA	NA	2.04×10^6	3.2	88.8
Flux	27	Base flow	Estimated values	2.75×10^{-4}	Varied	NA	7.15×10^6	11.2	100.0
Total	4,702	NA	NA	NA	NA	NA	6.36×10^7	100.0	NA

¹Used in some areas to prevent simulated groundwater flooding.

Calibration Constraints

Calibration is a compromise between reducing target residuals and other constraints that must be imposed so that the model overall is as close to reality as possible and thus is useful as a simulation tool. In addition to balancing the relative influences of the different target groups, other constraints were imposed on model parameters. One constraint was that upper and lower parameter bounds were set to limit calibrated values to realistic ranges (app. 1, table 1.12). Additionally, to prevent unnecessary spatial variability and over calibration of pilot points, Tikhonov regularization (Doherty, 2015, 2018) was used to constrain the variability of pilot point values within each K-zone.

Another constraint was related to well pumping reductions that result when the simulated saturated thickness becomes thin (Niswonger and others, 2011), which was set as 10 percent of the layer thickness for this model. To prevent these pumping reductions, K-zones were added in areas where large production wells caused enough HGU drawdown to reduce simulated pumping (table D5). Hydraulic conductivities were assigned to these K-zones that were large enough to reduce drawdown and prevent pumping reductions. These Kh values were manually adjusted prior to final automatic calibration to prevent pumping reductions and were set as fixed values during final automatic calibration.

Minor adjustments were made to some of the pumping wells to minimize pumping reductions. The Well Package simulates water taken from a group of three large springs that are located west of Lake Tapps along the river bluff. Groundwater use for this group of springs is represented by six pumping wells, which are named as follows in McLean and others (2024): (1) WgpADom00114 and (2) WgpAOther00114 for the north spring, (3) WgpADom00186 and (4) WgpAOther00186 for the south spring, and (5) WgpADom00185 and (6) WgpAOther00185 for the central spring. The north and south springs are separated by 0.6 mi. These names also are used in model input files for the Well Package (Wright and others, 2023) and precise locations are given in McLean and others (2024). To prevent pumping reductions occurring for the northernmost and central springs, part of the simulated pumping for these springs was transferred to the southernmost spring, where no pumping reduction occurred. Additionally, the locations of two production wells also were placed about 500 ft (one model cell) from the original locations specified in McLean and others (2024) to mitigate pumping reductions. After final automatic calibration, the overall reduction in pumping was 3.5 percent for the steady-state model version. Because of many uncertainties in groundwater-use estimates, as described in Chapter C, this pumping reduction is within the potential error of those estimates.

Transient Calibration

All calibrated parameter values from the steady-state model version were transferred into the transient model version. Additional parameters needed for the transient model version are Ss and Sy, which were distributed spatially by applying multiple zones within each model layer, with each zone containing a uniform value of Ss and Sy. Zones were added as needed for optimum calibration, and the number of zones for each model layer varied from 1 to 13 (table D7). The Ss and Sy zones are spatially identical. PEST was not used to calibrate the transient model version because of long model run times. The transient model version was calibrated by manual adjustment of the Ss and Sy values to match the time-series records for hydraulic head in wells and base flow at streamflow stations (app. 3, figs. 3.1 and 3.2). Equal preference was given to hydraulic head and base flow for calibration. In many cases, improving calibration to hydraulic head resulted in poorer calibration to base flow, and vice versa. Therefore, compromises were made between calibration to hydraulic head and base flow. Calibrated values for Ss and Sy are summarized by HGU in table D7. Simulated values and calibration targets for hydraulic head and base flow for the transient model version are in appendix 1, table 1.6 and McLean and others (2024).

Assessment of Model Fit

Simulated and measured hydraulic-head values from appendix 1, table 1.7, for the steady-state model version are plotted for comparison (fig. D4A). The steady-state model version also was calibrated to the estimated differences in hydraulic-head values between different HGUs in the vertical direction (fig. D4A, D4B; app. 1, table 1.10). A histogram provides additional detail on the distribution of hydraulic-head residuals for the steady-state model version (fig. D5), for which 75 percent of residuals were within ± 31.6 ft. The potentiometric surface for HGU A3 generated from the steady-state model version output is shown in figure D6 and is comparable to that constructed from measured groundwater levels, as described in Chapter B (fig. B20). Additional simulated potentiometric surface maps are available in Wright and others (2023).

Bar graphs provide a comparison of estimated and simulated base-flow values for station locations. Figure D7A shows total base flow, which includes the estimated base flow that enters from outside the AMA. Figure D7B is the same as figure D7A, except that estimated base flow entering from outside the model was subtracted to show base-flow gain or loss simulated within the AMA only. Plotted data are shown in appendix 1, table 1.9.

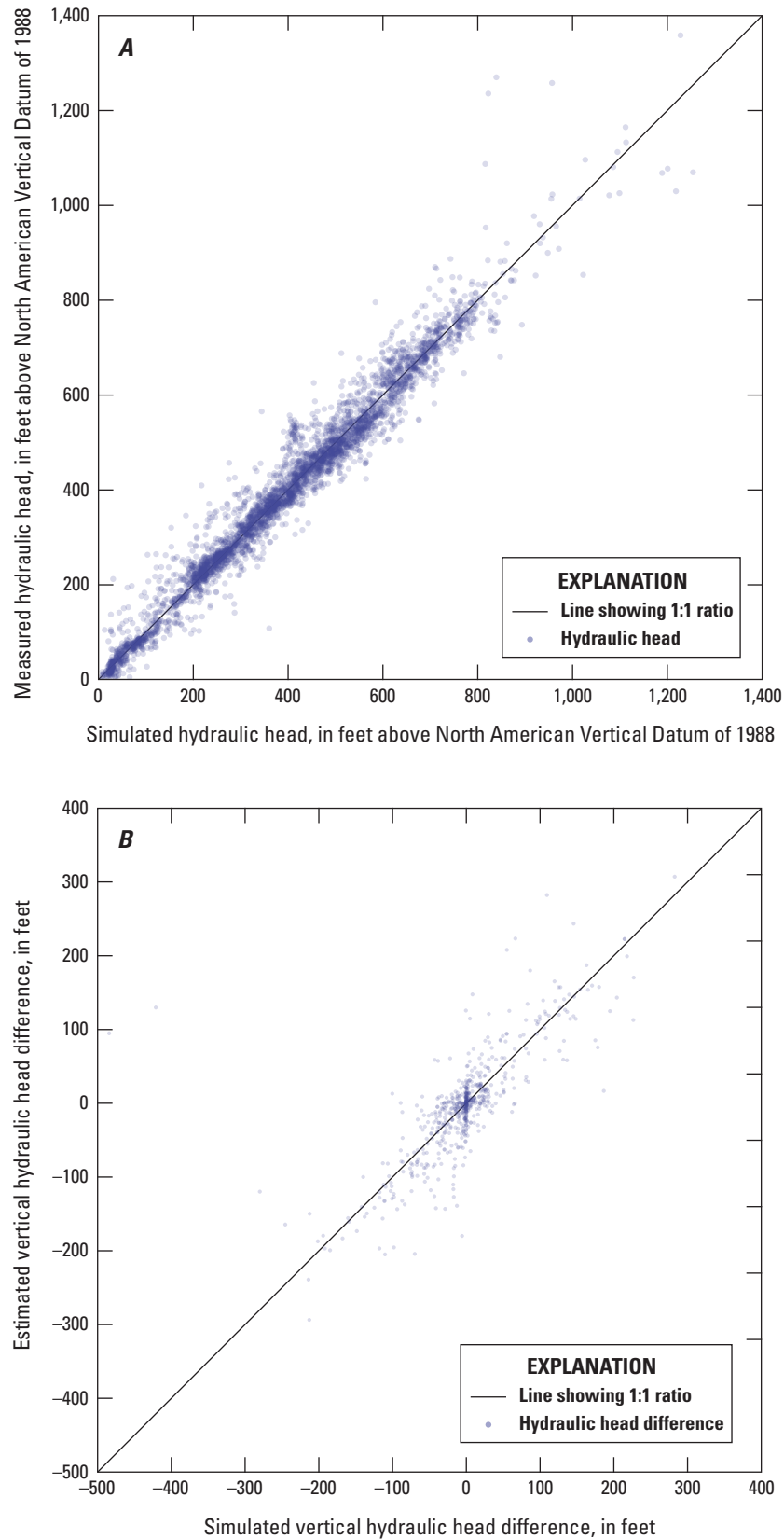


Figure D4. (A) Measured and simulated hydraulic-head values for the steady-state model version grouped by hydrogeologic unit and (B) estimated and simulated vertical hydraulic-head differences between model layers, near the southeastern part of Puget Sound, Washington. Dark shaded areas indicate high density of points.

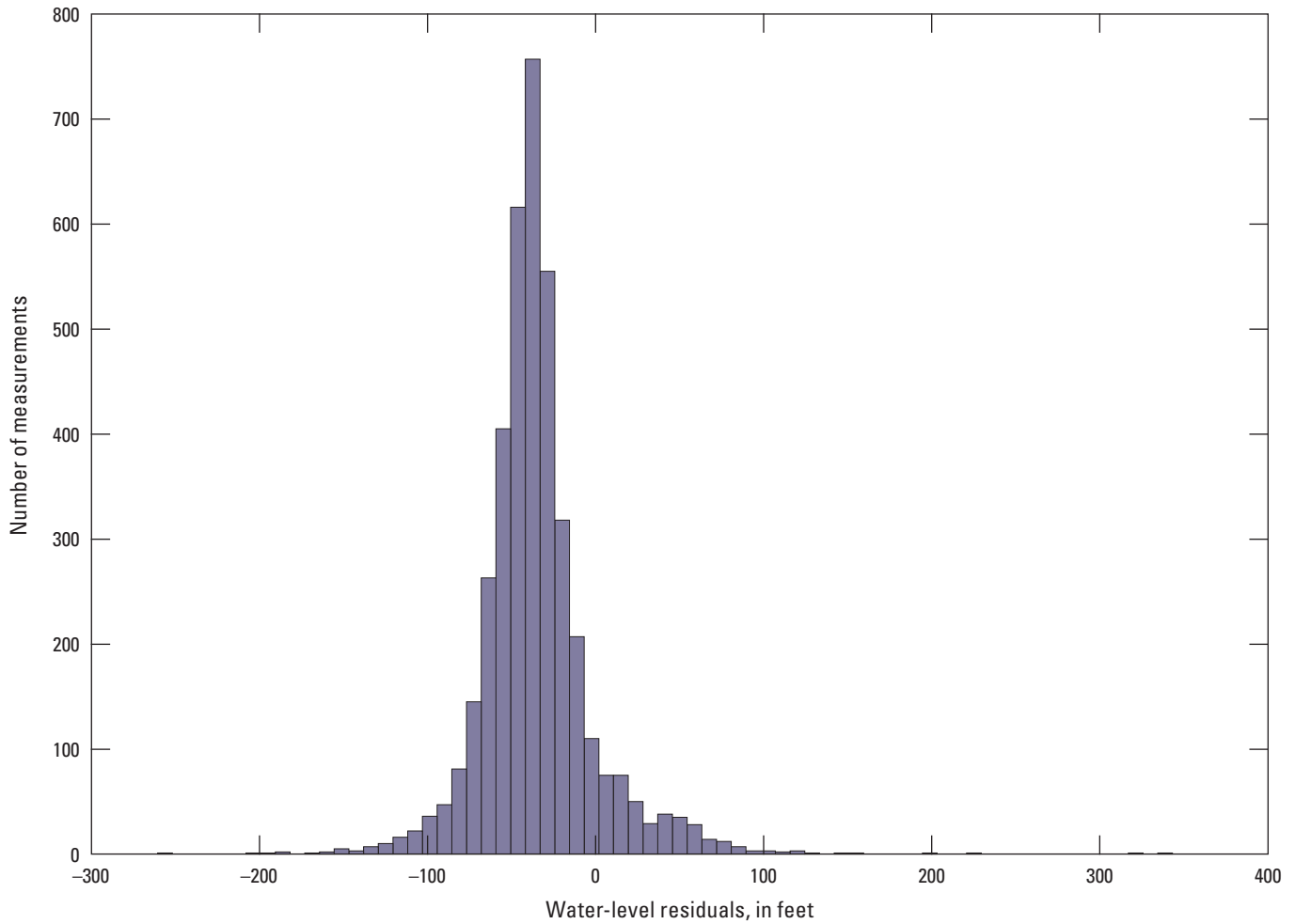


Figure D5. Hydraulic-head residuals for the steady-state model version, near the southeastern part of Puget Sound, Washington.

Calibration fitting metrics quantify the comparison of simulated values to target values (table D10). The mean of residuals indicates model bias (eq. D5), where a positive mean indicates that target values are higher than simulated values. The mean of residuals was slightly positive for the hydraulic head and base flow for the steady-state and transient model versions.

The mean absolute error is the average of the absolute values of all residuals (eq. D6). The root mean square error (RMSE, eq. D7) is a common metric that weights large residuals and generally is larger than the mean absolute error (Legates and McCabe, 1999). A useful way to evaluate the magnitudes of residuals in comparison to other models is by comparing the residuals to the overall range of targets, which is shown visually in figure D4A by the general scatter of residuals surrounding the 1:1 line. The range and mean of residuals generally are proportional to the range of target values. For example, a model simulating steep hydraulic gradients and a large range of target values likely will result in large residuals compared to a model with a small range of target values. Therefore, one way to evaluate residuals is to calculate the mean absolute error as a fraction of the target range (table D10), which preferably is less than about

5 percent. A similar comparison was made by Long and Putnam (2010). This metric does not exceed 2.0 percent for hydraulic-head residuals and is less than 1.0 percent for base-flow residuals.

$$\text{mean of residuals} = \frac{h_{tar} - h_{sim}}{n} \quad (D5)$$

$$\text{mean absolute error} = \frac{|h_{tar} - h_{sim}|}{n} \quad (D6)$$

$$RMSE = \sqrt{\sum \left[\frac{(h_{tar} - h_{sim})^2}{n} \right]} \quad (D7)$$

where

h_{tar} is the calibration target value,

h_{sim} is the simulated value,

n is the number of targets, and

$RMSE$ is root mean square error.

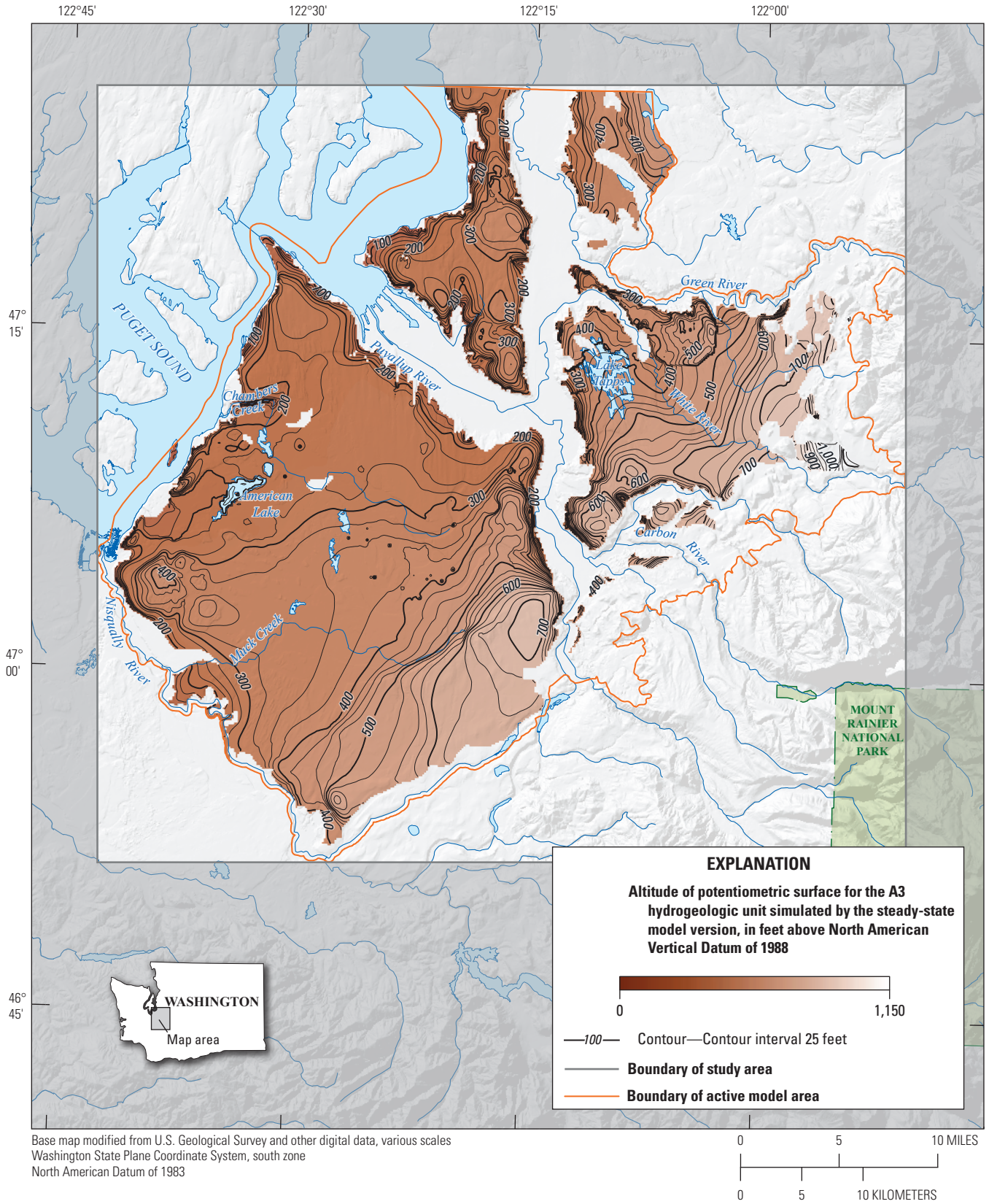


Figure D6. Potentiometric surface for hydrogeologic unit A3 simulated by the steady-state model version, near the southeastern part of Puget Sound, Washington.

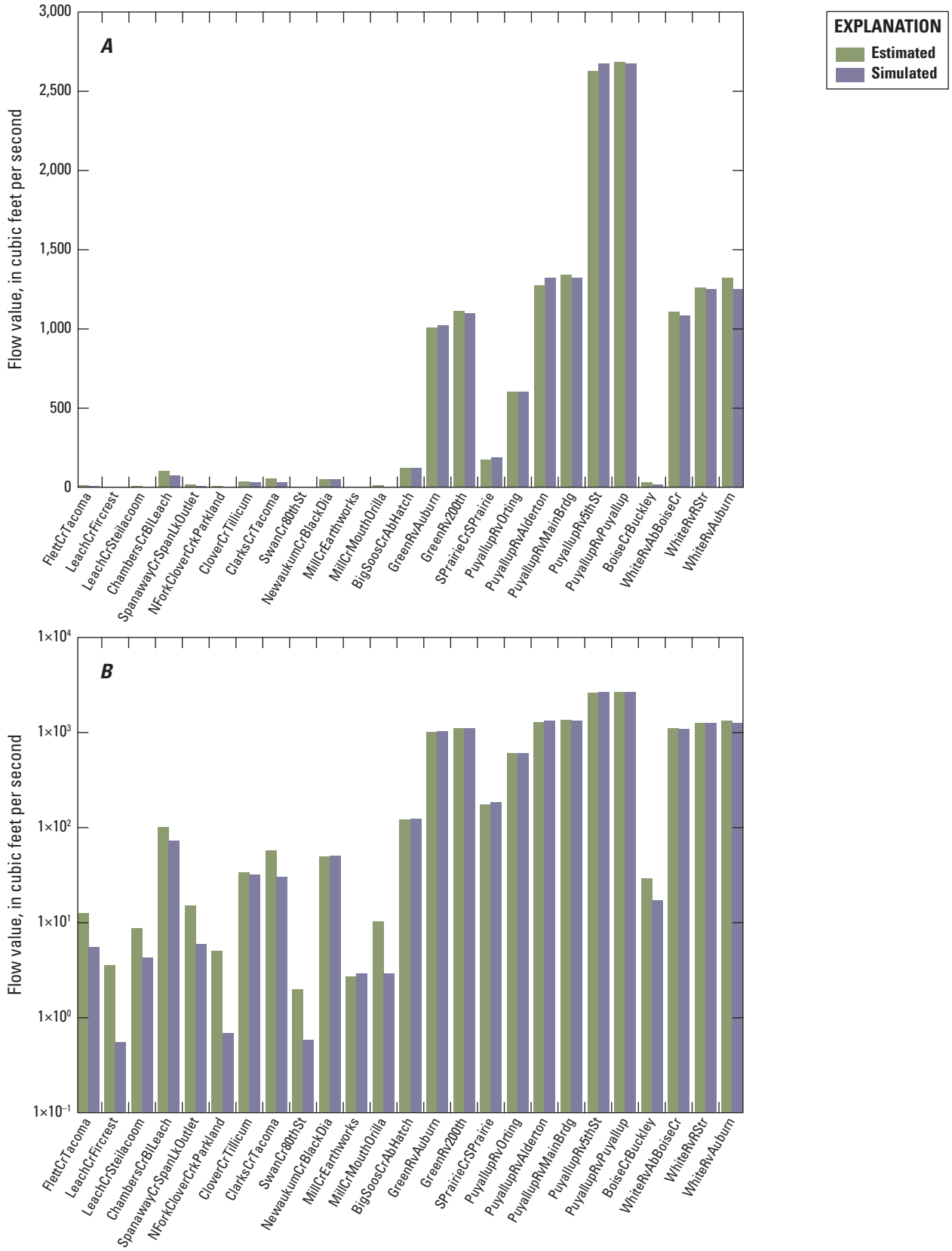


Figure D7. Estimated and simulated base flow for station locations for the steady-state model version, near the southeastern part of Puget Sound, Washington. *A.* Total base flow including estimated base flow for streams entering from outside the active model area. *B.* Same as *A*, except with a log scale to better show small flows. *C.* Base flow that is simulated within the active model area only (linear scale). [See [table D1](#) for full station names.]

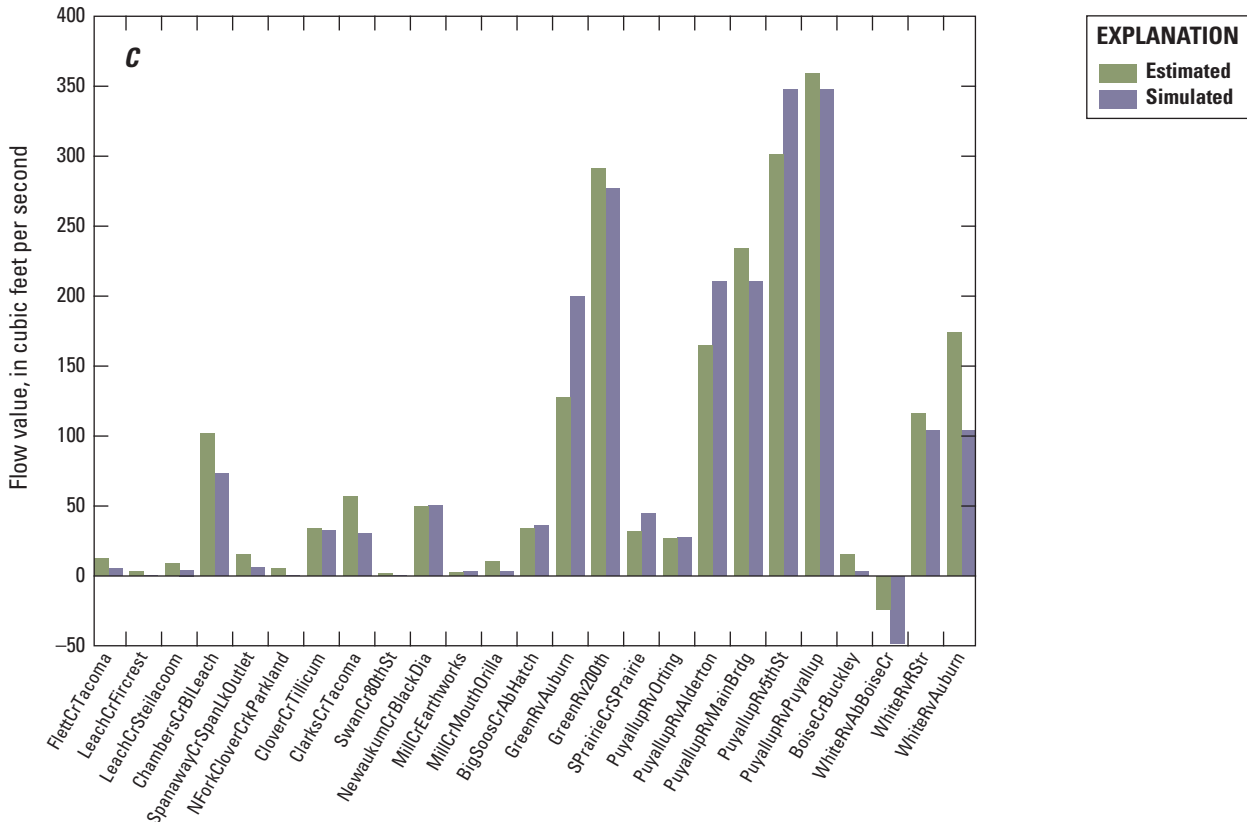


Figure D7.—Continued

The steady-state model version simulated dry cells in 2.4 percent of the cells containing hydraulic-head targets. Most of these cells are in areas where the simulated potentiometric surface is steep and difficult to calibrate to, such as along the river bluffs. Improved understanding of hydrogeologic properties, structure, heterogeneity, and connectivity along steep river bluffs, which most certainly is simplified in this model, would result in a better model for these areas. Other factors include the model's simplified representation of the complex interconnection of HGUs below these bluffs, where valley-fill materials are in contact with other HGUs.

Overcalibration of a model occurs when little or no constraints on parameter values are applied, which can result in unnecessary and unrealistic heterogeneity of HGU properties. Heterogeneity of hydraulic conductivity was limited by the density of pilot points. The model included a total of 216 and 192 pilot points for Kh and Kh/Kv, respectively. Limiting the number of pilot points serves two purposes: (1) limiting heterogeneity and helping prevent overcalibration and (2) reducing calibration run times. The result is that calibration targets are not matched as well as would be possible with a greater density of pilot points, but this compromise was considered appropriate.

Calibration results for the transient model version are shown in appendix 3 as hydrographs of simulated values and calibration targets for hydraulic head (fig. 3.1). The simulated

temporal changes in hydraulic head generally matched measured values well, even when the overall differences were large. Four of the 273 wells used in calibration of the transient model version (1.4 percent) were in areas of the model with dry cells and, therefore, were not plotted (o47, o49, o71, o74).

Simulated and estimated base flow for each station location consists of the base-flow gain that occurs within the AMA plus any additional base flow that enters streams from outside this area total base flow; fig. 3.2). This total base flow is plotted for all stations. For stations that include base flow from outside the AMA, a second plot was generated that shows only the base-flow gain occurring within the AMA. Many of the latter plots show that simulated flows do not track with the temporal changes in estimated flows as well those shown in the plots of total base flow. Not only is the base-flow-estimation method not accurate, as described in section, "Calibration Targets," but estimating base flow at locations entering the AMA is even less accurate because most of these locations do not have stations. The base-flow gain was determined by subtracting the upstream base flow from base flow at the station, compounding both sources of error. Therefore, it is unclear whether the estimated or simulated values provide better estimates of the base-flow gain in many cases.

Table D10. Model-calibration fitting metrics, near the southeastern part of Puget Sound, Washington.

[Description: RMSE, root mean square error. Units: ft, foot; ft³/s, cubic foot per second; NA, not applicable]

Description	Category	Value	Units
Steady-state model hydraulic-head targets			
Mean absolute error	Hydraulic head	25.0	ft
Mean of residuals ¹	Hydraulic head	2.4	ft
RMSE	Hydraulic head	38.6	ft
Minimum target value	Hydraulic head	-2.7	ft
Maximum target value	Hydraulic head	1,359	ft
Number of targets	Hydraulic head	3,992	NA
Number of wells with targets	Hydraulic head	3,992	NA
Mean absolute error as a fraction of the range	Hydraulic head	1.8	Percentage
Transient model hydraulic-head targets			
Mean absolute error	Hydraulic head	20.2	ft
Mean of residuals ¹	Hydraulic head	4.0	ft
RMSE	Hydraulic head	31.0	ft
Minimum value of targets	Hydraulic head	-5.1	ft
Maximum value of targets	Hydraulic head	1,114	ft
Number of targets	Hydraulic head	10,047	NA
Number of wells with targets	Hydraulic head	273	NA
Mean absolute error as a fraction of the range	Hydraulic head	1.8	Percentage
Steady-state model base-flow targets ²			
Mean absolute error	Base flow	15.1	ft ³ /s
Mean of residuals ¹	Base flow	3.5	ft ³ /s
RMSE	Base flow	23.4	ft ³ /s
Minimum target value	Base flow	2.0	ft ³ /s
Maximum target value	Base flow	2,681	ft ³ /s
Number of targets	Base flow	25	NA
Mean absolute error as a fraction of the range	Base flow	0.6	Percentage
Transient model base-flow targets ²			
Mean absolute error	Base flow	42.8	ft ³ /s
Mean of residuals ¹	Base flow	9.2	ft ³ /s
RMSE	Base flow	107.0	ft ³ /s
Minimum target value	Base flow	0.0	ft ³ /s
Maximum target value	Base flow	5,937	ft ³ /s
Number of targets	Base flow	2,746	NA
Mean absolute error as a fraction of the range	Base flow	0.7	Percentage

¹The residual is equal to the target (observed or estimated) value minus the simulated value.

²Excludes stations not used in calibration: two that coincide with specified inflows for the Green and White Rivers (stations 12106700 and 12097850) and the Nisqually River (station 12089500).

Sensitivity Analysis

A sensitivity analysis was applied to groups of parameters for the steady-state model version, in which parameters were varied by group, and a sensitivity metric (τ) was calculated for each parameter group, as described by

$$\tau = \sqrt{\sum_{i=1}^{N_{obs}} [w(O_{base,i} - O_{varied,i})]^2} \quad (D8)$$

where

- τ is the dimensionless sensitivity metric,
- \sum is a summation over the number of observations,
- N_{obs} is the number of observations,
- W represents the observation weights,

$O_{base,i}$ represents an observed value from the simulation with no parameter value change, and

$O_{varied,i}$ represents an observed value from the simulation with a varied parameter value.

The value of τ was plotted for each parameter group described in table D8 to summarize the relative sensitivities of target residuals to each parameter group (fig. D8). To assess the sensitivity of a parameter group, all parameters in that group were increased by 1 percent, and the outcome was compared with the outcome with no change in parameter values.

The highest sensitivity is for the recharge multiplier (rm0) because this parameter affects the recharge rate in every part of the model and, therefore, every calibration target. Other highly sensitive parameter groups (τ greater than 10) are those containing Kh and Kh/Kv parameters (fig. D8). Overall, Kh is more sensitive than Kh/Kv. Sensitivities for Kh in layers 5–13

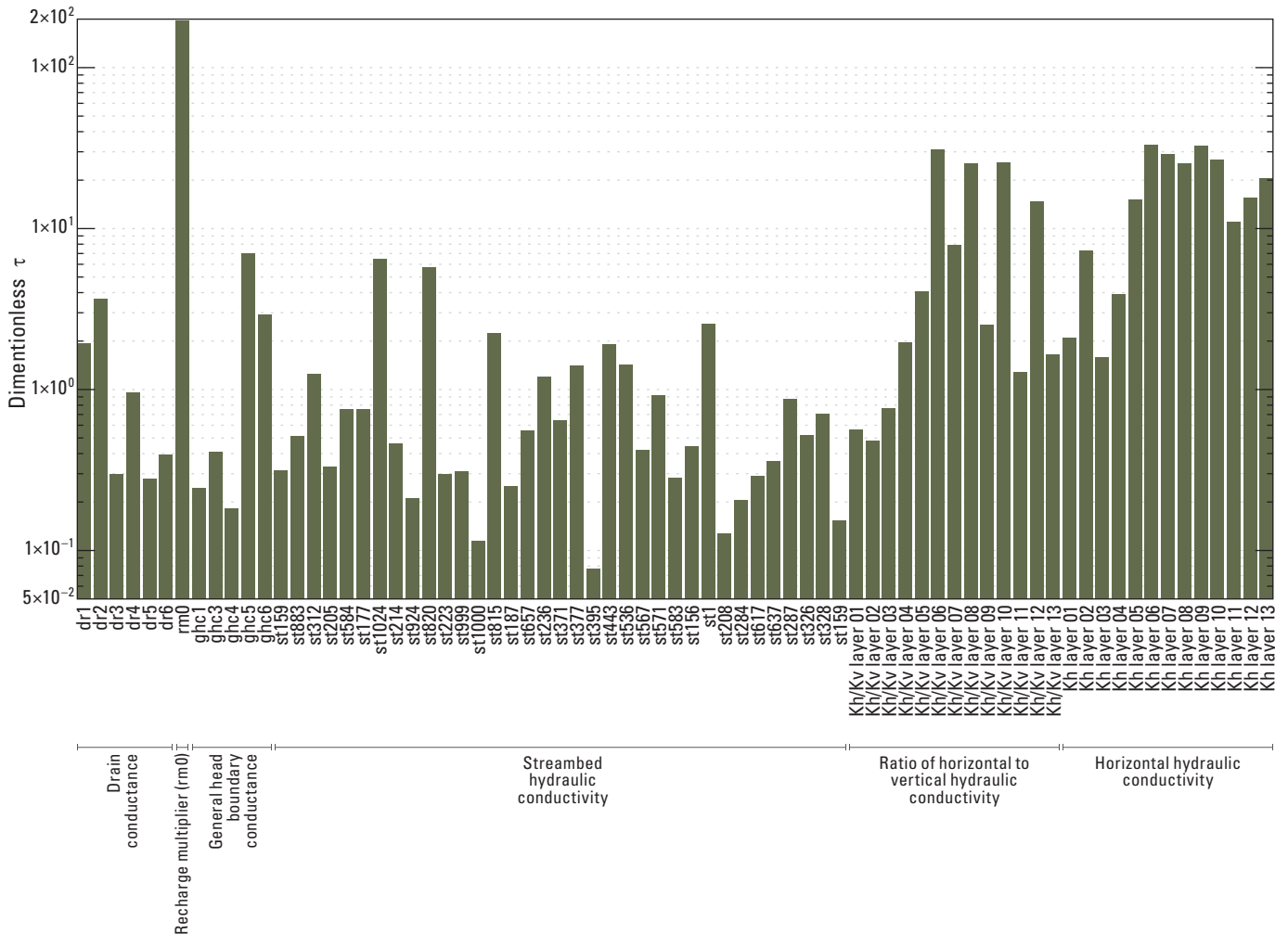


Figure D8. Model sensitivity for the steady-state model version by parameter group (see table D8), as represented by the sensitivity metric, τ (eq. D8), near the southeastern part of Puget Sound, Washington.

are all greater than $\tau = 10$. Parameter groups for Kh/Kv in layers 6, 8, 10, and 12 (confining units in layers 6 and below) also have values of τ greater than 10, with markedly higher sensitivity than for all HGU layers, indicating the importance of vertical hydraulic conductivity of confining layers in model function.

The highest drain-conductance sensitivities are for parameter groups dr1 and dr2 (River bluffs in HGUs A3 and C, respectively; [fig. D8](#); [table D8](#)). For streambed hydraulic conductivity, the highest sensitivities are for parameter groups st1024, st820, st815, and st1 (Diversion to Lake Tapps, Green River Auburn, Newaukum Creek at Black Diamond, and Southern model area, respectively). For GHB parameter groups, the highest sensitivities are for ghc5 and ghc6 (bed conductance for Lake Tapps and Puget Sound, respectively). For further discussion of parameter sensitivities and interpretation thereof, see Chapter E, section, “[Model Limitations and Potential Refinements](#).”

References Cited

- Anderson, M.P., Woessner, W.W., and Hunt, R.J., 2015, Applied groundwater modeling—Simulation of Flow and advective transport (2nd ed.): San Diego, Elsevier, 630 p.
- Aspect Consulting, LLC., 2009, Technical memorandum—Modeling analyses for Fort Lewis Sequelitchew Springs and Lake area: Seattle, Washington, Aspect Consulting, LLC Project No. 040001-012, accessed November 30, 2020, at <https://www.slideshare.net/sequelitchew/modeling-analyses-for-fort-lewis-jblm-drinking-water-system-aspect-2009>.
- Brown and Caldwell, 2016, Spanaway Lake management plan characterization memorandum: Seattle, Washington, Brown and Caldwell, accessed November 30, 2020, at <https://www.co.pierce.wa.us/Archive/ViewFile/Item/5118>. (Underlying data were provided directly by the Pierce Conservation District, Puyallup, Washington.)
- Doherty, J., 2015, Calibration and uncertainty analysis for complex environmental models: Brisbane, Australia, Watermark Numerical Computing, 227 p., accessed September 16, 2020, at <https://pesthompage.org/pest-book>.
- Doherty, J., 2018, PEST—Model-independent parameter estimation, User manual part I—PEST, SENSAN and Global Optimisers (7th ed.): Brisbane, Australia, Watermark Numerical Computing, 368 p., accessed September 16, 2020, at <https://pesthompage.org/documentation>.
- Gendaszek, A., 2023, Soil water balance model of the Puyallup and Chambers-Clover Basins, western Washington: U.S. Geological Survey data release, accessed March 15, 2023, at <https://doi.org/10.5066/P925FHGQ>.
- Harbaugh, A.W., 2005, MODFLOW-2005, The U.S. Geological Survey modular ground-water model—The ground-water flow process: U.S. Geological Survey Techniques and Methods, book 6, chap. A16 [variously paged].
- Harbaugh, A.W., and Hill, M.C., 2009, Observations in MODFLOW-2005: U.S. Geological Survey, 32 p., accessed January 8, 2021, at <https://water.usgs.gov/ogw/modflow-nwt/MODFLOW-NWT-Guide/OBS.pdf>.
- Langevin, C.D., Hughes, J.D., Banta, E.R., and Niswonger, R.G., Panday, Sorab, and Provost, A.M., 2017, Documentation for the MODFLOW 6 groundwater flow model: U.S. Geological Survey Techniques and Methods, book 6, chap. A55, 197 p., accessed November 30, 2020, at <https://doi.org/10.3133/tm6A55>.
- Legates, D.R., and McCabe, G.J., Jr., 1999, Evaluating the use of “goodness-of-fit” measures in hydrologic and hydroclimatic model validation: Water Resources Research, v. 35, no. 1, p. 233–241.
- Long, A.J., and Putnam, L.D., 2010, Simulated groundwater flow in the Ogallala and Arikaree aquifers, Rosebud Indian Reservation area, South Dakota—Revisions with data through water year 2008 and simulations of potential future scenarios: U.S. Geological Survey Scientific Investigations Report 2010–5105, 64 p.
- McLean, J.E., Welch, W.B., and Long, A.J., 2024, Spatial data in support of the characterization of water resources near the southeastern part of Puget Sound, Washington: U.S. Geological Survey data release, <https://doi.org/10.5066/P9JFKLMG>.
- Magirl, C.S., and Olsen, T.D., 2009, Navigability potential of Washington rivers and streams determined with hydraulic geometry and a geographic information system: U.S. Geological Survey Scientific Investigations Report 2009–5122, 22 p.
- National Oceanic and Atmospheric Administration, 2021, Tides and currents—Datums for 9446484, Tacoma WA: National Oceanic and Atmospheric Administration database, accessed January 7, 2021, at <https://tidesandcurrents.noaa.gov/datums.html?id=9446484>.
- Niswonger, R.G., Panday, S. and Ibaraki, M., 2011, MODFLOW-NWT, A Newton formulation for MODFLOW-2005: U.S. Geological Survey Techniques and Methods, book 6, chap. A37, 44 p.
- Pacific Groundwater Group, 1999, 1999 hydrogeologic characterization, City of Auburn: Prepared for the City of Auburn Department of Public Works Water Utility Engineering by Pacific Groundwater Group, Seattle, Washington, 91 p.

- Pierce County, 2017, Final Spanaway Lake watershed-scale stormwater management plan: Pierce County, Washington, [variously paged], accessed November 30, 2020, at <https://www.co.pierce.wa.us/Archive.aspx?AMID=389>.
- Puget Sound Lidar Consortium, 2011, Puget Sound lidar supermosaic: Puget Sound Lidar Consortium web page, accessed May 1, 2018, at <http://pugetsoundlidar.ess.washington.edu/lidardata/restricted/filegeodatabase/supermosaic/index.html>.
- Prudic, D.E., Konikow, L.F., and Banta, E.R., 2004, A new streamflow-routing (SFR1) package to simulate stream-aquifer interaction with MODFLOW-2000: U.S. Geological Survey Open-File Report 2004–1042, 104 p., accessed January 8, 2021, at <https://doi.org/10.3133/ofr20041042>.
- Sloto, R.A., and Crouse, M.Y., 1996, HYSEP—A computer program for streamflow hydrograph separation and analysis: U.S. Geological Survey Water-Resources Investigations Report 96–4040, 46 p.
- U.S. Environmental Protection Agency, 2020, NHD Plus (National Hydrography Dataset Plus): U.S. Environmental Protection Agency database, accessed November 30, 2020, at <https://www.epa.gov/waterdata/nhdplus-national-hydrography-dataset-plus>.
- U.S. Geological Survey, 2020, National Water Information System: U.S. Geological Survey National Water Information System web interface, <http://dx.doi.org/10.5066/F7P55KJN>, accessed July 1, 2020, at <https://waterdata.usgs.gov/nwis>.
- U.S. Geological Survey, 2021, StreamStats (ver. 4.4.0): U.S. Geological Survey web page, accessed January 8, 2021, at <https://streamstats.usgs.gov/ss/>.
- Van Heeswijk, M., and Smith, D.T., 2002, Simulation of the ground-water flow system at Naval Submarine Base Bangor and vicinity, Kitsap County, Washington: U.S. Geological Survey Water-Resources Investigations Report 2002–4261, 142 p., accessed January 7, 2021, at <https://doi.org/10.3133/wri024261>.
- Washington Lidar Portal, 2011, LiDAR data acquisition and processing—Pierce County, Washington Delivery 21: Washington State Department of Natural Resources web page, accessed December 13, 2011, at <https://lidarportal.dnr.wa.gov/>.
- Welch, W.B., Bright, V.A.L., Gendaszek, A.S., Dunn, S.B., Headman, A.O., and Fasser, E.T., 2024, Conceptual hydrogeologic framework and groundwater budget near the southeastern part of Puget Sound, Washington, chap. A–C of Welch, W.B., and Long, A.J., eds., Characterization of groundwater resources near the southeastern part of Puget Sound, Washington: U.S. Geological Survey Scientific Investigations Report 2024–5026–A–C, 71 p., 1 pl., <https://doi.org/10.3133/sir20245026v1>.
- Westenbroek, S.M., Kelson, V.A., Dripps, W.R., Hunt, R.J., and Bradbury, K.R., 2010, SWB—A modified Thornthwaite-Mather soil-water-balance code for estimating groundwater recharge: U.S. Geological Survey Techniques and Methods, book 6, chap. A31, 60 p., accessed November 30, 2020 at <https://doi.org/10.3133/tm6A31>.
- Wright, E.E., Long, A.J., and Fuhrig, L.T., 2023, MODFLOW-NWT model to simulate the groundwater flow system near Puget Sound, Pierce and King Counties, Washington: U.S. Geological Survey data release, accessed March 1, 2023, at <https://doi.org/10.5066/P9LU1PMQ>.

Chapter E. Numerical Model Results

By Andrew J. Long, Leland T. Fuhrig, Valerie A.L. Bright, Elise E. Wright, and Andrew S. Gendaszek

Introduction

This chapter summarizes model output for groundwater budgets and the results of several hydrologic scenarios. Although only selected model outputs are presented in tables and figures in this chapter, detailed output files are available in Wright and others (2023).

Groundwater Budgets

The steady-state simulated groundwater budget is summarized by flow rate and the percentage of total inflow or outflow for each category (table E1). Precipitation recharge

accounts for 97.8 percent of total simulated inflow. Some of the water removed from the groundwater system for human use is returned to groundwater through leaking distribution pipes, sewer pipes, and septic systems. These groundwater return flows account for 1.0 percent of total inflows. The water level in Lake Tapps is higher than the underlying groundwater hydraulic head because of controlled inflows from the Buckley Diversion (table D4), resulting in groundwater recharge from the lake. This simulated recharge accounts for 1.1 percent of inflows. Streams and large springs, small springs and seeps, and submarine groundwater discharge to Puget Sound account for 67.3, 10.0, and 15.1 percent of total outflows, respectively. Groundwater use accounts for 5.7 percent of outflow, but the net, or consumptive, groundwater use when return flows are

Table E1. Simulated groundwater budget for the steady-state model version, near the southeastern part of Puget Sound, Washington.

[MODFLOW package: NA, not applicable. Simulated flow rate: acre-ft/yr, acre-feet per year; ft³/d, cubic foot per day; ft³/s, cubic foot per second]

Category	MODFLOW package	Simulated flow rate			Percentage of total
		ft ³ /d	acre-ft/yr	ft ³ /s	
Inflows					
Precipitation recharge	Recharge Package	154,802,528	1,298,017	1,791.7	97.8
Groundwater return flows	Well Package	1,624,784	13,624	18.8	1.0
Lake Tapps seepage	General-Head Boundary Package	1,706,900	14,312	19.8	1.1
Seepage from other lakes ¹	General-Head Boundary Package	144,125	1,208	1.7	0.1
Total inflow	NA	158,278,337	1,327,162	1,831.9	100
Outflows					
Streams and large springs (net outflow)	Streamflow-Routing Package	106,483,948	892,866	1,232.5	67.3
Small springs and seeps	Drain Package	15,774,770	132,271	182.6	10.0
Submarine groundwater discharge to Puget Sound (net outflow)	General-Head Boundary Package	23,843,300	199,926	276.0	15.1
Seepage to lakes ¹	General-Head Boundary Package	3,220,556	27,004	37.3	2.0
Groundwater use	Well Package	8,967,444	75,192	103.8	5.7
Total outflow	NA	158,290,018	1,327,260	1,832.1	100
Outflows minus inflows	NA	11,681	97.9	0.1	0.0

¹American Lake, Lake Youngs, Lake Kapowsin, Steilacoom Lake, Spanaway Lake, and Lake Meridian.

E2 Numerical Model of the Groundwater-Flow System Near the Southeastern Part of Puget Sound, Washington

subtracted is 4.7 percent of outflow. The simulated monthly groundwater budget for the transient model version is shown in appendix 1, table 1.13.

Groundwater discharges to Puget Sound directly as submarine groundwater discharge and indirectly as base flow to rivers and streams that empty into the sound. All rivers and streams in the active model area (AMA) empty into Puget Sound. Therefore, the total simulated groundwater contribution to Puget Sound through rivers and streams is 1,233 cubic feet per second (ft³/s), which is more than four times larger than submarine groundwater discharge (276.0 ft³/s; table E1).

The average groundwater budget for 2005–15 for the AMA was estimated by Welch and others (2024, Chapter C, table C6). A comparison of the estimated groundwater budget to that of the steady-state model version shows that the percentages of total inflow or total outflow by category are similar for the two budgets (table E2). The largest difference is for well withdrawals: 7.3 percent of total outflow for the estimated budget compared with 5.7 percent for the simulated budget, as a result of simulated pumping reductions described in Chapter D (section, “Groundwater Use and Return Flow”).

The farthest right column of table E2 shows the percent difference in flow by category between the two budgets. All simulated inflow categories have higher values than estimated, including precipitation recharge, which is 25 percent higher than estimated because the calibrated recharge multiplier

is 1.25. The recharge multiplier allowed for as much as 25 percent error in the SWB recharge estimate, as described in Chapter D. Lake Tapps simulated seepage is 52 percent higher than the estimated value of 9,418 acre-feet per year (acre-ft/yr), which is about the mid-point between the upper and lower estimates of 16,228 and 2,680 acre-ft/yr reported by Pacific Groundwater Group (1999). The simulated value of 14,312 is within this range.

Total simulated outflow is 25 percent higher than estimated, which matches total simulated inflow (table E2). Net discharges to streams, springs, lakes, and Puget Sound were combined in table E2 so that a direct comparison could be made between the estimated and simulated budgets. These simulated combined discharges are 27 percent higher than those estimated, which is consistent with the increase in simulated inflows.

Scenario Simulations

Ten hydrologic scenarios, grouped into three suites, simulate variations of potential drought and water-use changes. Although useful insights may be gained from these scenarios, many other scenarios could be simulated by modifying model inputs that are available from Wright and others (2023).

Table E2. Estimated groundwater budget from Welch and others (2024, Chapter C, table C6) compared to that for the steady-state model version, near the southeastern part of Puget Sound, Washington.

[Estimated budget: Estimated groundwater budget from Welch and others (2024, Chapter C, table C6). Abbreviations: acre-ft/yr, acre-feet per year; NA, not available]

Category	Estimated budget		Simulated budget		Percent difference for simulated and estimated
	Flow rate, in acre-ft/yr	Percentage of total inflow or outflow	Flow rate, in acre-ft/yr	Percentage of total inflow or outflow	
Inflows					
Precipitation recharge	1,037,717	97.8	1,298,017	97.8	25
Groundwater return flows	13,631	1.3	13,624	1.0	-0.1
Lake Tapps seepage ¹	9,418	0.9	14,312	1.1	52
Seepage from other lakes ²	NA	NA	1,208	0.1	NA
Total inflow	1,060,766	100	1,327,162	100	25
Outflows					
Net discharge to streams, springs, lakes, and Puget Sound	982,837	92.7	1,252,068	94.3	27
Withdrawals from wells	77,929	7.3	75,192	5.7	-3.5
Total outflow	1,060,766	100	1,327,260	100	25

¹Seepage from other lakes is combined with net discharge outflows.

²American Lake, Lake Youngs, Lake Kapowsin, Steilacoom Lake, Spanaway Lake, and Lake Meridian.

Scenario 1 Suite—Drought

Scenarios 1a–1c simulate three different intensities of drought for long-term equilibrium conditions. The steady-state model version was run with 15-, 20-, and 25-percent reduction of precipitation recharge, which correspond to scenarios 1a, 1b, and 1c, respectively. Change in recharge for these scenarios ranged from -286.8 to -447.9 ft^3/s , corresponding to changes in base flow ranging from -207.7 to -352.9 ft^3/s (table E3). The change in base flow as a percentage of the change the recharge was 77.3, 78.5, and 78.8 percent for scenarios 1a, 1b, and 1c, respectively (table E3).

Scenario 1d simulated variable conditions with extended seasonal drought. The calibrated transient model version was modified to simulate 3 years of consecutive seasonal drought, defined by the months of May–September. This period was selected because this is when stream base flow is sensitive to low precipitation recharge. The estimated recharge for this 5-month period was lowest during 2007 (6.5 ft^3/s on average, or about 0.05 inches total) and was 0.42 percent of all May–September periods for 2005–15 (app. 1, table 1.13). By contrast, the driest year for 2005–15 was 2013, when recharge was 70 percent of average. Therefore, because the historical record indicates that the May–September period had a drought far more severe than the overall drought for the entire year and because May–September is a period characterized by low streamflows, these were the months selected to represent severe drought that could most affect streamflows.

The May–September period for 2007 was used as a proxy for the seasonal drought and hydrologic conditions for this period were inserted into the transient model version for the same months applied during 2009–11, replacing the original hydrologic conditions. The period 2009–11 was selected because this is a period with an average recharge rate of 1.83 ft^3/s , which is similar to the average for 2005–15 (1.92 ft^3/s ; app. 1, table 1.13).

This simulation was identical to the calibrated transient model version, except that hydrologic conditions for May–September 2009–11 were replaced with those of May–September 2007. The new hydrologic conditions applied for these months consisted of precipitation recharge, specified streamflow, groundwater use, and lake levels (Recharge, Streamflow-Routing [SFR], Well, and General-Head Boundary [GHB] Packages). Differences between August base flow simulated for scenario 1d and the calibrated transient model version are shown in table E4, where negative numbers indicate decreases for the scenario. Simulated base flow for August was evaluated because this commonly is when streamflow is at an annual minimum. Flow values in table E4 include simulated base-flow gains within the model area in addition to specified base flow entering from outside the model.

The change in the total simulated base-flow gain within the model area for August was compared to the change in precipitation recharge for the seasonal drought (May–September). The changes in recharge for 2009–11 ranged from -98.7 to -99.5 percent, which correspond to changes in base flow ranging from -1.8 to -13.3 ft^3/s (table E5). The change in August base flow as a percentage of the change in average recharge for May–August ranged from 10.6 to 36.0 percent for 2009–11. These flow percentages are much smaller than those of the steady-state scenarios (1a–1c), partly because high winter recharge rates provide much of the base flows that are sustained throughout the dry summers. Also, many streams are normally dry during August, which minimizes the overall base-flow reduction simulated by the scenario because simulated August flow did not change for these streams. Furthermore, these flow percentages do not account for effects of this simulated drought that continued into the post-drought years—namely, the change in base flow ranged from -12.1 to -103.1 ft^3/s for 2009–11 and from -4.2 to -15.7 ft^3/s for the post-drought period (2012–15).

Table E3. Changes in simulated steady-state base flow in the active model area for scenarios 1a, 1b, and 1c compared to the calibrated steady-state model version, near the southeastern part of Puget Sound, Washington.

[Negative numbers indicate a decrease for the scenario. Units: ft^3/s , cubic foot per second]

Description	Units	Scenario		
		1a	1b	1c
Percent change in recharge	Percent	-15.0	-20.0	-25.0
Percent change in average simulated base flow for all streams and springs ¹	Percent	-16.6	-22.5	-28.3
Change in recharge	ft^3/s	-268.8	-358.3	-447.9
Change in average simulated base flow for all streams and springs ¹	ft^3/s	-207.7	-281.3	-352.9
Change in base flow as a percentage of the change in recharge	Percent	77.3	78.5	78.8

¹The change in total base flow is equivalent to the change in model-area base flow for these scenarios.

Table E4. Change in simulated August base flow and precipitation recharge for scenario 1d (drought) for station locations compared to the calibrated transient model version, near the southeastern part of Puget Sound, Washington.—Continued

[Negative numbers indicate a decrease for the scenario. **Change in scenario 1d total August base flow compared to the calibrated transient model version:** Total base flow consists of base flow entering from outside of the active model area, in addition to base-flow gain simulated within the model. **Abbreviations:** BL, below; CR, Creek; E, East; ID, identifier; LK, Lake; NR, near; ST, Street; WA, Washington; ft³/s, cubic foot per second]

Station ID	Calibration target name	Station name	Average August base flow for the calibrated transient version (ft ³ /s)	Change in scenario 1d total August base flow compared to the calibrated transient model version (ft ³ /s)												
				2005	2006	2007	2008	2009	2010	2011	2012	2013	2014	2015		
12102190	o4689	SWAN CREEK AT 80TH ST EAST NEAR TACOMA, WA	0.0	0.0	0.0	0.0	0.0	0.0	0.0	0.0	0.0	0.0	0.0	0.0	0.0	0.0
12095000	o4687	SOUTH PRAIRIE CREEK AT SOUTH PRAIRIE, WA	62.0	0.0	0.0	0.0	-1.0	-15.0	-14.5	-0.4	-0.2	-0.2	-0.1			
12093500	o4686	PUYALLUP RIVER NEAR ORTING, WA	491.1	0.0	0.0	0.0	-61.8	-2.2	-122.8	-0.4	-0.3	-0.2	-0.2			
12096500	o4683	PUYALLUP RIVER AT ALDERTON, WA	921.9	0.0	0.0	0.0	-130.6	-21.0	-242.0	-2.6	-1.8	-1.4	-1.1			
12096505	o4684	PUYALLUP RIVER AT E MAIN BRIDGE AT PUYALLUP, WA	924.4	0.0	0.0	0.0	-130.7	-21.2	-242.1	-2.6	-1.8	-1.4	-1.1			
12101470	o4682	PUYALLUP RIVER AT 5TH ST BRIDGE AT PUYALLUP, WA	1,794	0.0	0.0	0.0	-265.5	-138.6	-626.8	-5.0	-3.2	-2.2	-1.6			
12101500	o4685	PUYALLUP RIVER AT PUYALLUP, WA	1,794	0.0	0.0	0.0	-265.5	-138.6	-626.8	-5.0	-3.2	-2.2	-1.6			
12099600	o4667	BOISE CREEK AT BUCKLEY, WA	0.0	0.0	0.0	0.0	0.0	0.0	0.0	0.0	0.0	0.0	0.0			
12097850	o4692	WHITE RIVER BELOW CLEARWATER RIVER NR BUCKLEY, WA	749.1	0.0	0.0	0.0	-129.8	-94.2	-405.7	0.0	0.0	0.0	0.0			

Table E4. Change in simulated August base flow and precipitation recharge for scenario 1d (drought) for station locations compared to the calibrated transient model version, near the southeastern part of Puget Sound, Washington.—Continued

[Negative numbers indicate a decrease for the scenario. **Change in scenario 1d total August base flow compared to the calibrated transient model version:** Total base flow consists of base flow entering from outside of the active model area, in addition to base-flow gain simulated within the model. **Abbreviations:** BL, below; CR, Creek; E, East; ID, identifier; LK, Lake; NR, near; ST, Street; WA, Washington; ft³/s, cubic foot per second]

Station ID	Calibration target name	Station name	Average August base flow for the calibrated transient version (ft ³ /s)	Change in scenario 1d total August base flow compared to the calibrated transient model version (ft ³ /s)											
				2005	2006	2007	2008	2009	2010	2011	2012	2013	2014	2015	
12099200	o4690	WHITE RIVER ABOVE BOISE CREEK AT BUCKLEY, WA	708.0	0.0	0.0	0.0	0.0	-130.7	-150.9	-396.4	-0.8	-0.5	-0.2	-0.2	
12100490	o4691	WHITE RIVER AT R STREET NEAR AUBURN, WA	830.6	0.0	0.0	0.0	0.0	-131.2	-147.8	-397.4	-2.1	-1.2	-0.7	-0.4	
12100496	o4703	WHITE RIVER NEAR AUBURN, WA	830.0	0.0	0.0	0.0	0.0	-131.2	-147.8	-397.4	-2.1	-1.2	-0.7	-0.4	
12108500	o4679	NEWAUKUM CREEK NEAR BLACK DIAMOND, WA	13.6	0.0	0.0	0.0	0.0	-0.4	-5.1	-2.5	-0.4	-0.2	-0.1	0.0	
12112600	o4666	BIG SOOS CREEK ABOVE HATCHERY NEAR AUBURN, WA	44.4	0.0	0.0	0.0	0.0	-1.7	-11.5	-5.8	-0.3	-0.1	-0.1	0.0	
12106700	o4673	GREEN RIVER AT PURIFICATION PLANT NEAR PALMER, WA	158.1	0.0	0.0	0.0	0.0	12.5	8.8	-27.3	0.0	0.0	0.0	0.0	
12113000	o4674	GREEN RIVER NEAR AUBURN, WA	293.1	0.0	0.0	0.0	0.0	9.3	-20.3	-42.9	-1.6	-0.7	-0.4	-0.2	
12113344	o4672	GREEN RIVER AT 200TH STREET AT KENT, WA	336.7	0.0	0.0	0.0	0.0	8.9	-22.8	-46.4	-2.0	-1.0	-0.6	-0.4	
12113347	o4677	MILL CREEK AT EARTHWORKS PARK AT KENT, WA	1.5	0.0	0.0	0.0	0.0	0.0	0.0	-0.1	0.0	0.0	0.0	0.0	
12113349	o4678	MILL CREEK NEAR MOUTH AT ORILLIA, WA	1.5	0.0	0.0	0.0	0.0	0.0	0.0	-0.1	0.0	0.0	0.0	0.0	

Table E5. Change in simulated August base flow and precipitation recharge in the active model area for scenario 1d (drought) compared to the calibrated transient model version, near the southeastern part of Puget Sound, Washington.

[Negative numbers indicate a decrease. Bold numbers indicate a change from the base model. **Units:** ft³/s, cubic foot per second. **Abbreviation:** NA, not applicable]

Description	Units	2005	2006	2007	2008	2009	2010	2011	2012	2013	2014	2015
Percent change in recharge for May–August	Percent	0.0	0.0	0.0	0.0	-98.7	-99.5	-99.3	0.0	0.0	0.0	0.0
Percent change in simulated base flow at end of August for all streams and springs ¹	Percent	0.0	0.0	0.0	0.0	-1.8	-13.3	-4.9	-2.0	-1.2	-0.7	-0.6
Average recharge for May–August (base model)	ft ³ /s	117.0	57.0	1.6	38.7	116.2	288.2	232.0	185.9	12.6	190.4	7.3
Average recharge for May–August (scenario 1)	ft ³ /s	117.0	57.0	1.6	38.7	1.6	1.6	1.6	185.9	12.6	190.4	7.3
Change in simulated base flow at end of August for all streams and springs ¹	ft ³ /s	0.0	0.0	0.0	0.0	-12.1	-103.1	-39.6	-15.7	-9.0	-6.3	-4.2
Change in base flow as a percentage of the change in recharge	Percent	NA	NA	NA	NA	10.6	36.0	17.2	NA	NA	NA	NA

¹Model-area base flow consists of base-flow gain simulated within the active model area only, excluding flows entering from outside of the active model area.

Scenario 2 Suite—Elimination of Groundwater Use

The intent of scenario 2 was to estimate the overall effects of current (2005–15) groundwater use on the groundwater system. The calibrated steady-state model version was used for this scenario, with the following change: All simulated groundwater use was removed from the model, which consisted of withdrawal from public-supply systems, domestic self-supply wells, and self-supply agricultural wells and return flow from septic system returns, pipeline leakage, and domestic and agricultural irrigation. This scenario addresses the differences between current land use and land use prior to the beginning of groundwater withdrawals. The purpose and scope of this scenario is to estimate the total effects of current groundwater withdrawals under current conditions of land use, land cover, and climate.

Output from scenario 2 was compared to output from the calibrated steady-state model version and showed an increase in altitude of the simulated potentiometric surface of HGU A3. The increase was less than 10 feet (ft) throughout most of the HGU's extent but ranged from 10 to more than 100 ft in several concentrated areas (fig. E1). Areas with 10–100 ft of change represent the effects pumping on the HGU.

The simulated change in base flow for station locations was more than 15 ft³/s for the Puyallup River and Chambers Creek, more than 8 ft³/s for the White River, and more than 4 ft³/s for the Clover and Clarks Creeks (table E6). The total change in simulated base flow was 64.1 ft³/s compared with a change in groundwater use of 85 ft³/s; therefore, the change in base flow as a percentage of the change in groundwater use was 75.4 percent (table E7).

Scenario 3 Suite—Cyclic Equilibrium with Increased Groundwater Use

This scenario suite includes five variations of groundwater use (scenarios 3a–3e), all of which use the same base hydrologic conditions that repeat year after year. The purpose was to test different groundwater-use scenarios occurring during a typical annual cycle of changing monthly hydrologic conditions and assess the effects on the interaction of groundwater and surface water. All hydrologic

conditions, other than groundwater use, were identical for scenarios 3a–3e. The base hydrologic conditions consist of a 4-year period (48 stress periods), in which each of the annual cycles are identical, to achieve cyclic equilibrium. Hydrologic conditions for each annual cycle of 12 months were determined by calculating mean monthly values of model inputs for the calibrated transient model version (2005–15); these inputs consist of precipitation recharge, specified flows for the SFR Package, and lake levels specified for the GHB Package.

Scenario 3a is the baseline scenario to which the other four scenarios are compared. Water-use rates from the calibrated transient model version for 2014 were used primarily because 2014 was the most recent non-anomalous year for 2005–15 (McLean and others, 2024). Exceptions to those rates consisted of groundwater use for the City of Sumner and the Spanaway Water Company, which provided current groundwater-use rates for their water supplies (app. 1, table 1.14). These rates were assumed to be more accurate than the 2014 estimated values for representing current groundwater use and, therefore, provided a more accurate baseline for comparison to scenarios 3d and 3e, which simulated increased pumping from these wells. Scenario 3a was simulated several times, each time using the output hydraulic-head values from the previous run as initial conditions for the next run to achieve equilibrium. Station 12113344 (Green River at 200th Street at Kent, WA) was removed from the analysis because its location is 0.5 mile from a no-flow boundary, which interferes with accurate simulation of small changes in flow to SFR cells.

Except for agricultural areas, scenarios of increased water use imply increases in demand that might result from population growth. In many parts of the AMA, population growth would be associated with forest clearing. Although it could be argued that clearing forests might decrease evapotranspiration, leading to increased precipitation recharge and base flow, this relation is not well understood. For example, Perry and Jones (2017) reported that in the Pacific Northwest, streamflow in 34- to 43-year-old forest plantations was 50 percent lower than streamflow in 150- to 500-year-old forests. Therefore, an attempt to adjust for land-use and forest changes and the associated changes to recharge that might result from population growth would be a complex endeavor and is beyond the scope of these scenarios.

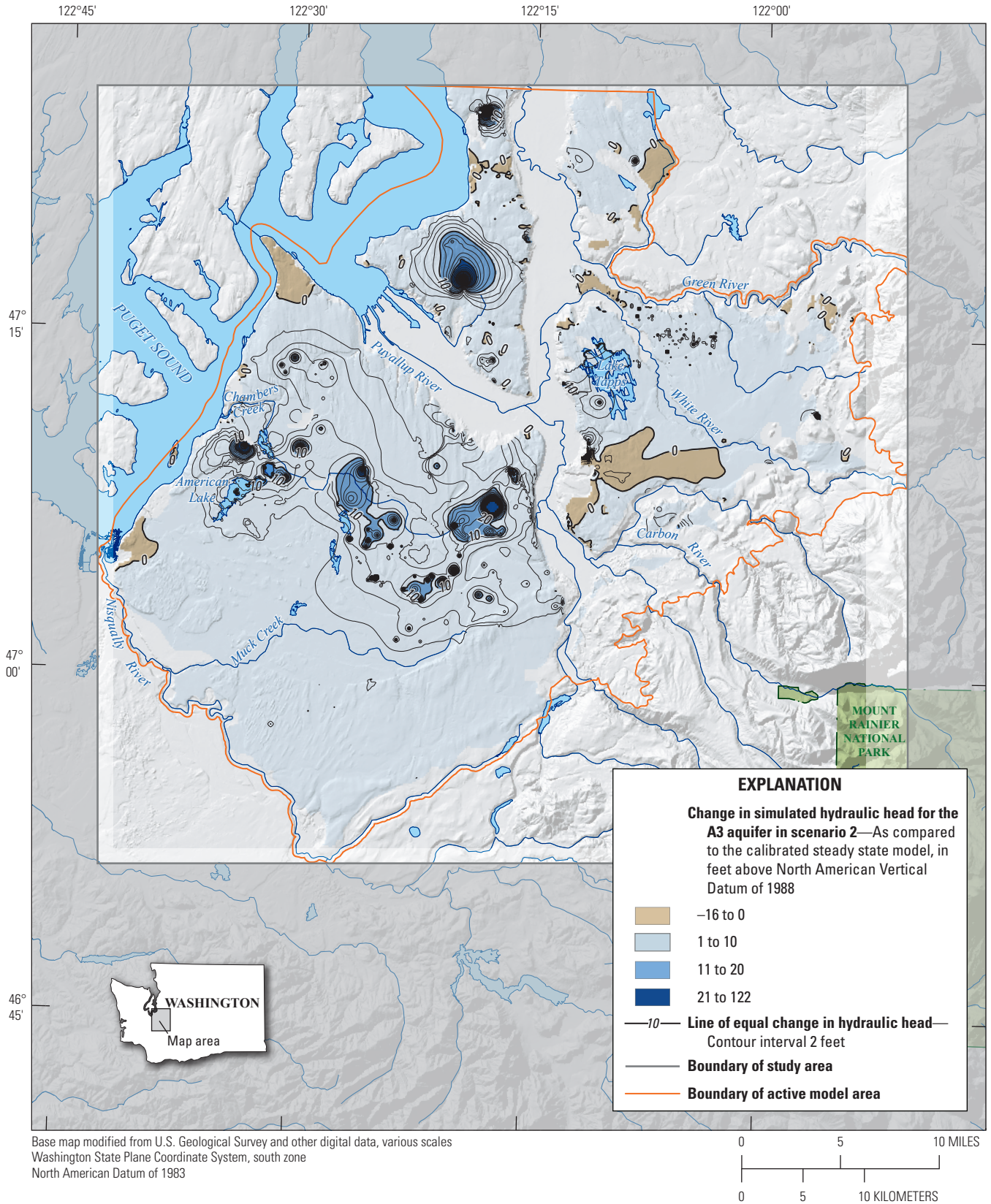


Figure E1. Change in simulated hydraulic head for hydrogeologic unit A3 resulting from scenario 2 (elimination of all human groundwater use), near the southeastern part of Puget Sound, Washington. Map shows the difference between the simulated potentiometric surface for scenario 2 and that of the calibrated steady-state model version.

E10 Numerical Model of the Groundwater-Flow System Near the Southeastern Part of Puget Sound, Washington

Table E6. Changes in simulated steady-state base flow for station locations for scenario 2 (elimination of groundwater use) compared to the calibrated steady-state model, near the southeastern part of Puget Sound, Washington.

[Positive numbers indicate an increase for the scenario. **Station name:** Station 12113344 (GREEN RIVER AT 200TH STREET AT KENT, WA) is not shown because model boundary conditions influenced results. **Change in simulated base flow:** Change in total base flow is equivalent to the change in model-area base flow for this scenario. **Abbreviations:** BL, below; CR, Creek; E, East; ID, identifier; LK, Lake; NR, near; ST, Street; WA, Washington; ft³/s, cubic foot per second]

Station ID	Calibration target name	Station name	Change in simulated base flow (ft ³ /s)
12090400	o4681	NORTH FORK CLOVER CREEK NEAR PARKLAND, WA	0.0
12090452	o4688	SPANAWAY CR AT SPANAWAY LK OUTLET NR SPANAWAY, WA	1.5
12090500	o4670	CLOVER CREEK NEAR TILLICUM, WA	6.7
12091100	o4671	FLETT CREEK AT TACOMA, WA	1.8
12091200	o4675	LEACH CREEK NEAR FIRCREST, WA	0.3
12091300	o4676	LEACH CREEK NEAR STEILACOOM, WA	0.5
12091500	o4668	CHAMBERS CREEK BL LEACH CREEK NEAR STEILACOOM, WA	15.2
12102075	o4669	CLARKS CREEK AT TACOMA ROAD NEAR PUYALLUP, WA	4.6
12102190	o4689	SWAN CREEK AT 80TH ST EAST NEAR TACOMA, WA	0.0
12095000	o4687	SOUTH PRAIRIE CREEK AT SOUTH PRAIRIE, WA	0.2
12093500	o4686	PUYALLUP RIVER NEAR ORTING, WA	0.0
12096500	o4683	PUYALLUP RIVER AT ALDERTON, WA	4.1
12096505	o4684	PUYALLUP RIVER AT E MAIN BRIDGE AT PUYALLUP, WA	4.2
12101470	o4682	PUYALLUP RIVER AT 5TH ST BRIDGE AT PUYALLUP, WA	15.1
12101500	o4685	PUYALLUP RIVER AT PUYALLUP, WA	15.1
12099600	o4667	BOISE CREEK AT BUCKLEY, WA	0.9
12097850	o4692	WHITE RIVER BELOW CLEARWATER RIVER NR BUCKLEY, WA	0.0
12099200	o4690	WHITE RIVER ABOVE BOISE CREEK AT BUCKLEY, WA	0.2
12100490	o4691	WHITE RIVER AT R STREET NEAR AUBURN, WA	8.2
12100496	o4703	WHITE RIVER NEAR AUBURN, WA	8.2
12108500	o4679	NEWAUKUM CREEK NEAR BLACK DIAMOND, WA	1.0
12112600	o4666	BIG SOOS CREEK ABOVE HATCHERY NEAR AUBURN, WA	-0.4
12106700	o4673	GREEN RIVER AT PURIFICATION PLANT NEAR PALMER, WA	0.0
12113000	o4674	GREEN RIVER NEAR AUBURN, WA	0.8
12113347	o4677	MILL CREEK AT EARTHWORKS PARK AT KENT, WA	0.2
12113349	o4678	MILL CREEK NEAR MOUTH AT ORILLIA, WA	0.2

Scenario 3b (increased public-supply groundwater use) was the same as scenario 3a with the following changes: Groundwater use (pumping) and return flows associated with Groups A and B public-supply wells were increased by 15 percent uniformly for each of these simulated features (pumping well or point of return flow) in the model. These changes resulted in an average net increase of 12.8 ft³/s specified as model input; however, the actual simulated increase was only 10.3 ft³/s because of simulated pumping reductions. Return flows consisted of recharge from pipeline leakage, lawn irrigation, public-supplied agricultural irrigation, large-onsite septic systems, and Group B septic

systems. Simulated base flow for scenario 3b was compared to that of scenario 3a, where negative numbers indicate decreases for the scenario (table E8). Decreases in simulated base flow for station locations (shown as negative values in table E8) were as large as 2.5 ft³/s for Chambers Creek during March and 1.5 ft³/s for the Puyallup River during March and April, with the smallest changes occurring during summer and autumn for most locations (table E8). Stations on Clarks and Big Soos Creeks and the Green River resulted in simulated base-flow increases of 0.1–0.2 ft³/s for some months, possibly resulting from simulated pumping reductions occurring for some wells because of increased pumping in other wells

Table E7. Change in simulated steady-state base flow in the active model area for scenario 2 (elimination of groundwater use) compared to the calibrated steady-state model, near the southeastern part of Puget Sound, Washington.[Positive numbers indicate an increase in base flow. Units: ft³/s, cubic foot per second]

Description	Units	Steady-state results	Comments
Percent change in average simulated base flow for all streams and springs ¹	Percent	5.14	Base flow increased
Percent change in average consumptive water use	Percent	-100.0	Consumptive water use decreased
Change in average simulated base flow for all streams and springs ¹	ft ³ /s	64.1	Base flow increased
Change in average consumptive water use	ft ³ /s	-85.0	Consumptive water use decreased
Change in base flow as a percentage of the change in consumptive water use	Percent	75.4	Base flow increased

¹Change in total base flow is equivalent to the change in model-area base flow for this scenario.

that resulted in reduced saturated thickness, or because of increased return flows. Base flow entering from outside the active model is the same for scenarios 3a–3e; therefore, the values in [table E8](#) are independent of these flows and represent changes for base flow within the AMA only.

Scenario 3c (increased self-supply groundwater use) was the same as scenario 3a, with the following changes: Groundwater use (pumping) for domestic and agricultural self-supply wells was increased by 15 percent, and recharge from septic systems and self-supplied agricultural irrigation was increased by the same amount. This resulted in an average net increase of 0.2 ft³/s specified as model input overall. The actual simulated increase also was 0.2 ft³/s because no simulated pumping reductions occurred. These changes were applied in the same way as for scenario 3b. Simulated base flow for this scenario was compared to that of scenario 3a. Decreases in simulated base flow for station locations were as large as 0.2 ft³/s for the Puyallup River and South Prairie Creek ([table E9](#)). Clarks Creek resulted in base flow increases of 0.1 ft³/s for some months for similar reasons to those of scenario 3b.

Scenario 3d was focused on Spanaway, which is an unincorporated, census-designated place near Spanaway Lake. This scenario was same as scenario 3a, except that groundwater use (pumping) for the Spanaway Water Company was increased overall by 67 percent (from scenario 3a), with increases applied to 10 water-supply wells. The model-specified pumping rate increased from 5.0 to 8.4 ft³/s on average, an increase of 3.4 ft³/s. The actual simulated increase was slightly less (3.3 ft³/s) because of simulated pumping reductions. The percent increases varied spatially (by well) and temporally for scenarios 3a, 3d, and 3e, as

shown in [appendix 1, table 1.14](#). Simulated base flow for scenario 3d was compared to that of scenario 3a. Changes in simulated base flow for station locations were as much as -2.4, -2.1, and -0.8 ft³/s for Chambers, Clover, and Spanaway Creeks, respectively ([table E10](#)). The smallest changes occurred during summer, which was when the smallest groundwater-use changes occurred ([app. 1, table 1.14](#)); however, a month-by-month correlation is not evident because the effects of pumping on streamflows are spread over time. Chambers Creek resulted in a base flow increase of 0.6 ft³/s for October for similar reasons to those of previous scenarios. Other increases (Puyallup River and South Prairie Creek) did not exceed 0.2 ft³/s.

Scenario 3e was the same as scenario 3a, except that groundwater use for the City of Sumner was increased overall by 103 percent (from scenario 3a), with variable increases applied to five water-supply wells ([app. 1, table 1.14](#)). The model-specified pumping rate increased from 2.4 to 4.9 ft³/s on average, an increase of 2.5 ft³/s. The actual simulated increase was only 2.3 ft³/s because of simulated pumping reductions. Simulated base flow for this scenario was compared to that of scenario 3a. Changes in simulated base flow for station locations were as much as -2.0 ft³/s for the Puyallup River ([app. 1, table E11](#)). Scenario 3e differed from the previous scenarios in that the largest changes in base flow occurred during summer, corresponding to larger pumping rate changes during summer ([app. 1, table 1.14](#)). Like scenario 3d, a month-by-month correlation for scenario 3e is not evident because of antecedent effects. Chambers and Clarks Creeks and the Puyallup and White Rivers resulted in increases in base flow of 0.1–0.2 ft³/s, each for 1 month out of the year.

Table E8. Changes in simulated monthly base flow resulting from scenario 3b (increased public-supply groundwater use), near the southeastern part of Puget Sound, Washington.

[Results are shown as the difference between scenarios 3b and 3a, with negative numbers indicating a decrease in base flow for the station location. Station name: Station 12113344 (GREEN RIVER AT 200TH STREET AT KENT, WA) is not shown because model boundary conditions influenced results. Change in simulated base flow: Change in total base flow is equivalent to the change in model-area base flow for these scenarios. Total base flow consists of flows from the Streamflow-Routing, Drain, and General-Head Boundary Packages. Abbreviations: Apr., April; Aug., August; BL., below; Dec., December; E., East; Feb., February; ID, identifier; Jan., January; Mar., March; Nov., November; NR, near; Oct., October; Sept., September; ST, Street; WA, Washington; ft³/s, cubic foot per second]

Station ID	Target name	Station name	Change in simulated base flow (ft ³ /s)												Minimum value	Maximum value		
			Jan.	Feb.	Mar.	Apr.	May	June	July	Aug.	Sept.	Oct.	Nov.	Dec.				
12090400	o4681	NORTH FORK CLOVER CREEK NEAR PARKLAND, WA	0.0	0.0	0.0	0.0	0.0	0.0	0.0	0.0	0.0	0.0	0.0	0.0	0.0	0.0	0.0	
12090452	o4688	SPANAWAY CREEK AT SPANAWAY LAKE OUTLET NEAR SPANAWAY, WA	-0.2	-0.2	-0.2	-0.2	-0.1	-0.1	-0.1	-0.1	-0.1	-0.1	-0.1	-0.1	-0.1	-0.2	-0.2	-0.1
12090500	o4670	CLOVER CREEK NEAR TILlicum, WA	-0.7	-0.7	-0.7	-0.7	-0.6	-0.5	-0.5	-0.5	-0.5	0.0	0.0	-0.5	-0.7	-0.8	-0.8	0.0
12091100	o4671	FLETT CREEK AT TACOMA, WA	-0.4	-0.4	-0.4	-0.4	-0.3	-0.3	-0.3	-0.3	-0.2	-0.2	-0.2	-0.2	-0.2	-0.3	-0.4	-0.2
12091200	o4675	LEACH CREEK NEAR FIRCREST, WA	0.0	0.0	0.0	0.0	0.0	0.0	0.0	0.0	0.0	0.0	0.0	0.0	0.0	0.0	-0.1	0.0
12091300	o4676	LEACH CREEK NEAR STEILACOOM, WA	-0.1	-0.1	-0.1	-0.1	0.0	0.0	0.0	0.0	0.0	0.0	0.0	0.0	0.0	-0.1	-0.1	0.0
12091500	o4668	CHAMBERS CREEK BL LEACH CREEK NEAR STEILACOOM, WA	-2.3	-2.3	-2.5	-2.4	-2.0	-1.7	-1.3	-1.0	-1.0	-1.0	-1.0	-1.1	-1.9	-2.1	-2.5	-1.0
12102075	o4669	CLARKS CREEK AT TACOMA ROAD NEAR PUYALLUP, WA	0.0	-0.2	-0.2	-0.3	-0.3	-0.5	-0.6	-0.6	-0.6	-0.6	-0.5	-0.3	-0.4	0.2	-0.6	0.2
12102190	o4689	SWAN CREEK AT 80TH STREET NEAR TACOMA, WA	0.0	0.0	0.0	0.0	0.0	0.0	0.0	0.0	0.0	0.0	0.0	0.0	0.0	0.0	0.0	0.0
12095000	o4687	SOUTH PRAIRIE CREEK AT SOUTH PRAIRIE, WA	-0.2	-0.1	-0.1	-0.1	0.0	0.0	0.0	0.0	0.0	0.0	0.0	0.0	0.0	-0.2	-0.2	0.0
12093500	o4686	PUYALLUP RIVER NEAR ORTING, WA	0.0	0.0	0.0	0.0	0.0	0.0	0.0	0.0	0.0	0.0	0.0	0.0	0.0	0.0	0.0	0.0
12096500	o4683	PUYALLUP RIVER AT ALDERTON, WA	-0.5	-0.4	-0.4	-0.3	-0.3	-0.3	-0.4	-0.4	-0.4	-0.4	-0.4	-0.4	-0.4	-0.5	-0.5	-0.3

Table E10. Changes in simulated monthly base flow resulting from scenario 3d (Spanaway Water Company groundwater use), near the southeastern part of Puget Sound, Washington.

[Results are shown as the difference between scenarios 3d and 3a, with negative numbers indicating a decrease in simulated base flow. **Station name:** Station 12113344 (GREEN RIVER AT 200TH STREET AT KENT, WA) is not shown because model boundary conditions influenced results. **Change in simulated base flow:** Change in total base flow is equivalent to the change in model-area base flow for these scenarios. Total base flow consists of flows from the Streamflow-Routing, Drain, and General-Head Boundary Packages. **Abbreviations:** Apr., April; Aug., August; BL, below; Dec., December; E, East; Feb., February; ID, identifier; Jan., January; Mar., March; Nov., November; NR, near; Oct., October; Sept., September; ST, Street; WA, Washington; ft³/s, cubic foot per second]

Station ID	Target name	Station name	Change in simulated base flow (ft ³ /s)												Minimum value	Maximum value	
			Jan.	Feb.	Mar.	Apr.	May	June	July	Aug.	Sept.	Oct.	Nov.	Dec.			
12090400	o4681	NORTH FORK CREEK NEAR PARKLAND, WA	0.0	0.0	0.0	0.0	0.0	0.0	0.0	0.0	0.0	0.0	0.0	0.0	0.0	0.0	0.0
12090452	o4688	SPANAWAY CREEK AT SPANAWAY LAKE OUTLET NEAR SPANAWAY, WA	-0.8	-0.7	-0.8	-0.6	-0.5	-0.4	-0.4	-0.3	-0.3	-0.3	-0.3	-0.5	-0.7	-0.8	-0.3
12090500	o4670	CLOVER CREEK NEAR TILLICUM, WA	-2.0	-1.8	-1.8	-1.6	-1.4	-1.3	-1.2	-1.2	0.0	0.0	-1.3	-1.9	-2.1	-2.1	0.0
12091100	o4671	FLETT CREEK AT TACOMA, WA	-0.1	0.0	0.0	0.0	0.0	0.0	-0.1	-0.1	-0.1	-0.1	-0.1	-0.1	-0.1	-0.1	0.0
12091200	o4675	LEACH CREEK NEAR FIRCREST, WA	0.0	0.0	0.0	0.0	0.0	0.0	0.0	0.0	0.0	0.0	0.0	0.0	0.0	0.0	0.0
12091300	o4676	LEACH CREEK NEAR STEILACOOM, WA	0.0	0.0	0.0	0.0	0.0	0.0	0.0	0.0	0.0	0.0	0.0	0.0	0.0	0.0	0.0
12091500	o4668	CHAMBERS CREEK BL LEACH CREEK NEAR STEILACOOM, WA	-2.3	-2.0	-2.0	-1.8	-1.5	-1.3	-0.8	-0.8	-0.4	-0.4	0.6	-2.3	-2.4	-2.4	0.6
12102075	o4669	CLARKS CREEK AT TACOMA ROAD NEAR PUYALLUP, WA	-0.1	0.0	-0.1	-0.1	0.0	0.0	0.0	0.0	0.0	0.0	0.0	0.0	-0.1	-0.1	0.0

For scenarios 3b–3e, the change in the total simulated base flow within the model area was compared to the change in groundwater use (app. 1, table E12). For example, scenario 3b consisted of a 13.0 percent total increase in groundwater use (10.3 ft³/s), which resulted in a 0.48 percent reduction in total base flow (6.8 ft³/s). For scenarios 3b, 3d, and 3e, the reductions in base flow as a percentage of the change in groundwater use were 65.3, 73.8, and 80.8 percent, respectively (app. 1, table E12). Scenario 3c consisted of a small increase in groundwater use (0.21 percent), which resulted in a larger change in base flow than groundwater use (–0.3 and 0.2 ft³/s, respectively). This result is owing to model error for scenarios with very small changes such as in this example because the model cannot simulate the effects of these small changes to the degree of accuracy required for an analysis like this.

Model Limitations and Potential Refinements

Uncertainty is associated with most model inputs. Groundwater levels, lake levels, and land-surface altitudes are relatively certain; other model inputs are far less certain, including precipitation recharge, base flow, hydraulic properties, groundwater use, and the three-dimensional structure of subsurface HGUs. Little information was available for aquicultural groundwater use, which, therefore, was not accounted for; such use was assumed to be small as a fraction of all groundwater use and negligible as a fraction of the overall groundwater budget. Models are useful not because of high levels of accuracy of all model inputs, but because they

combine the best information and estimates available, thereby providing the best predictions available related to physical processes.

The model described in this report simulates groundwater flow on a regional scale, which has inherent limitations for simulating hydrologic scenarios at local scales. Model structures and inputs were generalized to suit the scope and purpose of this regional-scale model. For example, the actual groundwater system has greater heterogeneity of horizontal hydraulic conductivity (K_h) than is possible with the model's density of pilot points. Although a greater density of pilot points would allow greater heterogeneity that would improve model calibration, caution should be exercised to limit over-calibration that could risk degrading the model's ability to simulate predictive scenarios well (Anderson and others, 2015; Doherty, 2015, 2018). Additionally, an increase in calibration run times should be expected if pilot-point density is increased. Calibration is sensitive to the placement of pilot points, which could be tested if further calibration refinement is done.

The model has a grid cell spacing of 500 ft, which is not a limitation for heterogeneity of hydraulic properties at the overall scale of the model. However, hydraulic gradient variations over distances less than 500 ft will be smoothed. A pumping well located 250 ft from a stream might have been placed either within the same model cell as the stream or in an adjacent cell, depending on the location of the stream and well in relation to the model grid. Two boundary conditions placed in the same cell are co-located at the center of the cell, and if these are placed in two adjacent cells, the distance between them is 500 ft. The cell spacing also prevents accurate simulation of drawdown from a pumped well at locations closer than 750 ft from the well. For pumping scenarios in which small distances are critical, any revised model version should include grid refinement.

Table E12. Changes in August base flow resulting from scenarios 3b–3e (increased groundwater use) in the active model area, near the southeastern part of Puget Sound, Washington.

[Results are shown as the change between each scenario and scenario 3a, with negative numbers indicating a decrease. **Scenario 3b:** Fifteen-percent increase in groundwater use for Group A and Group B public-supply wells. **Scenario 3c:** Fifteen-percent increase in groundwater use self-supply wells. **Scenario 3d:** Increase in groundwater use to simulate the Spanaway pilot project. **Scenario 3e:** Increase in groundwater use to simulate the Sumner pilot project. **Abbreviations:** ft³/s, cubic foot per second; NA, not applicable]

Description	Units	Scenario 3b	Scenario 3c	Scenario 3d	Scenario 3e
Percent change in average groundwater use	Percent	13.0	0.21	4.09	2.93
Percent change in average simulated base flow for all streams and springs ¹	Percent	–0.48	–0.02	–0.17	–0.13
Change in average groundwater use	ft ³ /s	10.3	0.2	3.3	2.3
Change in average simulated base flow for all streams and springs ¹	ft ³ /s	–6.8	–0.3	–2.4	–1.9
Change in base flow as percentage of the change in groundwater use	Percent	–65.3	NA ²	–73.8	–80.8

¹The change in total base flow is equivalent to the change in model-area base flow for these scenarios.

²Model error resulted in a change in base flow that is larger than the change in consumptive water use.

All simulated groundwater inflows and outflows were larger than those estimated, except for withdrawals from wells (table E2). This result occurred primarily for two reasons. First, the simulated precipitation recharge was allowed to be as much as 25 percent higher than estimated to allow for error in the SWB model estimates, which are uncertain because of the potential range of error in soil properties and precipitation rates. Second, the simulated net discharge to streams, springs, lakes, and Puget Sound (table E2) largely is the result of calibration to estimated base flow for individual stations. Because this base-flow calibration was a priority, no attempt was made to match the estimated value in table E2, and the goal of matching estimated base flow at stations resulted in the need to increase precipitation recharge to balance inflows and outflows.

Thin saturated thicknesses leading to simulated pumping reductions caused pumping rates to be reduced overall by 3.5 percent for the steady-state model version. Because of uncertainty of groundwater-use estimates, this pumping reduction is assumed to be smaller than the potential error of the estimates, accounting for only 0.3 percent of total simulated outflow. A larger concern is the use of the model to simulate groundwater pumping scenarios, which may be affected by simulated pumping reductions. For example, if the specified pumping rate for a simulated well is increased from 1 to 2 ft³/s, and the layer's saturated thickness becomes small, then the model would reduce the specified pumping rate, and the increase in pumping would be less than expected. In this case, the actual pumping rate can be obtained from model output, and this value (not the specified rate) should be used for comparison to the simulated effects on base-flow and groundwater levels. In some cases, turning off surrounding pumping wells might reduce or eliminate the pumping reduction, and the scenario could proceed with the desired pumping rate.

The model simulates only the base-flow component of streamflow; therefore, variations in stream stage resulting from runoff events cannot be simulated. Simulated stream stage is constant for major rivers but varies with base flow for all other streams.

Model scenarios presented in the report were used to estimate changes in base flow that occur at stations. These estimates were useful because the model's accuracy can be assessed at these locations, for which data are available. However, base-flow changes can be simulated for any location on any stream in the model, except with less certainty of model accuracy if no streamflow data are available.

Model error is associated with changes in base flow simulated by model scenarios. Simulated changes in base flow less than about 0.5 ft³/s should not be considered accurate. Changes in base flow are largest near the location of a change in pumping and are smallest at farther distances. These base-flow changes decrease asymptotically as the distance from the pumping well increases, and the changes can be simulated at tiny flow rates of as little 10⁻⁸ ft³/s in this model.

Although tiny changes such as this may be theoretically possible, these model outputs are not meaningful in any practical sense.

Additional calibration targets could be added as new data become available, which would be particularly useful for a detailed study of a local area. Additional calibration targets for a local area would justify a greater density of pilot points and storage property zones in that area. Although this increase would add to the total number of parameters, recalibration could be applied to parameters within and near the local area, with parameters farther away having fixed values. This application would result in the recalibration of far fewer parameters than those included originally. Localized grid refinement could be applied in addition but might not be necessary, in many cases, to achieve a large benefit from recalibration. The model simulated groundwater flooding in some areas; that is, a water table above the land surface. These simulated flooded areas were not calibrated to data, but if this was done, the model could potentially be used to predict groundwater flooding for periods of high precipitation.

Simulated pumping wells influenced model calibration because hydraulic head declines resulting from pumping might have degraded the model's fit to calibration targets at the beginning of automatic calibration. As calibration continued, such degradation could have caused increases in Kh near these wells. Because Kh must be large enough to accommodate these pumping wells, simulating these wells helps to better calibrate the model. Furthermore, these necessary increases in Kh indicate that heterogeneity in the HGU may be greater than what is represented in the model, particularly in areas void of large pumping wells. If the model is used to simulate a new pumping well that was not included during model calibration, the simulated Kh surrounding that well might not be large enough to accommodate the simulated pumping rate without large drawdown. In these cases, recalibration of the model with new data may be needed.

Some HGUs have wide ranges of Kh values, ranging by five orders of magnitude for HGUs A1, A3, and B between minimum and maximum values (table D6). HGUs A1 and A3 have minimum values of 0.011 and 0.003 ft/d, respectively, indicating that although these HGUs are generally considered to be aquifers, they are similar to confining units in some areas. Although HGU B is considered a confining unit, a maximum Kh value of 500 ft/d indicates that this HGU is an aquifer in some places. The degree to which these values represent reality is uncertain, and this uncertainty results partly from simplifications and uncertainty of the hydrogeologic framework described in Chapter B. Revisions to this model could include additional sensitivity analysis and testing whether large ranges of Kh values are critical to calibration.

Part of the reason for large ranges in Kh may have resulted from the fact that Kh is tied to the ratio of horizontal to vertical hydraulic conductivity (Kh/Kv). Limits were set for the range of Kh/Kv so that Kv would not be many orders of magnitude smaller than Kh. Therefore, if the calibration favors a low Kv value in some areas, then Kh also may need to be

reduced, even if the model would be better calibrated with a larger Kh value. Another option would be to calibrate Kv and Kh independently, but this makes it more difficult to restrict the range of Kh/Kv.

A sensitivity analysis is primarily important for understanding the functionality of the model but does not necessarily provide a quantitative assessment of the relative confidence in parameters or their values. A parameter with a high sensitivity does not necessarily mean that there is higher confidence in that parameter value than for a parameter with lower sensitivity. For example, the highest parameter sensitivity is for the recharge multiplier (rm0) because rm0 affects the recharge rate in every part of the model and because precipitation recharge accounts for 97.8 percent of model inflow (table E1). As a comparison, the largest outflow component is to streams and large springs (67.3 percent; table E1). The individual sensitivities for each streambed Kh parameter are much smaller than that of rm0 because each of the streambed parameters affect only a small part of the model. Therefore, although the sensitivity of a streambed parameter is much lower than for rm0, the confidence in the two parameter values is not necessarily proportional to their sensitivities.

Alternatively, comparing parameter sensitivities within parameter groups may yield a useful assessment of parameter confidence. For example, Kh pilot points will have the highest sensitivities in areas where calibration targets are plentiful and the lowest sensitivities in areas where targets are sparse. Areas where Kh sensitivities are low indicate that the model could be improved by adding calibration data. Therefore, the model can be useful for planning new data-collection efforts, and new data can be applied to the future refinements of the model.

HGU A1 is an important water source for the area west of the Puyallup River. The station at the outlet of Spanaway Lake (station ID 12090452; fig. D1) is the only base-flow calibration target to assist with calibration of HGU A1 in the area to the south of this location. On average, simulated transient base-flow values are about 30 percent of the estimated flows (app. 1, table 1.8); however, estimated base flow is only available for the last 14 months of the model period. Future revisions to the model would benefit from current streamflow data for this station, as well as stations at additional locations if they were to be installed.

Although useful insights may be gained from these scenarios, many other scenarios could be simulated. For example, scenarios 1a, 1b, and 1c simulate a long-term drought at steady-state conditions, and 1d simulates 3 consecutive years of summer drought. Another useful scenario would be one that simulates 3 or more years of year-long drought or 3 years of winter drought. A comparison of the effects of winter versus summer drought could help to plan

for future changes in seasonal precipitation or air temperature. Several scenarios related to groundwater use were described, but numerous other scenarios of single or multiple pumping wells could be simulated and used for water-supply planning. Scenarios of climate change also can be applied. Changes in air temperature, precipitation, or both can be applied to the SWB model (Gendaszek, 2023) to simulate precipitation recharge, which then can be applied to the groundwater-flow model. The effects of sea level rise on groundwater and base flow could be simulated by moving the Puget Sound boundary condition inland.

References Cited

- Anderson, M.P., Woessner, W.W., and Hunt, R.J., 2015, Applied groundwater modeling—Simulation of flow and advective transport (2nd ed.). San Diego, Elsevier, 630 p.
- Doherty, J., 2015, Calibration and uncertainty analysis for complex environmental models: Watermark Numerical Computing, Brisbane, Australia, 227 p., accessed September 16, 2020, at <https://pesthhomepage.org/pest-book>.
- Doherty, J., 2018, PEST—Model-independent parameter estimation, User manual part I—PEST, SENSAN and Global Optimisers (7th ed.): Brisbane, Australia, Watermark Numerical Computing, 368 p., accessed September 16, 2020, at <https://pesthhomepage.org/documentation>
- Gendaszek, A., 2023, Soil-water balance model of the Puyallup and Chambers-Clover Basins, western Washington: U.S. Geological Survey data release, accessed March 15, 2023, at <https://doi.org/10.5066/P925FHGQ>.
- McLean, J.E., Welch, W.B., and Long, A.J., 2024, Spatial data in support of the characterization of water resources near the southeastern part of Puget Sound, Washington: U.S. Geological Survey data release, <https://doi.org/10.5066/P9JFKLMG>.
- Pacific Groundwater Group, 1999, 1999 hydrogeologic characterization, City of Auburn: Prepared for the City of Auburn Department of Public Works Water Utility Engineering by Pacific Groundwater Group, Seattle, Washington, 91 p.
- Perry, T.D., and Jones, J.A., 2017, 2017, Summer streamflow deficits from regenerating Douglas-fir forest in the Pacific Northwest, USA: Ecohydrology, v. 10, no. 2, p. e1790, accessed July 28, 2022, at <https://doi.org/10.1002/eco.1790>.

Welch, W.B., Bright, V.A.L., Gendaszek, A.S., Dunn, S.B., Headman, A.O., and Fasser, E.T., 2024, Conceptual hydrogeologic framework and groundwater budget near the southeastern part of Puget Sound, Washington, chap. A–C of Welch, W.B., and Long, A.J., eds., *Characterization of groundwater resources near the southeastern part of Puget Sound, Washington*: U.S. Geological Survey Scientific Investigations Report 2024–5026–A–C, 71 p., 1 pl., <https://doi.org/10.3133/sir20245026v1>.

Wright, E.E., Long, A.J., and Fuhrig, L.T., 2023, MODFLOW-NWT model to simulate the groundwater flow system near Puget Sound, Pierce and King Counties, Washington: U.S. Geological Survey data release, accessed March 1, 2023, at <https://doi.org/10.5066/P9LU1PMQ>.

Appendix 1. Supplementary Tables

The following tables are available from the Wright and others (2023) data release. The tables linked to from here are referred to throughout this report and are provided as individual sheets within a single Microsoft Excel® workbook and also as separate text files with a “.csv” extension. Also included in the Wright and others (2023) data release is a ancillary.zip folder with additional figures and other materials helpful for describing the model. Tables 1.1–1.14 are available for download as .csv files and as tabs within an Excel file at <https://doi.org/10.3133/sir20245026v2>.

Table 1.1. Streamflow-Routing (SFR) Package specifications by reach (Prudic and others, 2004).

Table 1.2. Estimated monthly average base flow estimated for Coal, Boise, and Scatter Creeks where they enter the active model area, near the southeastern part of Puget Sound, Washington, 2005–15.

Table 1.3. Estimated monthly average base flow estimated for selected streams where they enter the active model area, the Buckley diversion (inflow to Lake Tapps), and outflow from Lake Tapps, near the southeastern part of Puget Sound, Washington, 2005–15.

Table 1.4. Monthly average water levels for American, Gravelly, Steilacoom, and Spanaway Lakes, and Lake Tapps, derived from measured and estimated values, near the southeastern part of Puget Sound, Washington, 2005–15.

Table 1.5. Measured water levels for American, Gravelly, and Spanaway Lakes, near the southeastern part of Puget Sound, Washington, 2000–18.

Table 1.6. Time-series records of measured and simulated hydraulic-head values (transient model version) for selected wells used, near the southeastern part of Puget Sound, Washington, 2005–15.

Table 1.7. Averages of measured hydraulic-head values for selected wells and corresponding simulated steady-state values, near the southeastern part of Puget Sound, Washington, 2005–15.

Table 1.8. Estimated and simulated monthly average base flow for selected stations, near the southeastern part of Puget Sound, Washington, 2005–15.

Table 1.9. Estimated and simulated base-flow values for the steady-state model version for stations with continuous records, near the southeastern part of Puget Sound, Washington, 2005–15.

Table 1.10. Estimated and simulated vertical hydraulic-head differences for the steady-state model version between an upper and lower model layer for selected locations, near the southeastern part of Puget Sound, Washington, 2005–15.

Table 1.11. Supplemental hydraulic-head targets for the steady-state model version set equal to the land surface to prevent groundwater flooding and corresponding simulated values, near the southeastern part of Puget Sound, Washington.

Table 1.12. Model calibration parameters showing input to the control file for the Model-Independent Parameter Estimation (PEST) program (Doherty, 2018).

Table 1.13. Simulated groundwater budget for the calibrated transient model version, near the southeastern part of Puget Sound, Washington, 2005–15

Table 1.14. Groundwater use applied to scenario 3 for the Spanaway Water Company and the City of Sumner, near the southeastern part of Puget Sound, Washington.

References Cited

- Doherty, J., 2018, PEST—Model-independent parameter estimation, User manual part I—PEST, SENSAN and Global Optimisers (7th ed.): Brisbane, Australia, Watermark Numerical Computing, 368 p., accessed September 16, 2020, at <https://pesthhomepage.org/documentation>.
- Prudic, D.E., Konikow, L.F., and Banta, E.R., 2004, A new streamflow-routing (SFR1) package to simulate stream-aquifer interaction with MODFLOW-2000: U.S. Geological Survey Open-File Report 2004–1042, accessed January 8, 2021, at <https://doi.org/10.3133/ofr20041042>.
- Wright, E.E., Long, A.J., and Fuhrig, L.T., 2023, MODFLOW-NWT model to simulate the groundwater flow system near Puget Sound, Pierce and King Counties, Washington: U.S. Geological Survey data release, accessed March 1, 2023, at <https://doi.org/10.5066/P9LU1PMQ>.

Appendix 2. Estimation of Base Flow for Points of Inflow to the Active Model Area (AMA)

Streams enter the active model area (AMA) at 10 points of inflow (fig. D1), and monthly base flow was estimated at these locations for 2005–15. Average monthly base-flow estimates at the points of inflow for Coal, Boise, and Scatter Creeks were described in Gendaszek (2023) and are available in appendix 1, table 1.2. Average monthly base-flow rates for the Green, White, Carbon, and Puyallup Rivers and for Big Soos, South Prairie, and Voight Creeks were estimated by methods described in this appendix and are available in appendix 1, table 1.3. Data for stations used in these estimates were obtained from the U.S. Geological Survey (USGS) National Water Information System (U.S. Geological Survey, 2020).

Estimation Methods

Green and White Rivers

For the Green and White Rivers, stations with continuous streamflow data are located at the points of inflow (fig. D1; stations 12106700 and 12097850). Daily streamflow data were available for the White River station for October 2008–December 2015. To estimate monthly base flow for January 2005–September 2008, a least squares linear regression was applied to the estimated base flow for station 12097850 and a downstream station (USGS 12099200; app. 1, table 1.8), with a coefficient of determination (R^2) of 0.88. The equation derived from the regression was applied to the base flow for the White River inflow point for the missing period (app. 1, table 1.2).

Big Soos Creek

Monthly inflows for Big Soos Creek were estimated on the basis of Station 12112600 located 11 miles (mi) downstream from the point of inflow (fig. D1). The monthly specified inflow record was estimated by assuming that this would be proportional to the monthly base flow for station 12112600 (app. 1, table 1.8), and the watershed areas for the two stream locations were used to estimate this proportionality. The watershed area for the inflow point divided by that of the station is 0.72, as determined by StreamStats v4.4.0 (U.S. Geological Survey, 2021). This ratio was multiplied by the monthly base-flow values for the station and used as the specified inflow for Big Soos Creek (app. 1, table 1.3). The average of monthly values was used as the steady-state inflow value (table D4). This inflow rate was assumed to include flow from a tributary to Big Soos Creek that flows along the northeastern boundary of the AMA, where it joins Big Soos Creek.

Carbon River

The approach taken for Big Soos Creek also was applied to an estimated monthly inflow record for the Carbon River. This record was assumed to be proportional to the estimated monthly base flow for Station 12094000 (app. 1, table 1.8), which is located 3 mi upstream from the point of inflow for the Carbon River (fig. D1), resulting in a watershed ratio of 1.02. Monthly and steady-state inflow values are shown in tables 1.3 and D4, respectively.

Voight Creek

Station 12095500 is located 1 mi downstream from the point of inflow for Voight Creek (fig. D1). Because of the proximity of the station to the inflow point, estimated base flow for the station was used as the model specified inflow. However, because daily streamflow data for the station were available for only July–October 1949 (U.S. Geological Survey, 2020), hydrograph separation could not be used to estimate monthly base flow for the 11-year model period. Therefore, we assumed that monthly average streamflow for station 12095500 would be proportional to that of station 12095000 on South Prairie Creek (fig. D1), and least squares linear regression was applied to the monthly streamflow for these two stations for July–October 1949 ($R^2 = 0.87$). We further assumed that this relation for monthly streamflow would be applicable to monthly base flow for the model period. Therefore, the equation derived from the regression was applied to monthly base flow for South Prairie Creek (station 12095000, app. 1, table 1.8) to estimate base flow for the Voight Creek station for the model period, and this was used as the specified inflow for Voight Creek (app. 1, table 1.3).

Puyallup River and South Prairie Creek

A first attempt at estimating specified inflow values for the Puyallup River and South Prairie Creek consisted of the same watershed scaling method applied to Big Soos Creek and the Carbon River. The resulting monthly inflow rates for the two streams were applied as specified flow rates in the Streamflow-Routing Package. Output from the transient model version resulted in a poor match to measured streamflow gains and losses obtained from seepage runs that were described in Chapter C of Welch and others (2024). The stream reaches used in this comparison are the uppermost reaches in the AMA, consisting of (1) the Puyallup River between stations 12093500 and 12092505 and (2) South Prairie Creek upstream from 12095000 and downstream from stations 12094425 and 12094498 (fig. D1). The watershed scaling method resulted in a variable streamflow gain for these reaches.

In a second attempt at estimating specified inflow values, we assumed that the base-flow gain for these two reaches is constant for both streams rather than variable, even as streamflow varies. These constants were subtracted from the respective monthly base-flow records for the two stations (app. 1, table 1.8), the results of which were used as the specified inflow records for the two streams in the transient model version (app. 1, table 1.3).

To estimate a constant base-flow gain for the Puyallup River, a specified inflow rate was applied to the steady-state model version that resulted in a simulated base-flow rate for station 12093500 that was similar to the estimated value. A specified inflow of 576.2 cubic feet per second (ft³/s) (table D4) resulted in simulated base flow for the station of 604.6 ft³/s (after final model calibration), which is similar to the estimated base flow of 602.5 ft³/s (table D1). This equates to a simulated base-flow gain of 28.4 ft³/s for the stream reach, which was compared with measured gains available from discrete measurements during the seepage runs. Discrete streamflow measurements for station 12092505 near the inflow point (fig. D1) were available to determine the gain for two different occasions. The difference in measured streamflow between stations 12092505 and 12093500 indicates a gain of 28 and 47 ft³/s on October 17, 2011, and October 10, 2012, respectively (U.S. Geological Survey, 2020), and the simulated base-flow gain of 28.4 ft³/s is within this range.

The approach taken for the Puyallup River specified inflow also was applied to the South Prairie Creek inflow point. A specified inflow rate of 142.3 ft³/s (table D4) was applied to the steady-state model version, resulting in simulated base flow for station 12095000 of 186.3 ft³/s (after final model calibration), which is about 7 percent larger than the estimated value of 173.9 ft³/s (table D1). This equates to a simulated base-flow gain of 44.0 ft³/s for the stream reach, which was compared with measured gains available from discrete measurements during the seepage runs. Station 12094425 is on South Prairie Creek near the model boundary, and Station

12094498 is on Wilkeson Creek, a tributary to South Prairie Creek, also near the model boundary (fig. D1). An inflow point for the tributary was not explicitly included in the model and was grouped together with the specified inflow for South Prairie Creek. The difference in measured streamflow between the sum of the two upstream stations and station 12095000 indicates a gain of 27.4 and 10.2 ft³/s on October 17, 2011, and October 10, 2012, respectively (U.S. Geological Survey, 2020). The simulated base-flow gain of 44.0 ft³/s is outside of the range of measured values but was considered acceptable and used as the constant base-flow gain.

References Cited

- Gendaszek, A., 2023, Soil-water balance model of the Puyallup and Chambers-Clover Basins, western Washington: U.S. Geological Survey data release, accessed March 15, 2023, at <https://doi.org/10.5066/P925FHGQ>.
- U.S. Geological Survey, 2020, National Water Information System, U.S. Geological Survey National Water Information System web interface, <http://dx.doi.org/10.5066/F7P55KJN>, accessed July 1, 2020, at <https://waterdata.usgs.gov/nwis>.
- U.S. Geological Survey, 2021, StreamStats (ver. 4.4.0): U.S. Geological Survey web page, accessed January 8, 2021, at <https://streamstats.usgs.gov/ss/>.
- Welch, W.B., Bright, V.A.L., Gendaszek, A.S., Dunn, S.B., Headman, A.O., and Fasser, E.T., 2024, Conceptual hydrogeologic framework and groundwater budget near the southeastern part of Puget Sound, Washington, chap. A–C of Welch, W.B., and Long, A.J., eds., Characterization of groundwater resources near the southeastern part of Puget Sound, Washington: U.S. Geological Survey Scientific Investigations Report 2024–5026–A–C, 71 p., 1 pl., <https://doi.org/10.3133/sir20245026v1>.

Appendix 3. Supplementary Figures

The following time-series plots provide a comparison of simulated values to measured or estimated values of hydraulic head in calibration wells and base flow at streamgages for the transient model version. Calibration was focused on matching simulated values to the temporal changes in measured or observed values, rather than the absolute differences.

Time series of hydraulic head

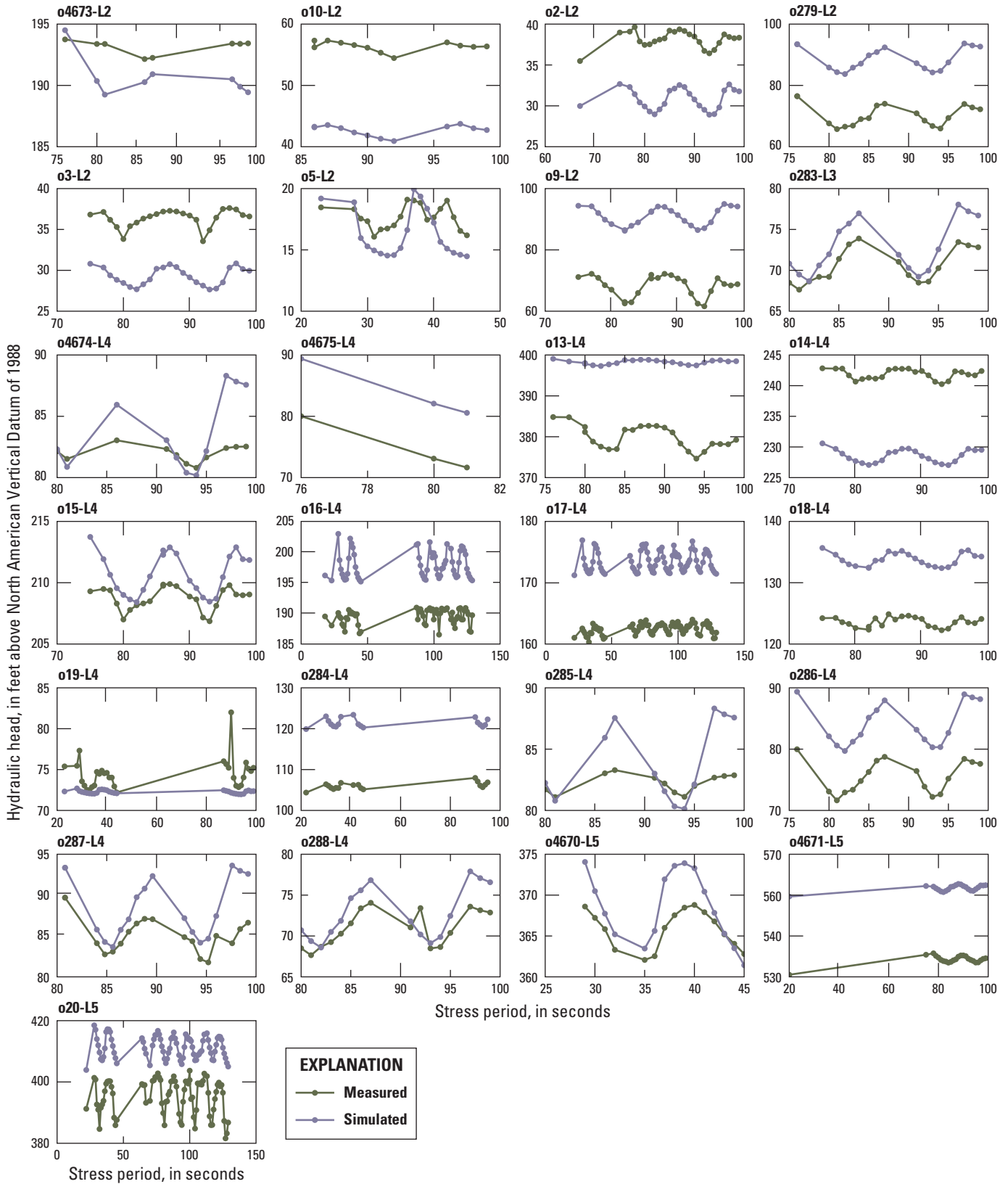


Figure 3.1. Hydrographs showing measured and simulated hydraulic-head values for 271 wells used in calibration of the transient model version, near the southeastern part of Puget Sound, Washington.

Time series of hydraulic head

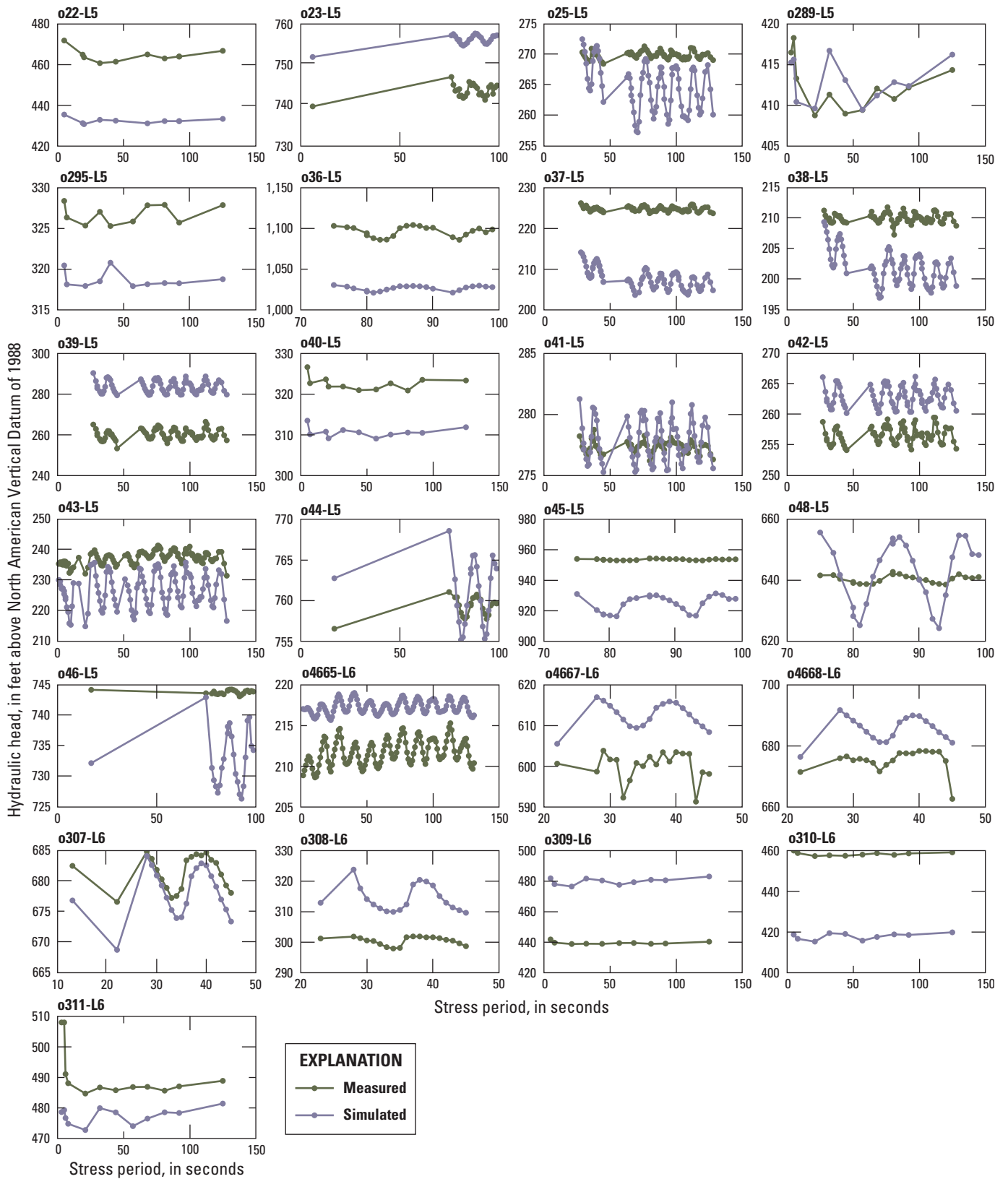


Figure 3.1.—Continued

Time series of hydraulic head

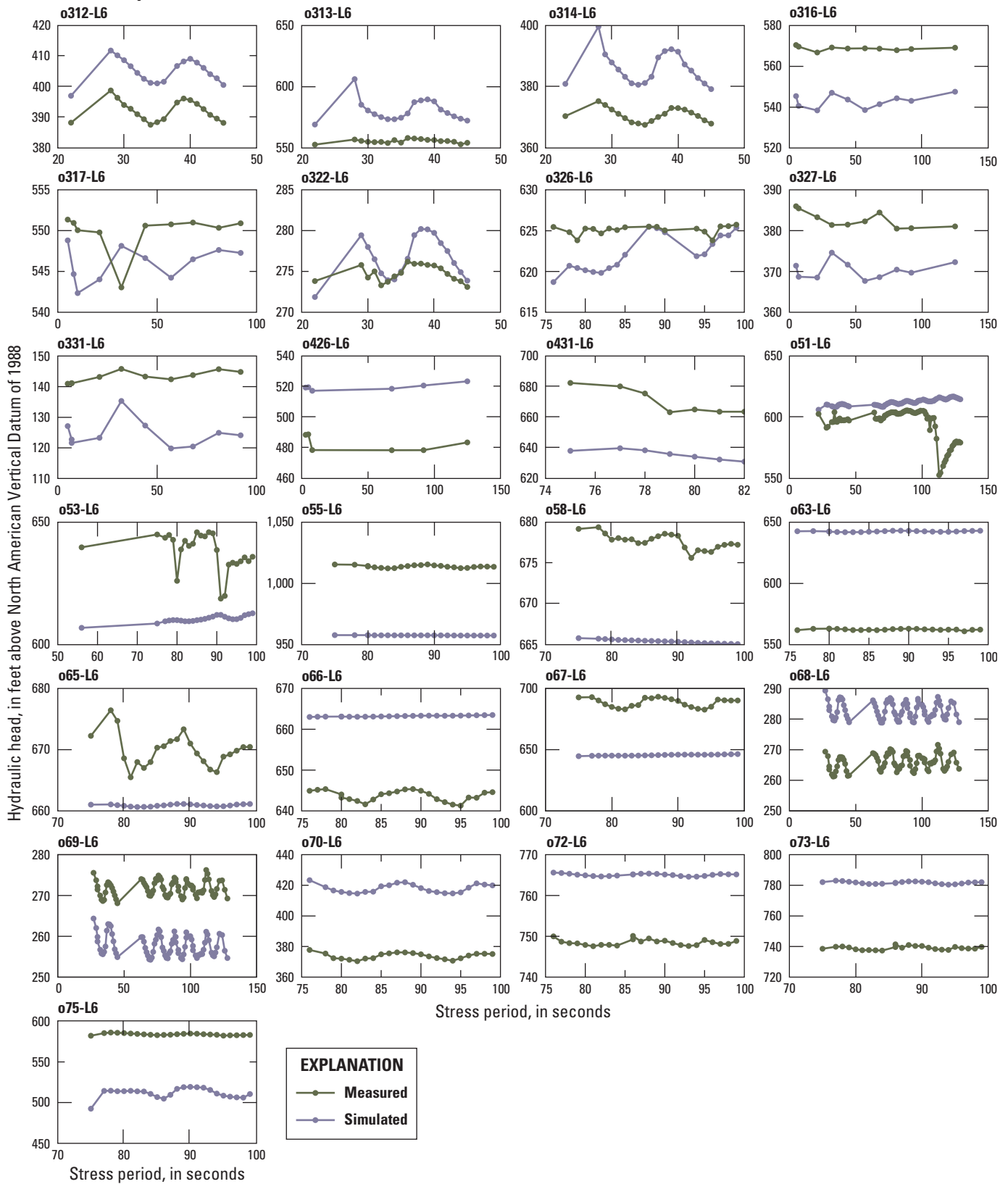


Figure 3.1.—Continued

Time series of hydraulic head

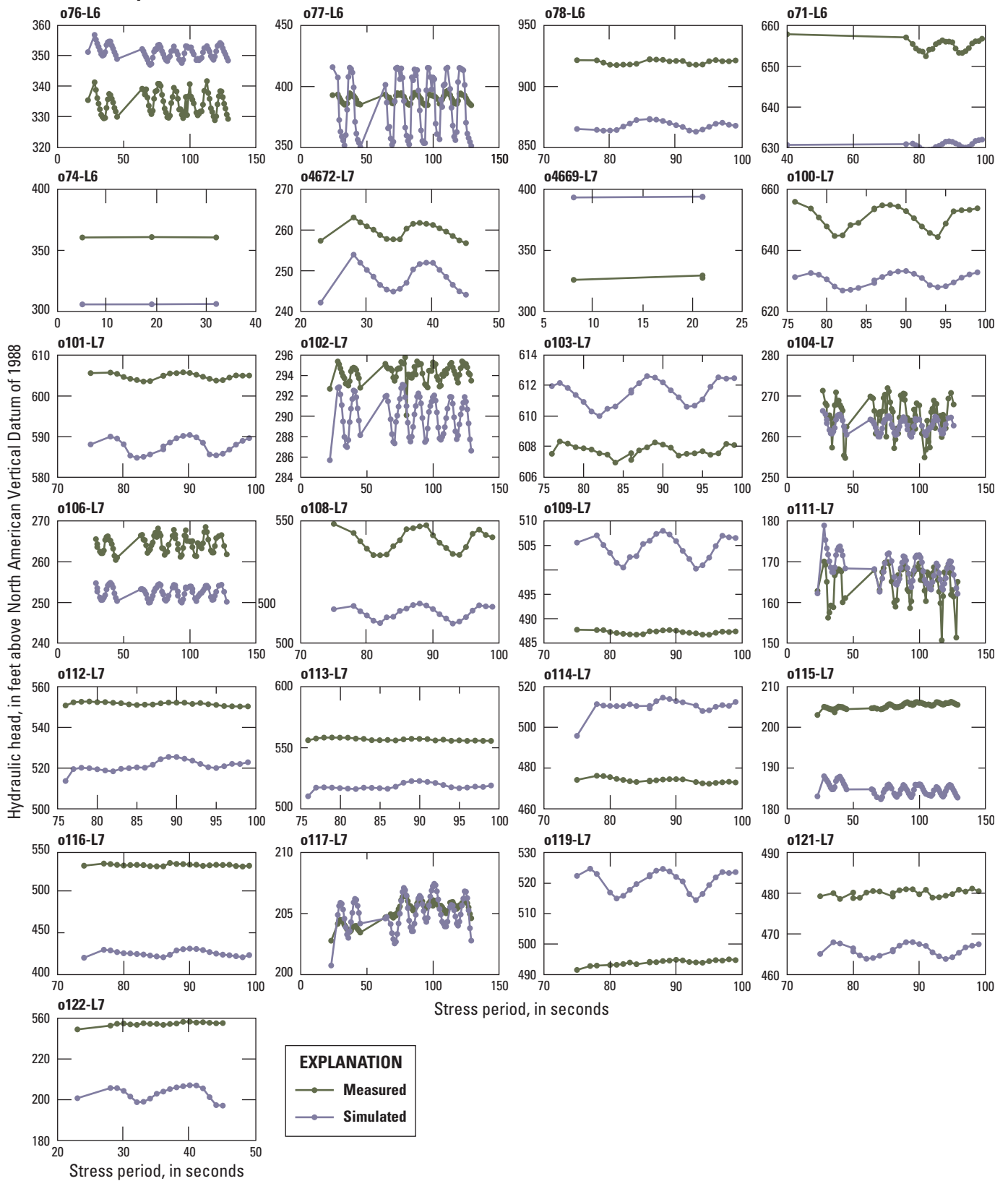


Figure 3.1.—Continued

Time series of hydraulic head

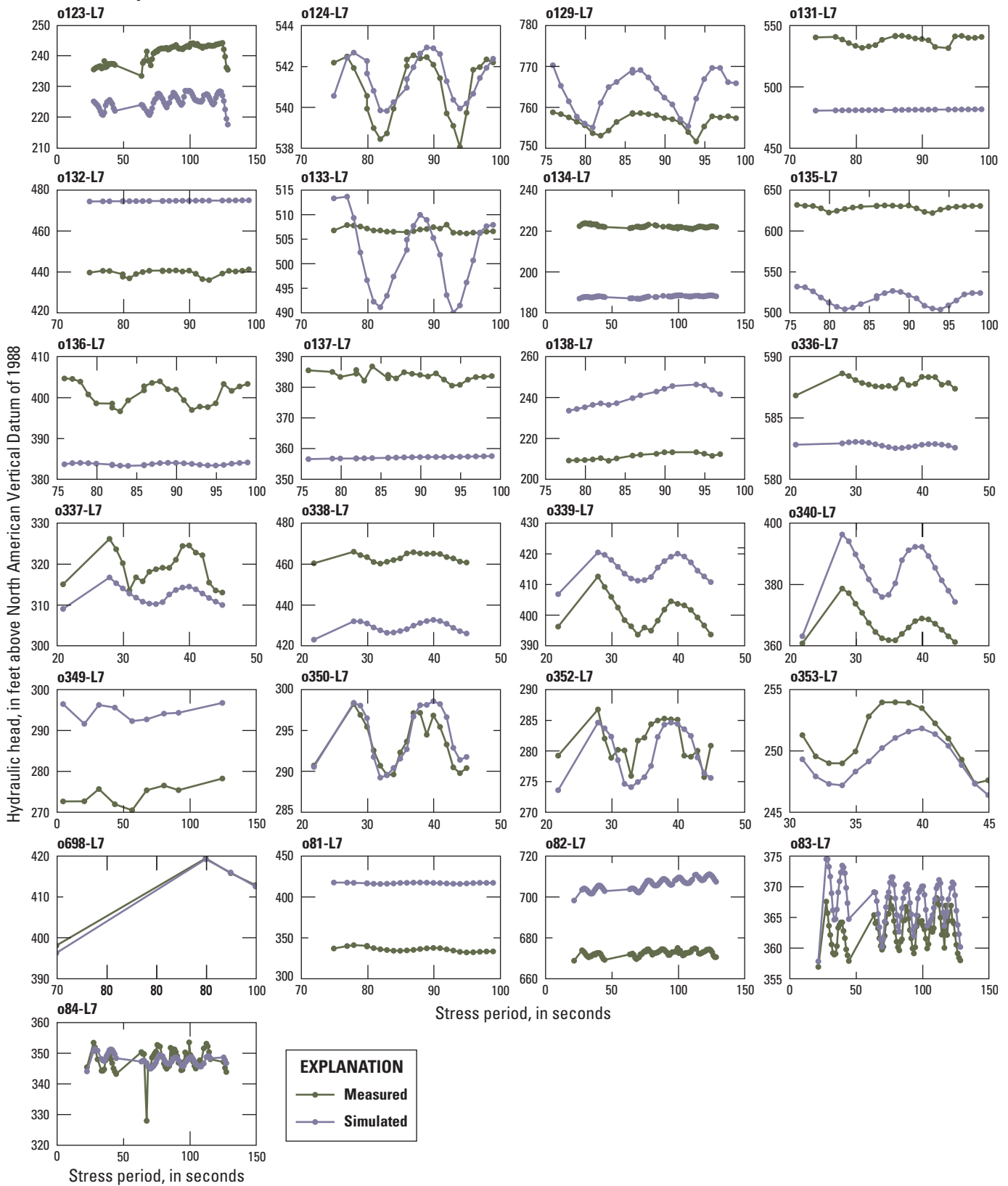


Figure 3.1.—Continued

Time series of hydraulic head

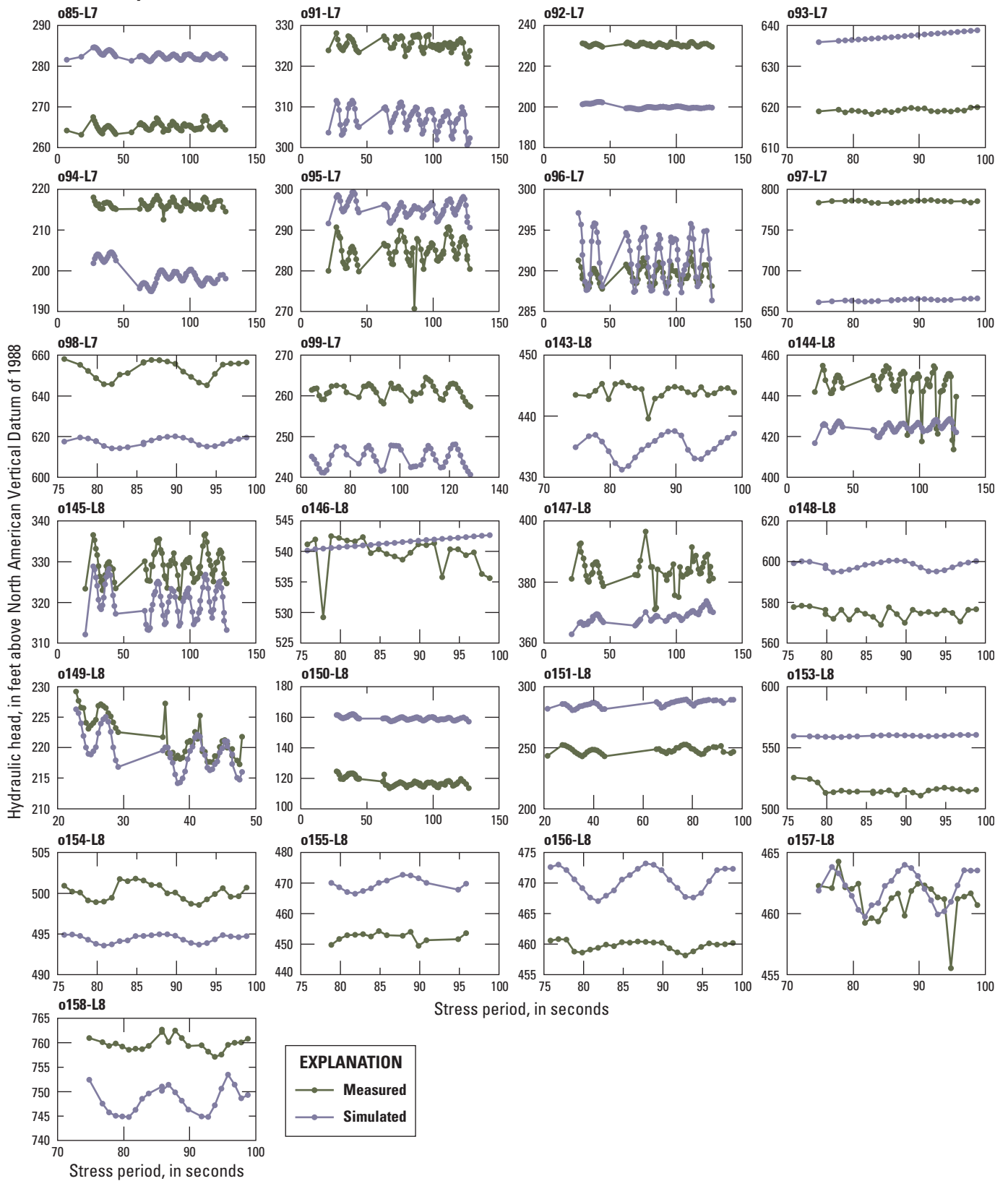


Figure 3.1.—Continued

Time series of hydraulic head

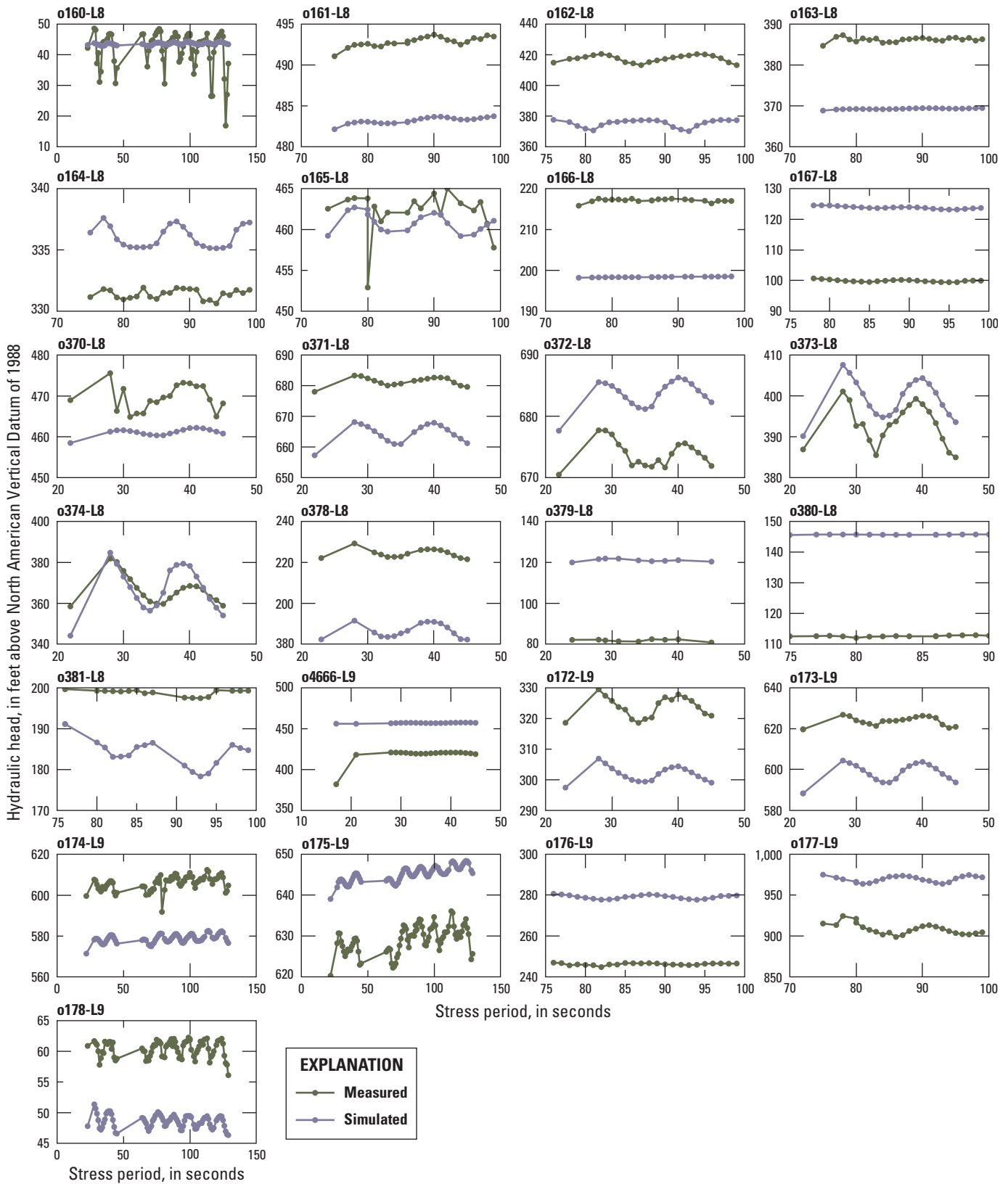


Figure 3.1.—Continued

Time series of hydraulic head

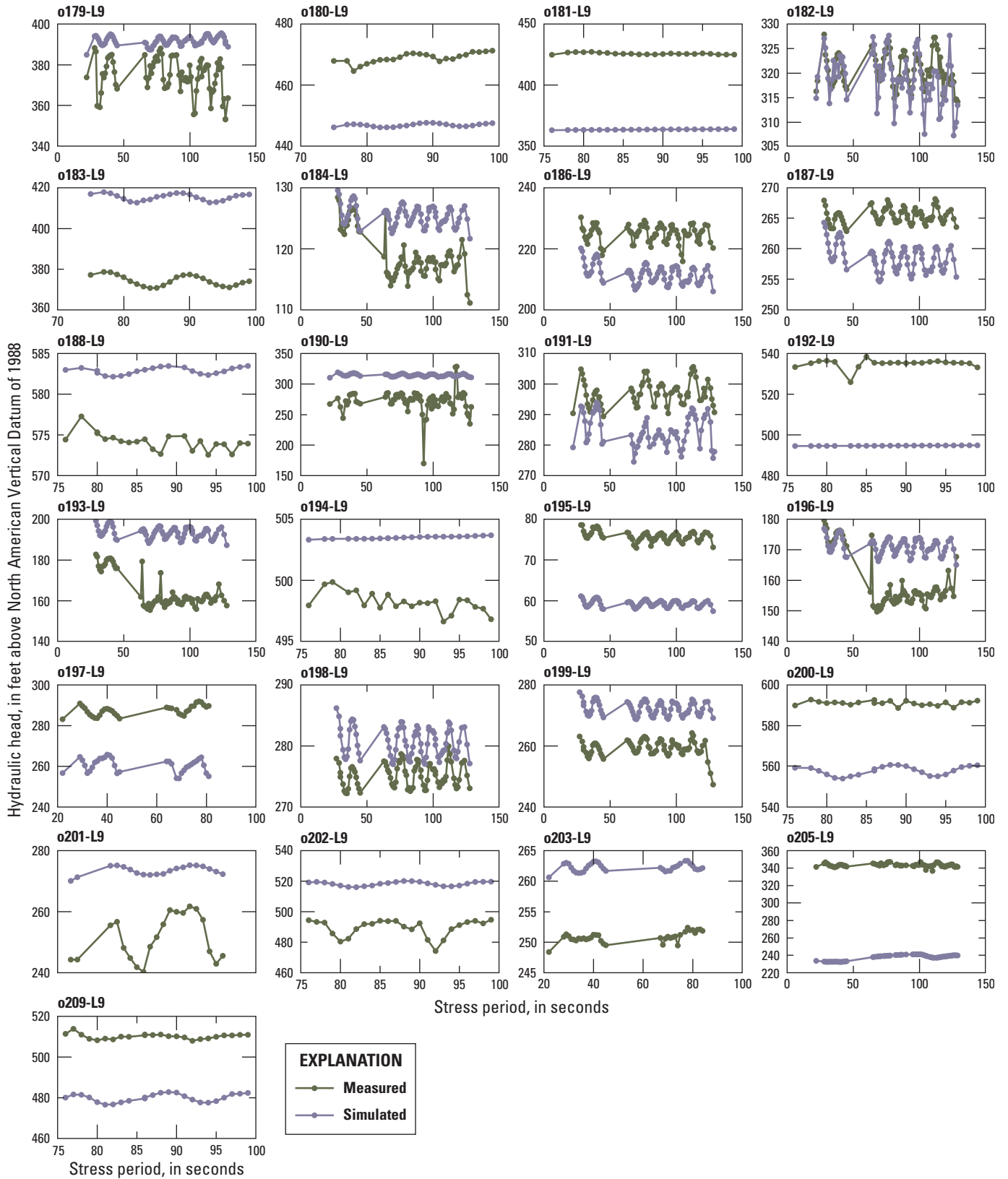


Figure 3.1.—Continued

Time series of hydraulic head

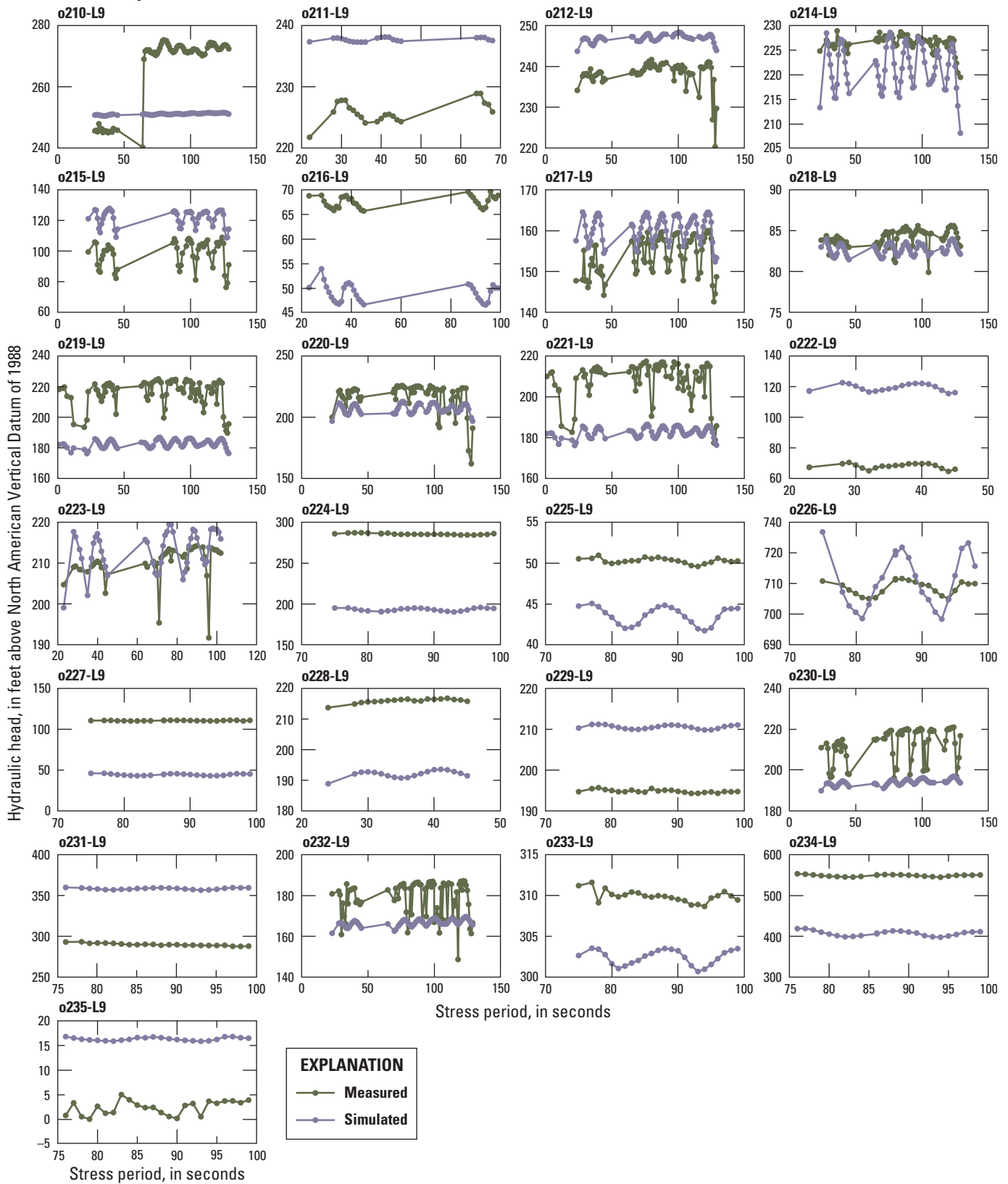


Figure 3.1.—Continued

Time series of hydraulic head

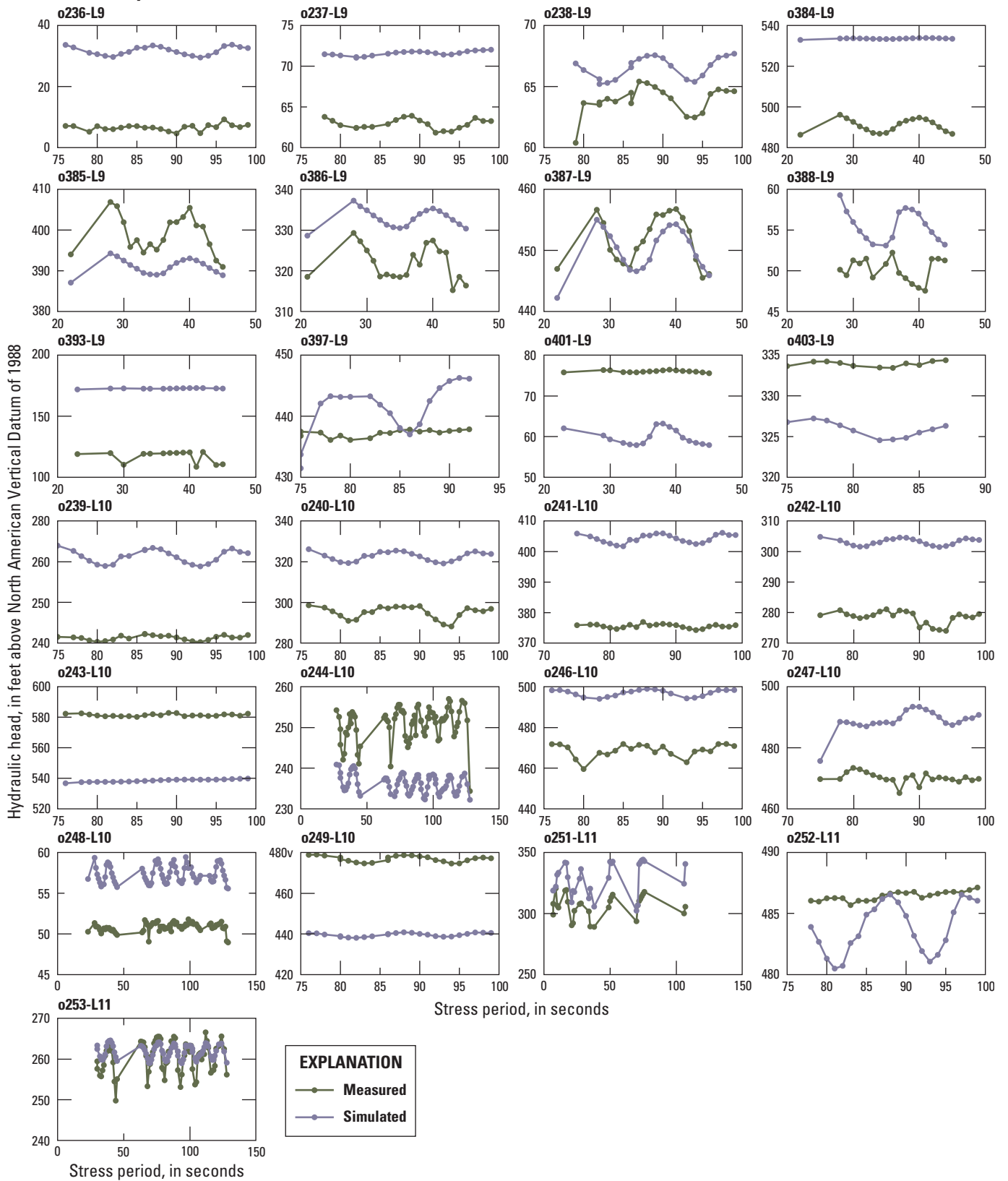


Figure 3.1.—Continued

Time series of hydraulic head

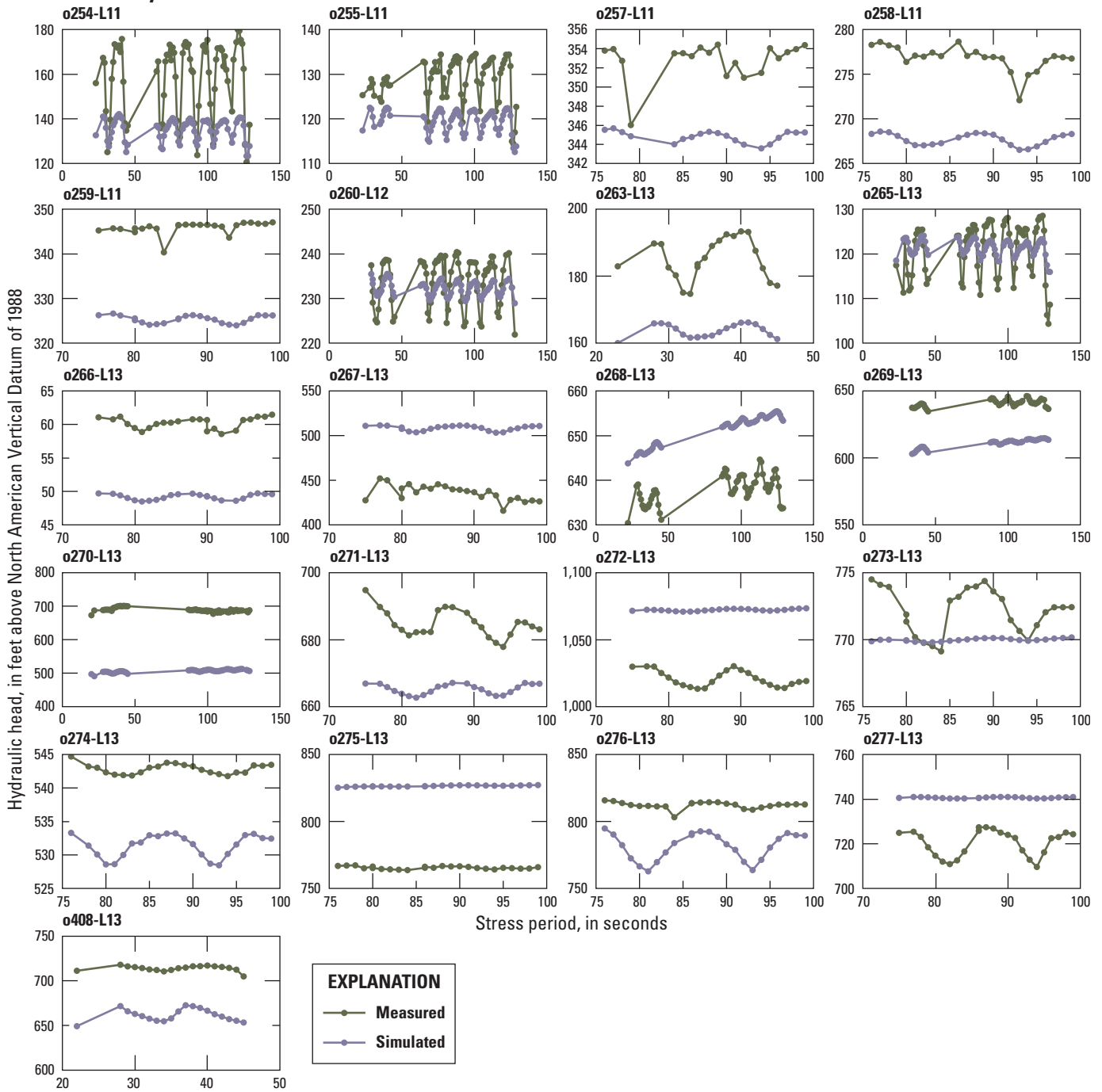


Figure 3.1.—Continued

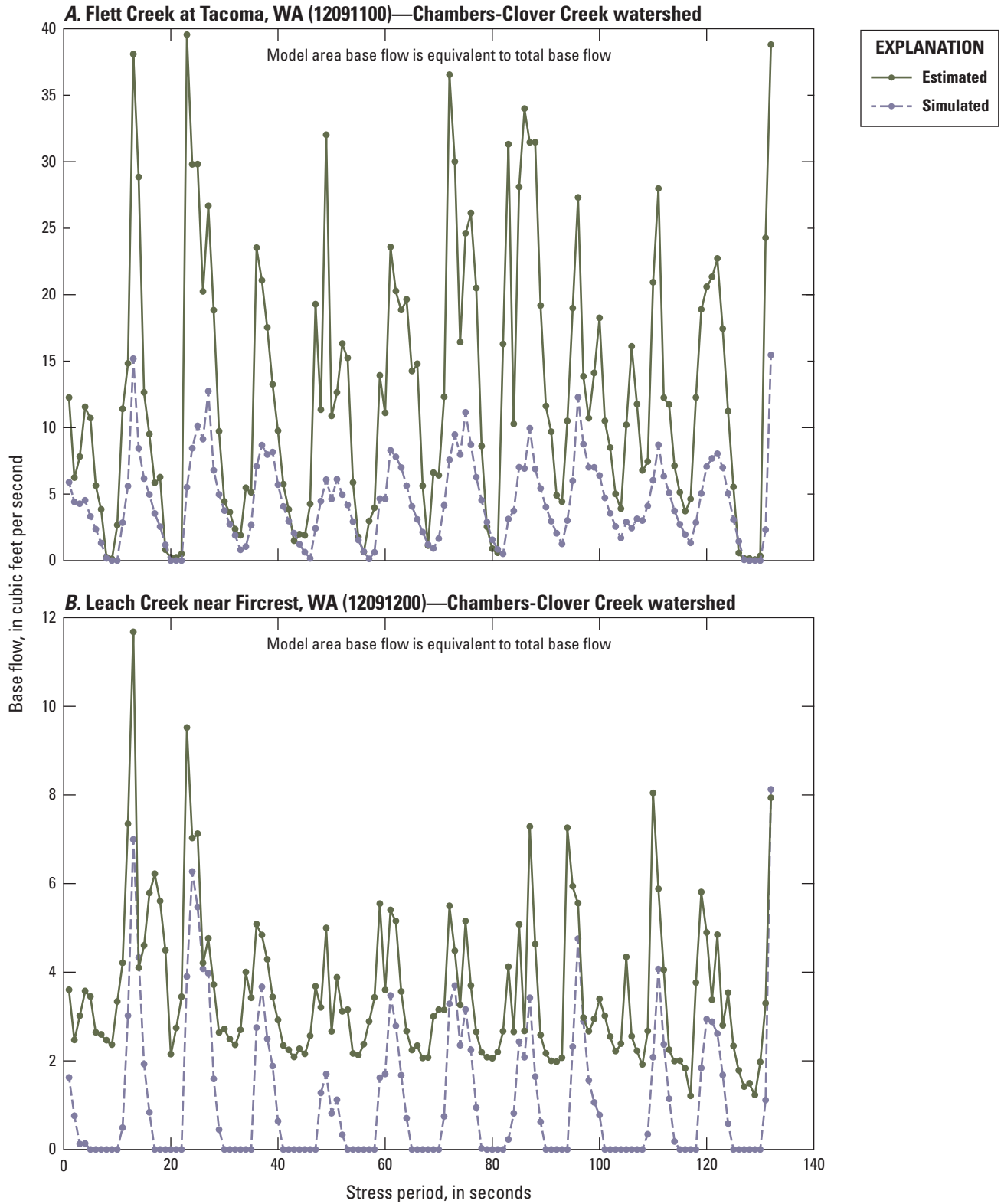


Figure 3.2. Hydrographs showing estimated and simulated base flow for transient model version, near the southeastern part of Puget Sound, Washington, WA, Washington.

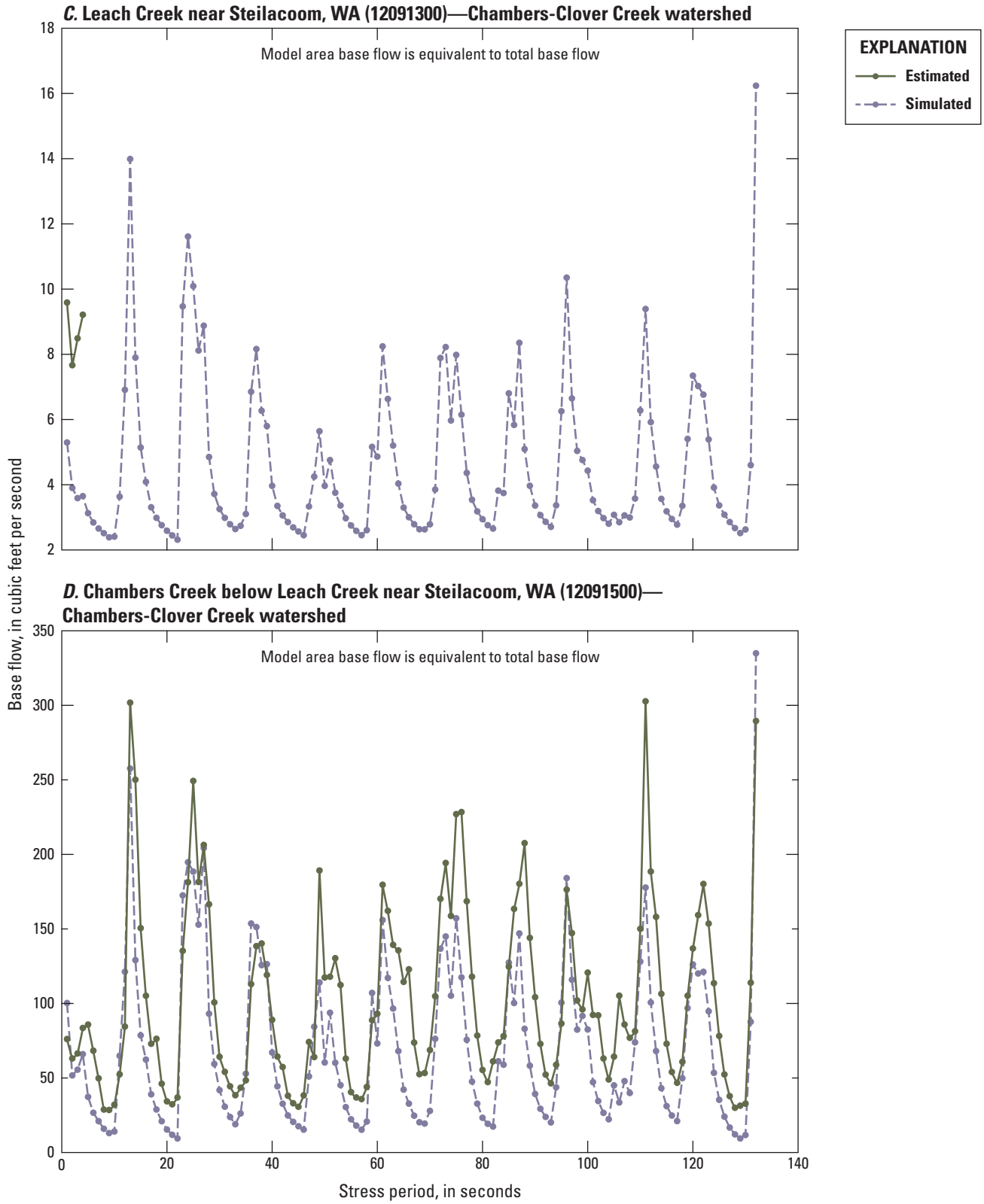
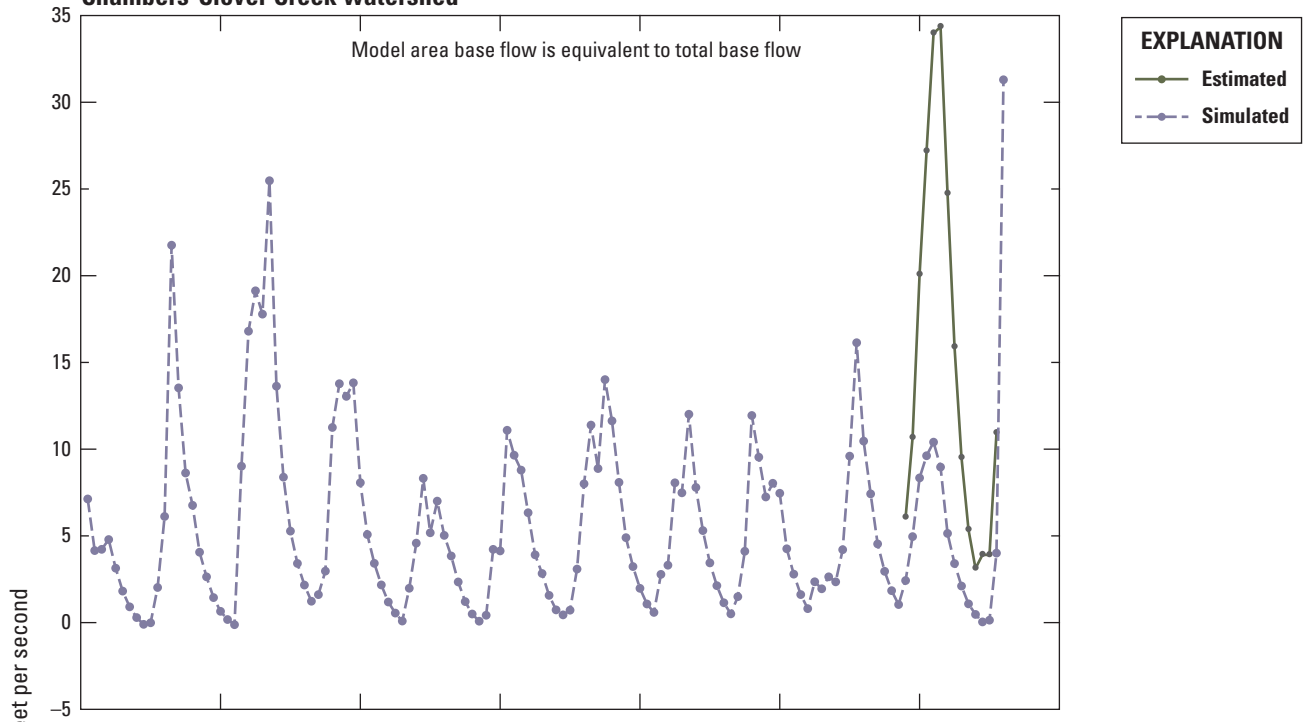


Figure 3.2.—Continued

**E. Spanaway Creek at Spanaway Lake outlet near Spanaway, WA (12090452)—
Chambers-Clover Creek watershed**



**F. North Fork Clover Creek near Parkland, WA (12090400)—
Chambers-Clover Creek watershed**

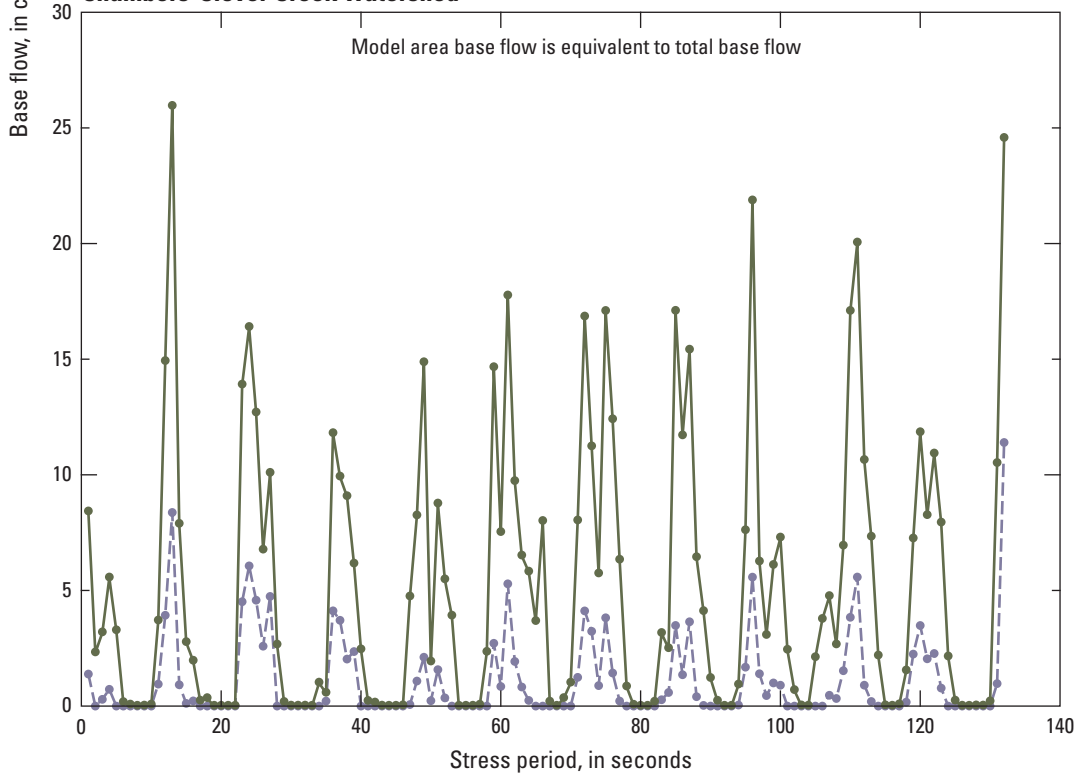


Figure 3.2.—Continued

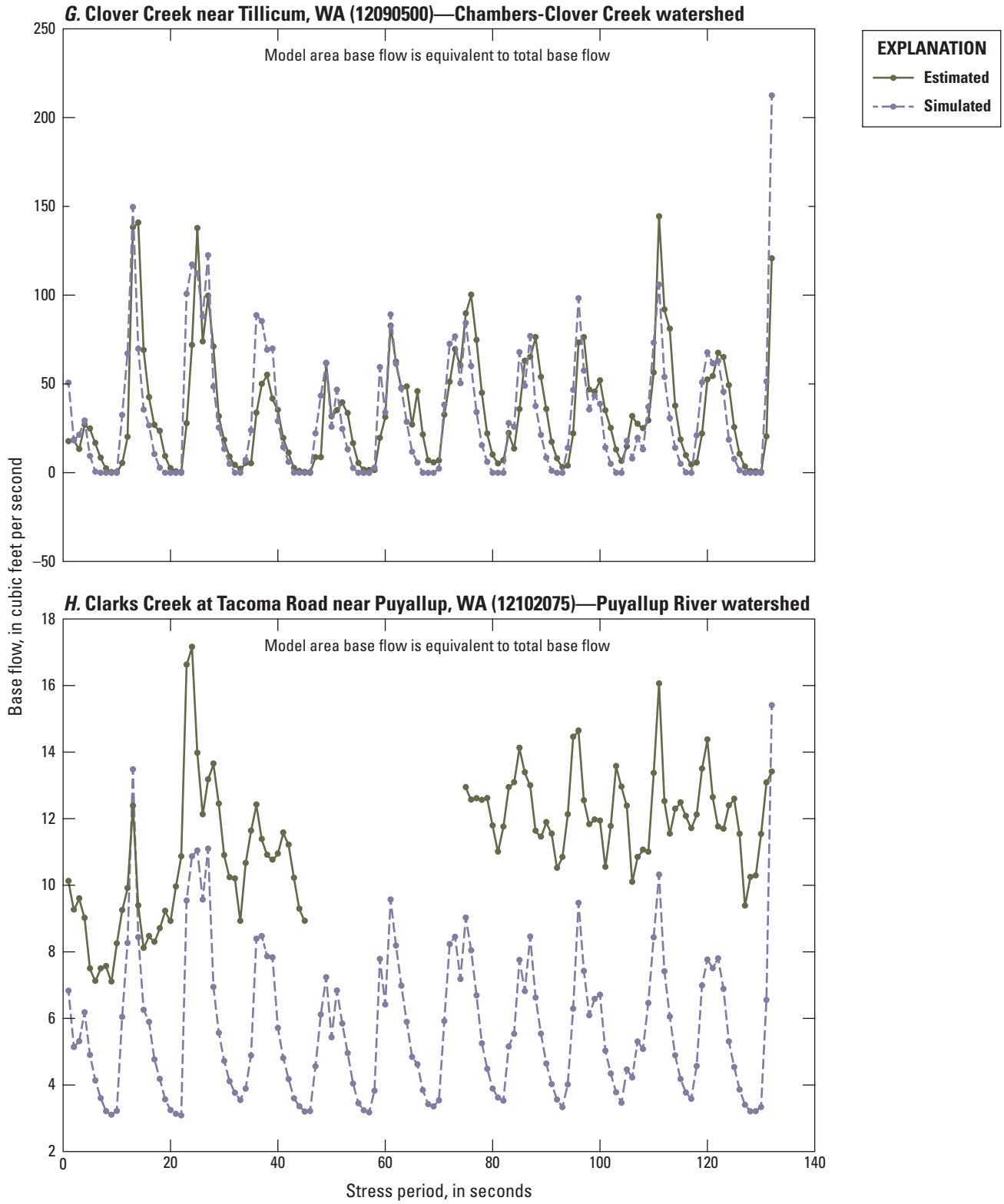


Figure 3.2.—Continued

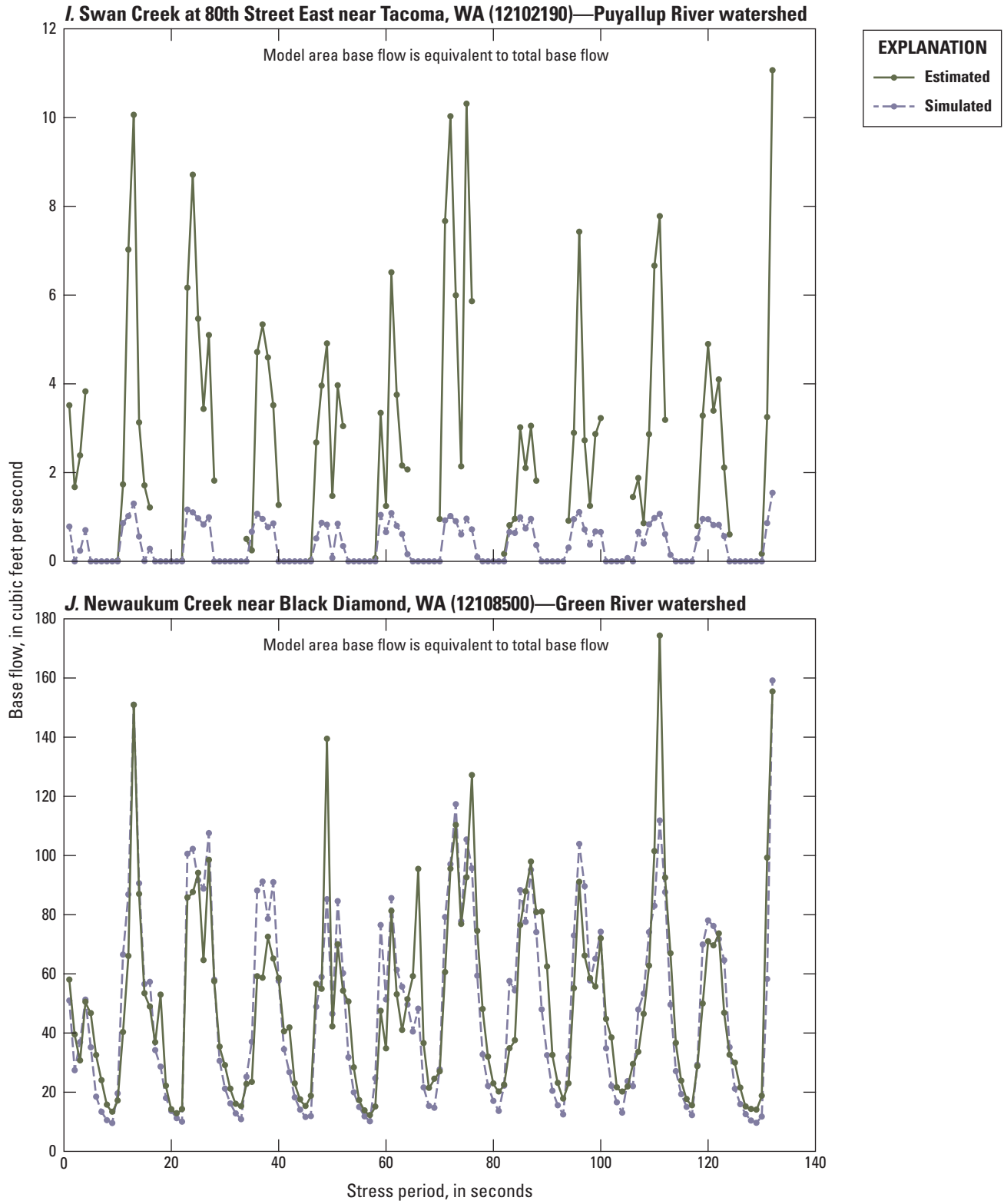


Figure 3.2.—Continued

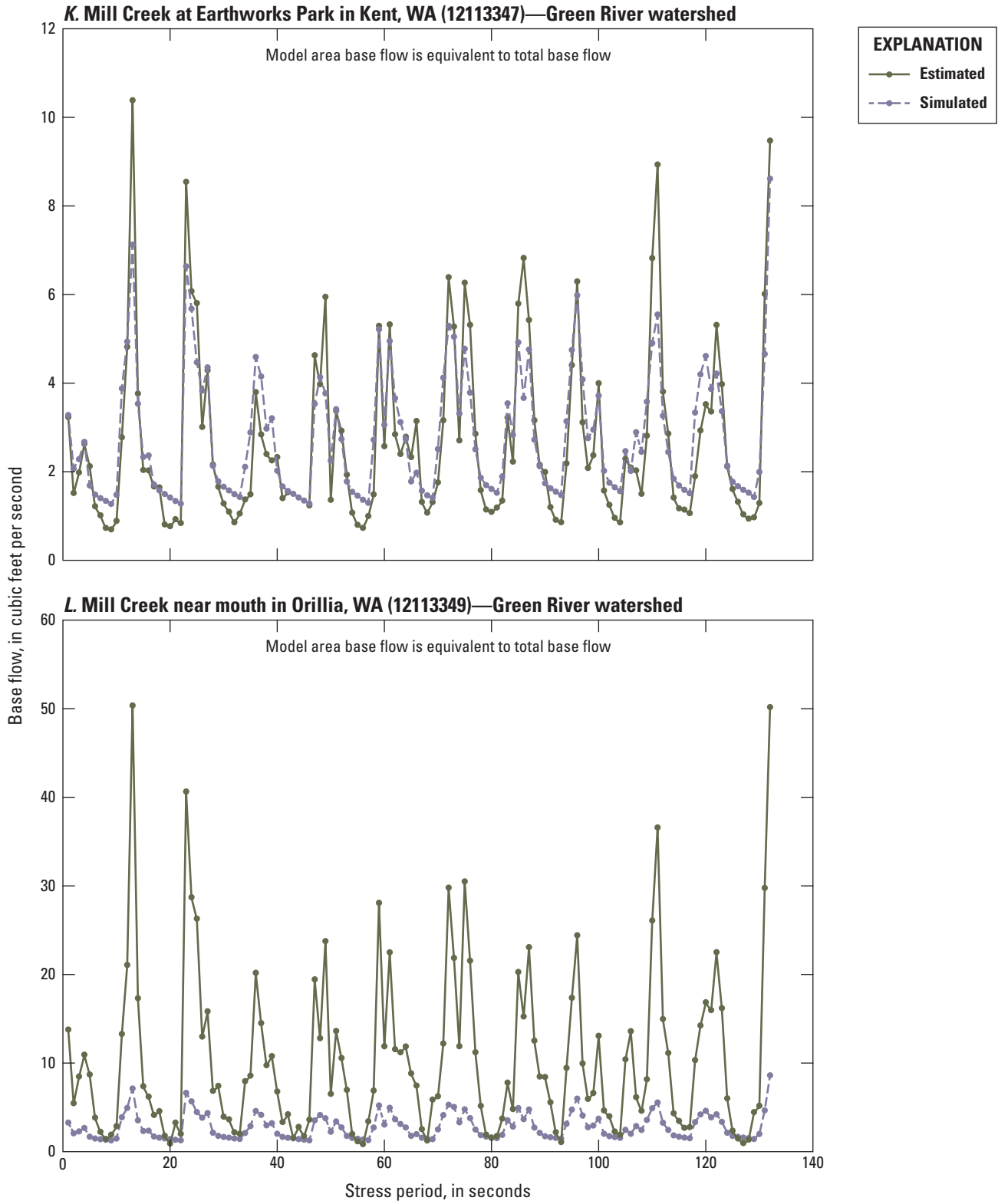


Figure 3.2.—Continued

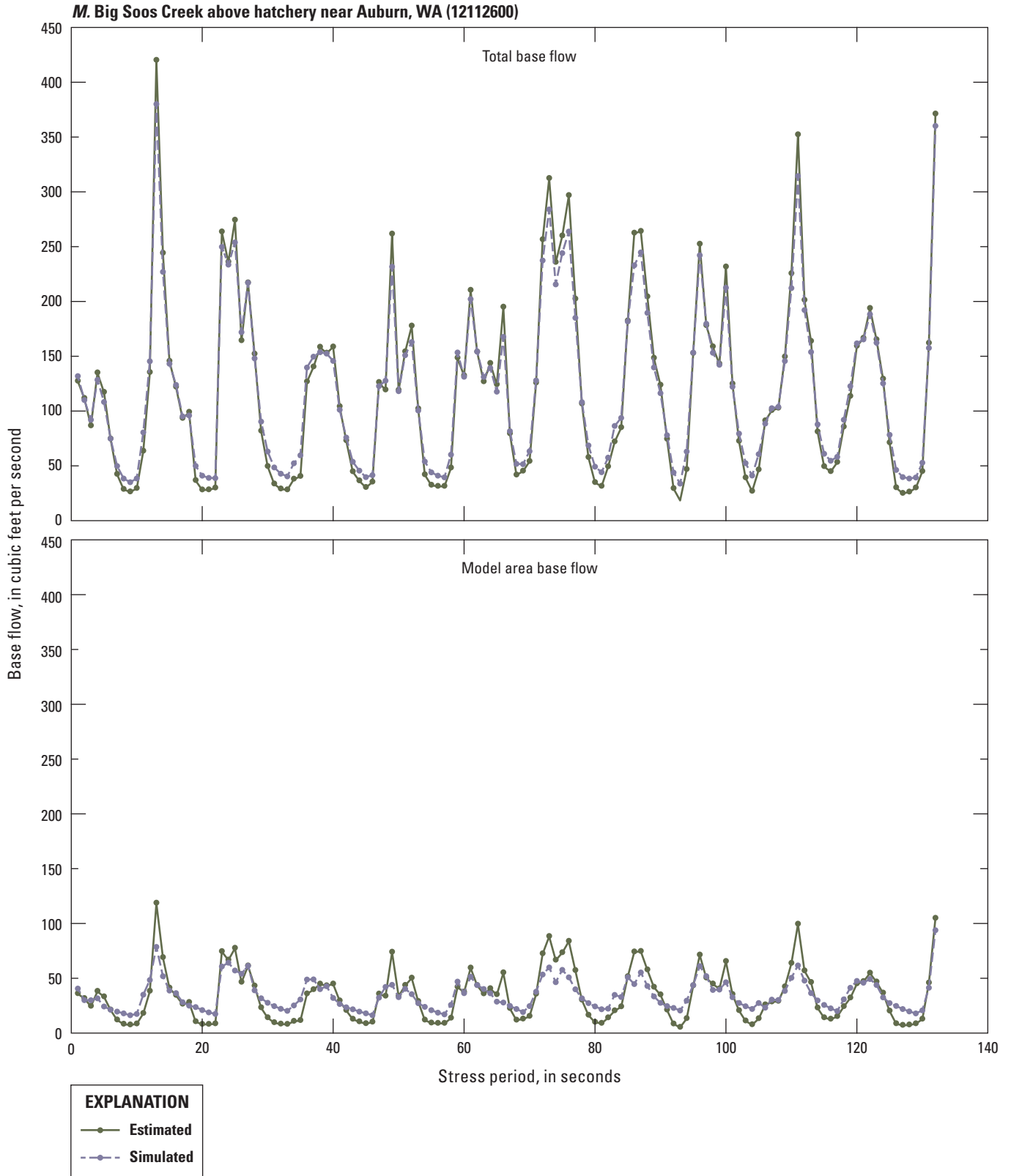


Figure 3.2.—Continued

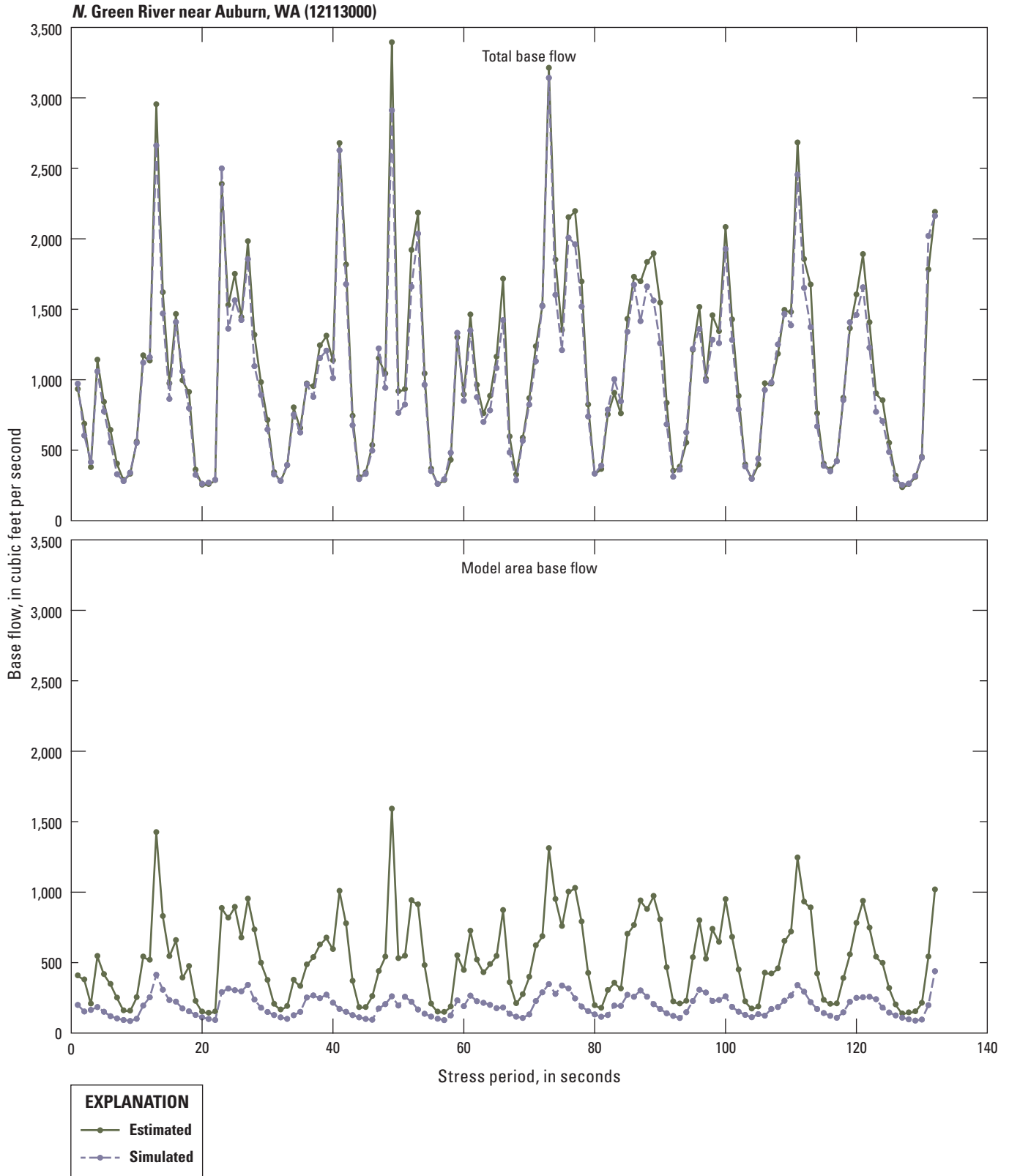


Figure 3.2.—Continued

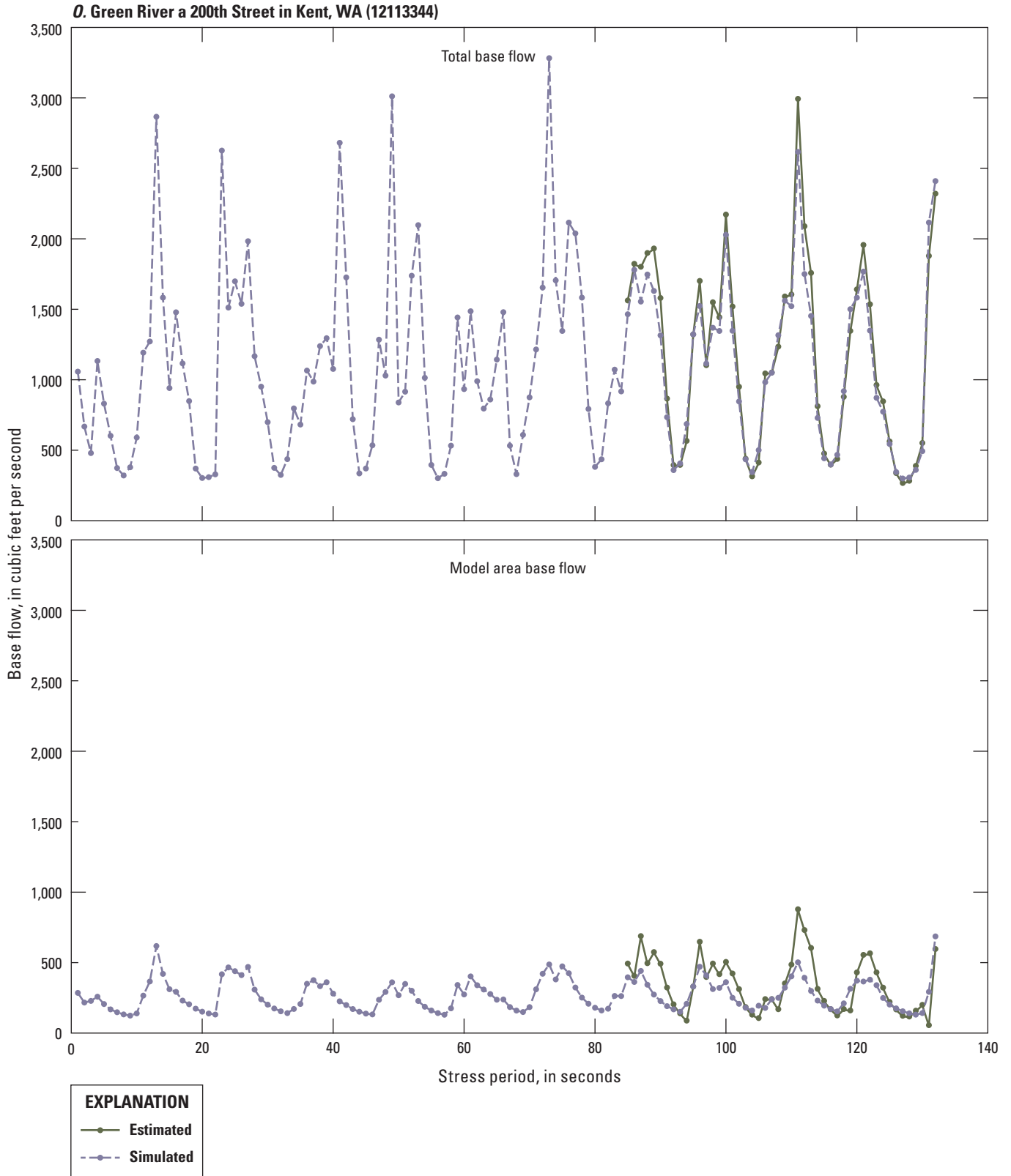


Figure 3.2.—Continued

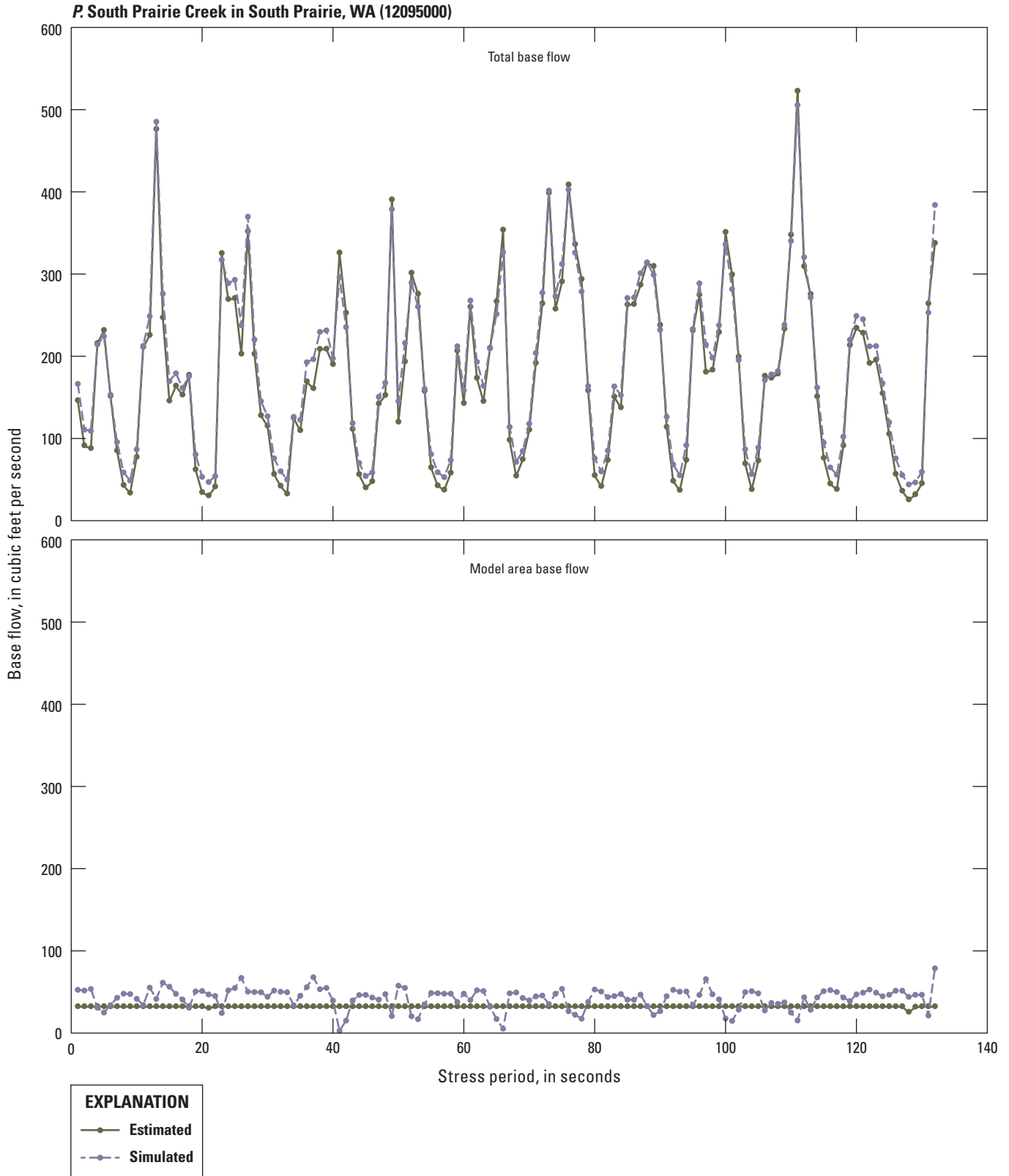


Figure 3.2.—Continued

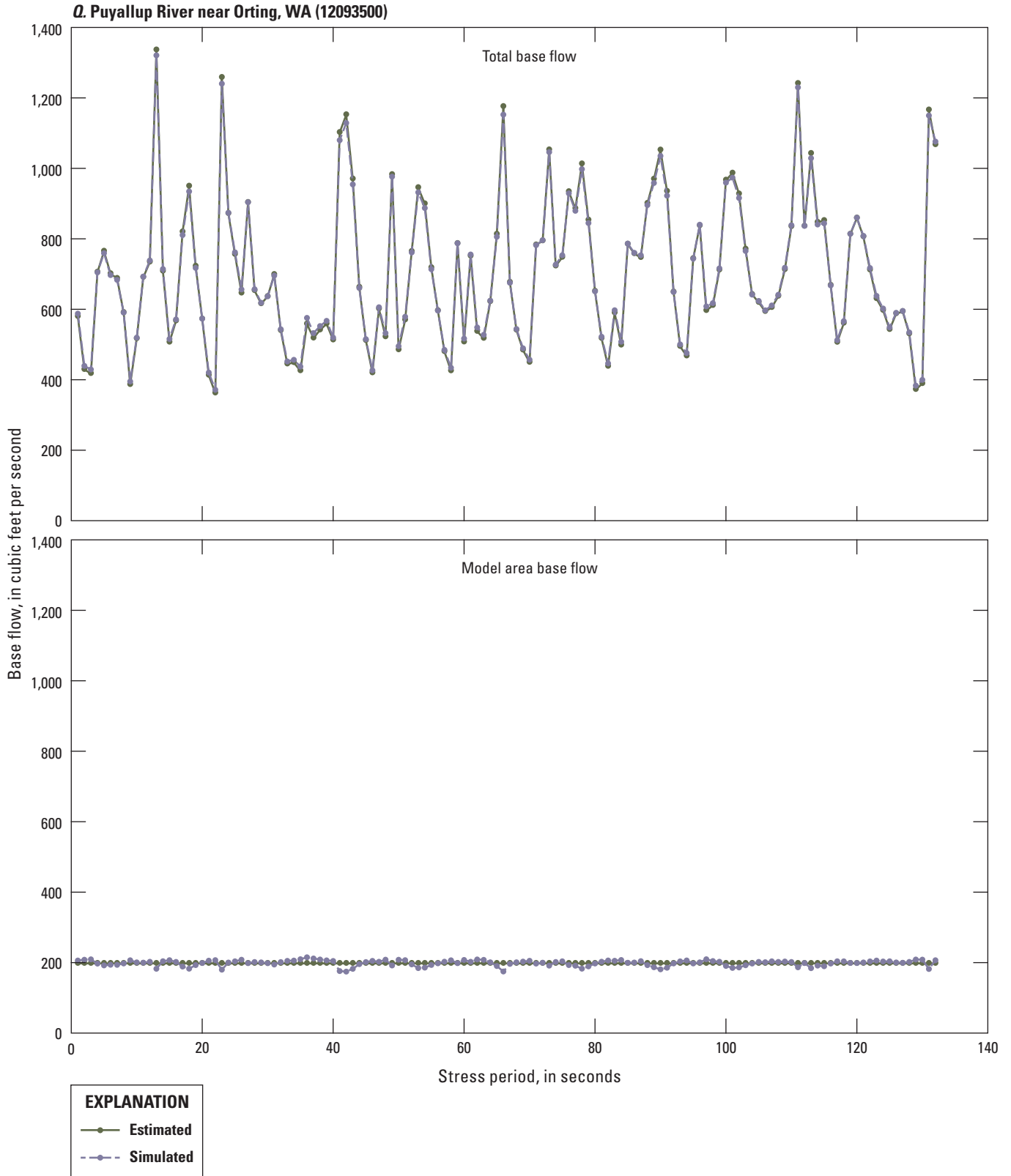


Figure 3.2.—Continued

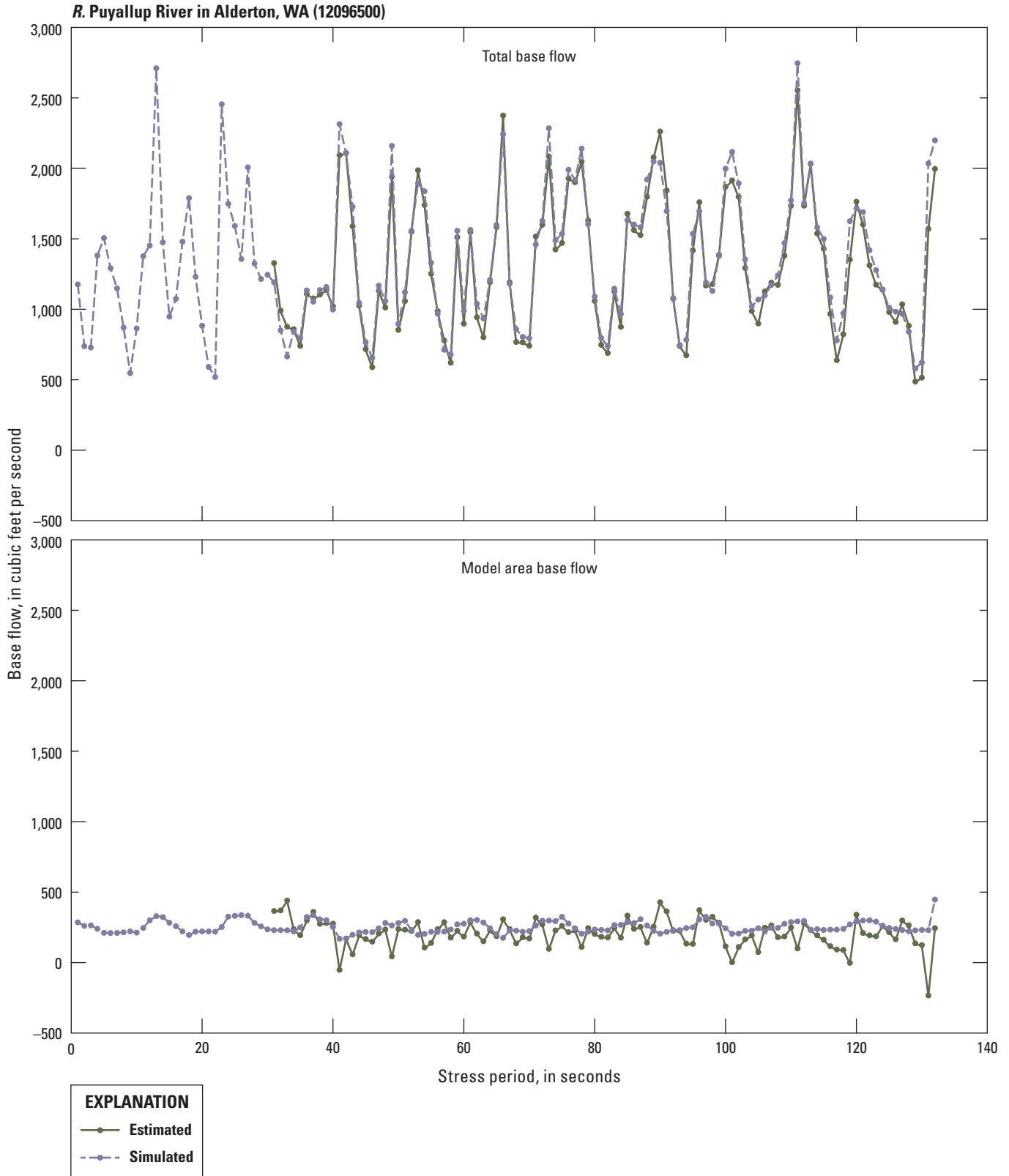


Figure 3.2.—Continued

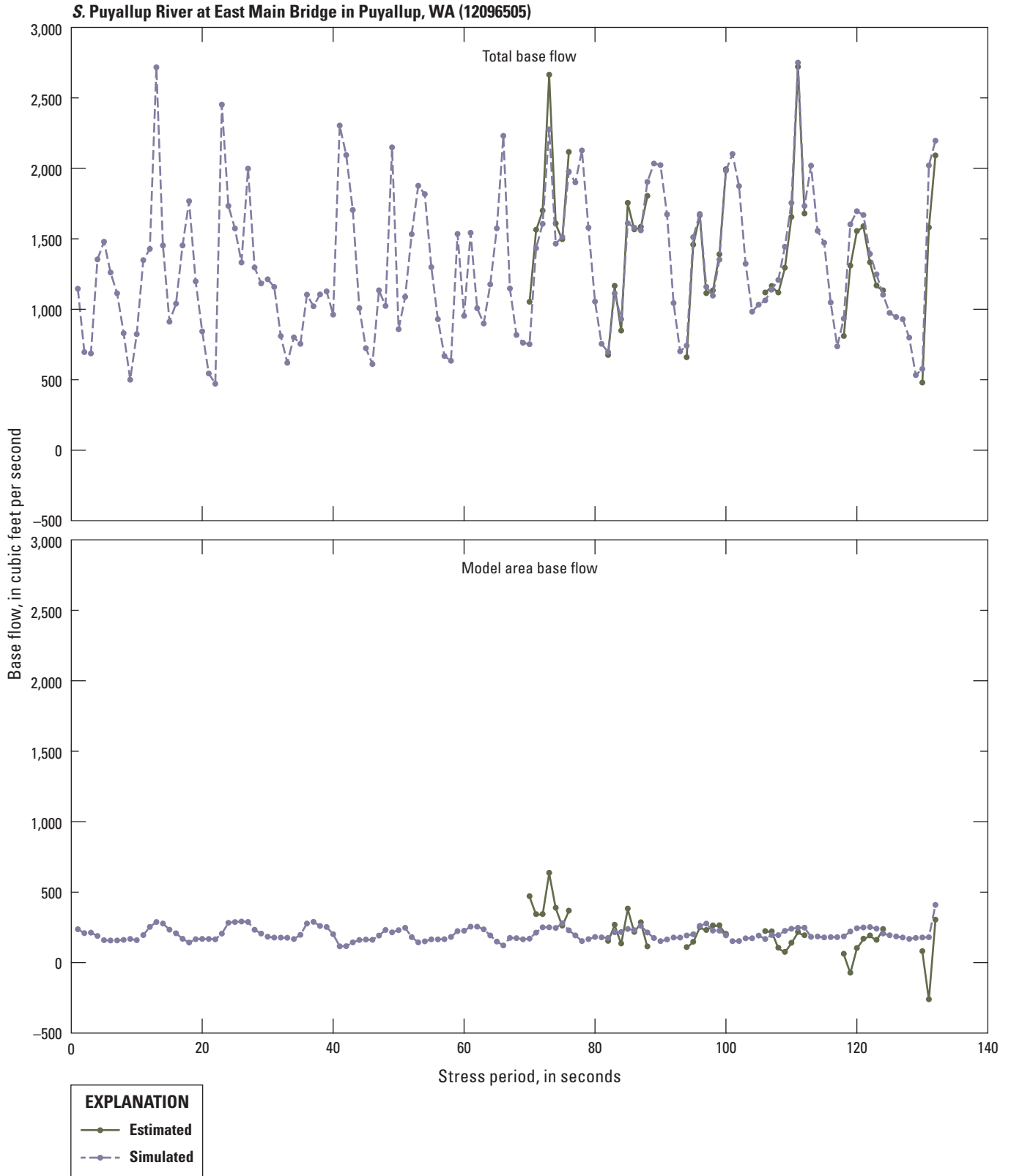


Figure 3.2.—Continued

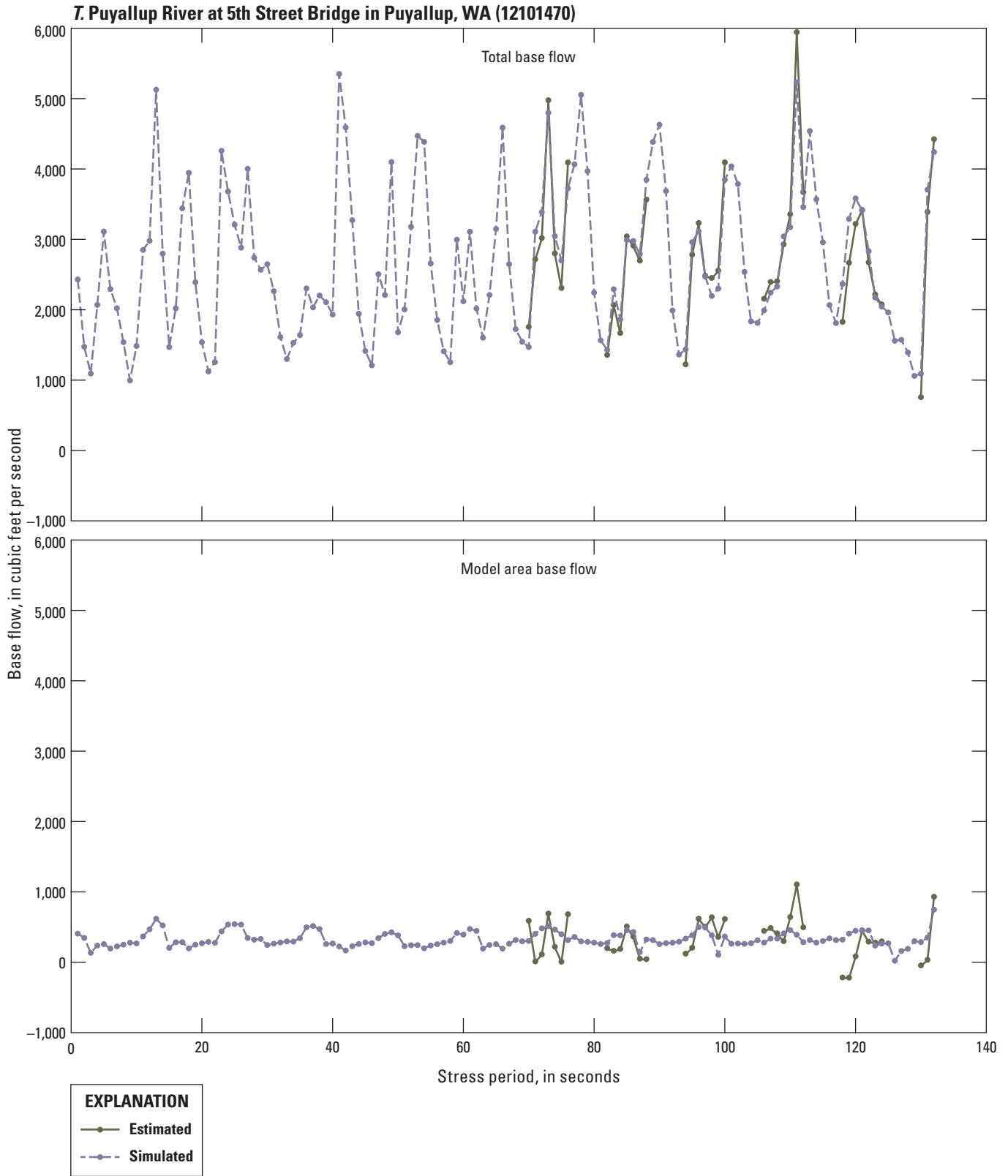


Figure 3.2.—Continued

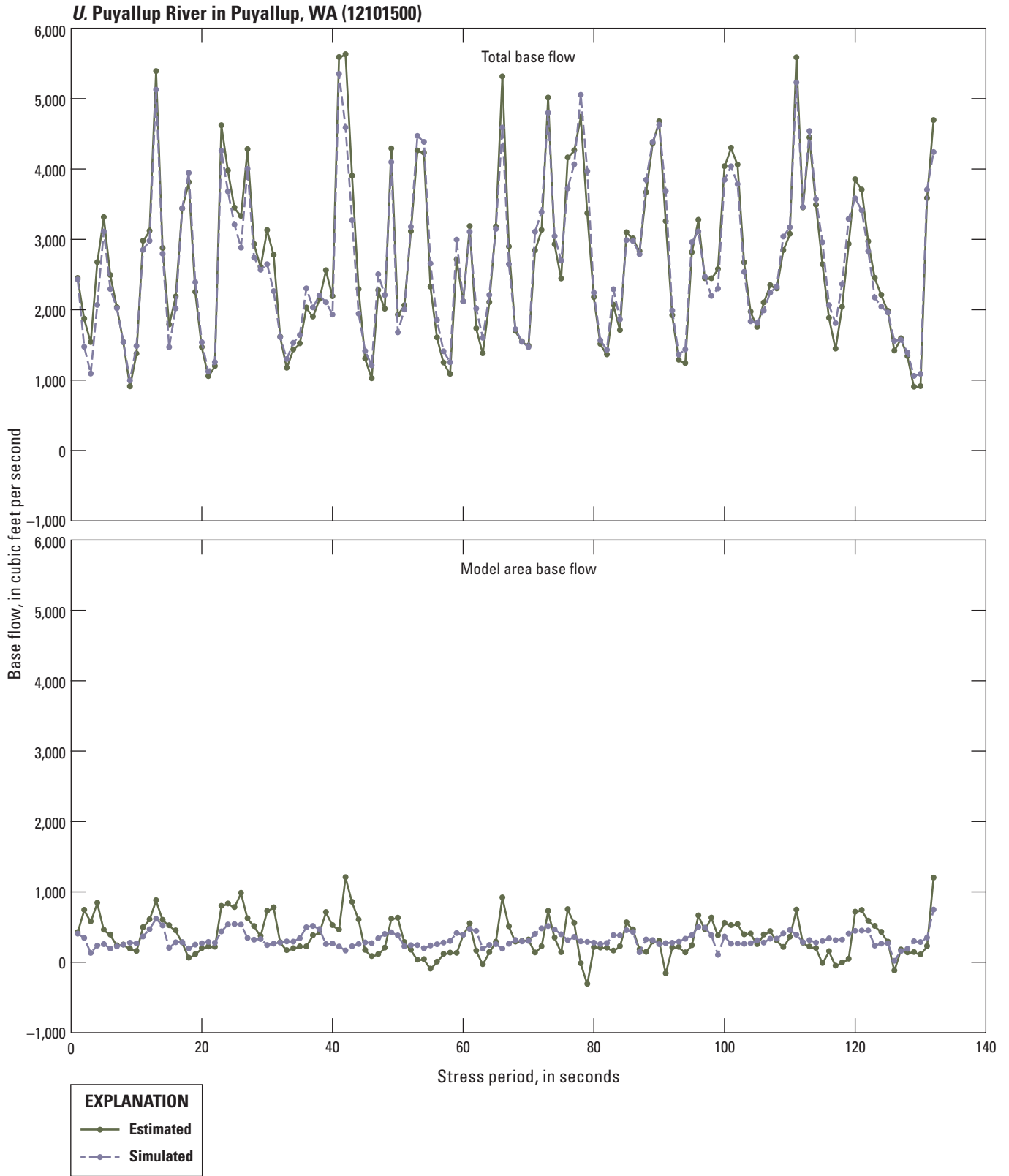


Figure 3.2.—Continued

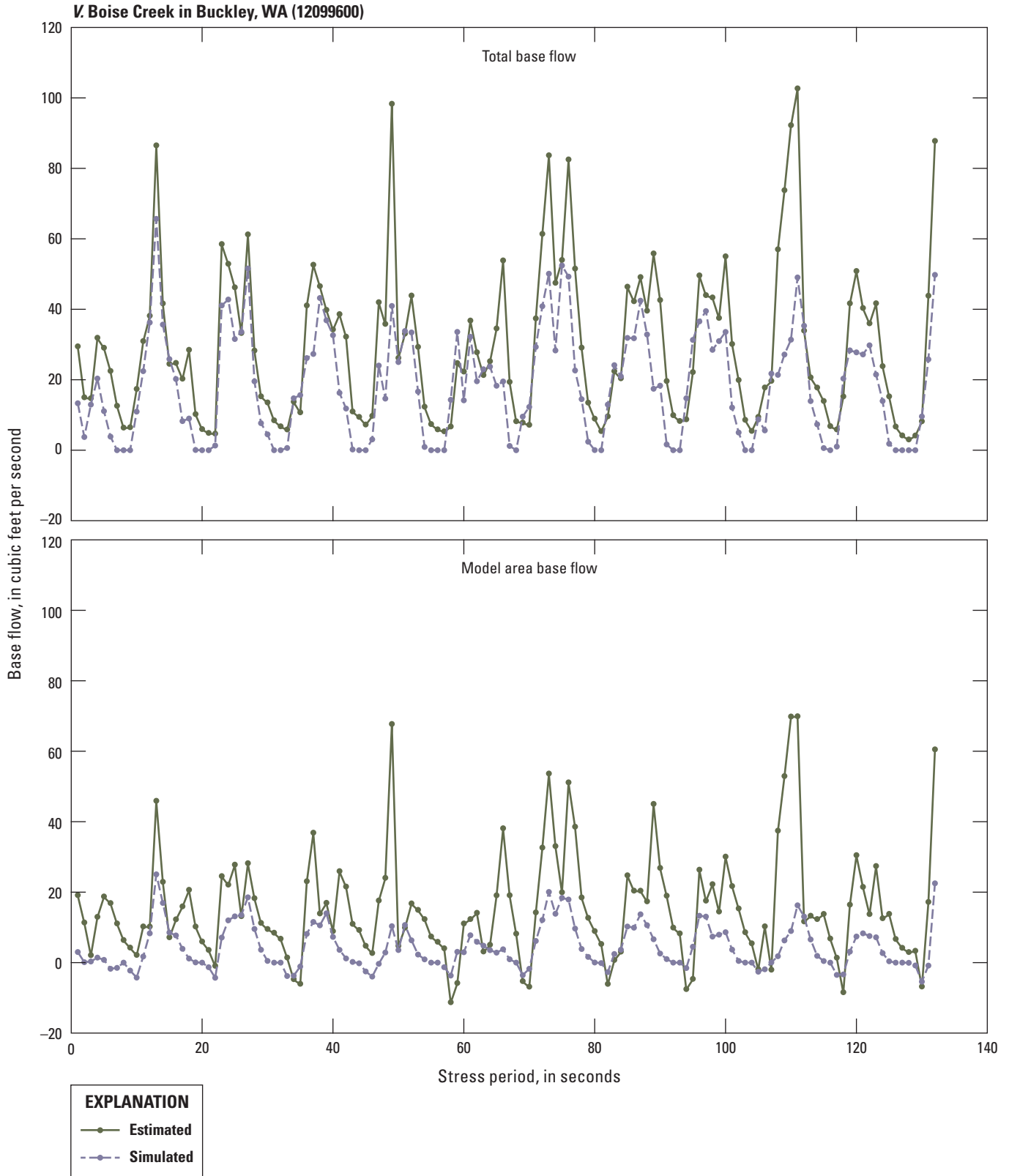


Figure 3.2.—Continued

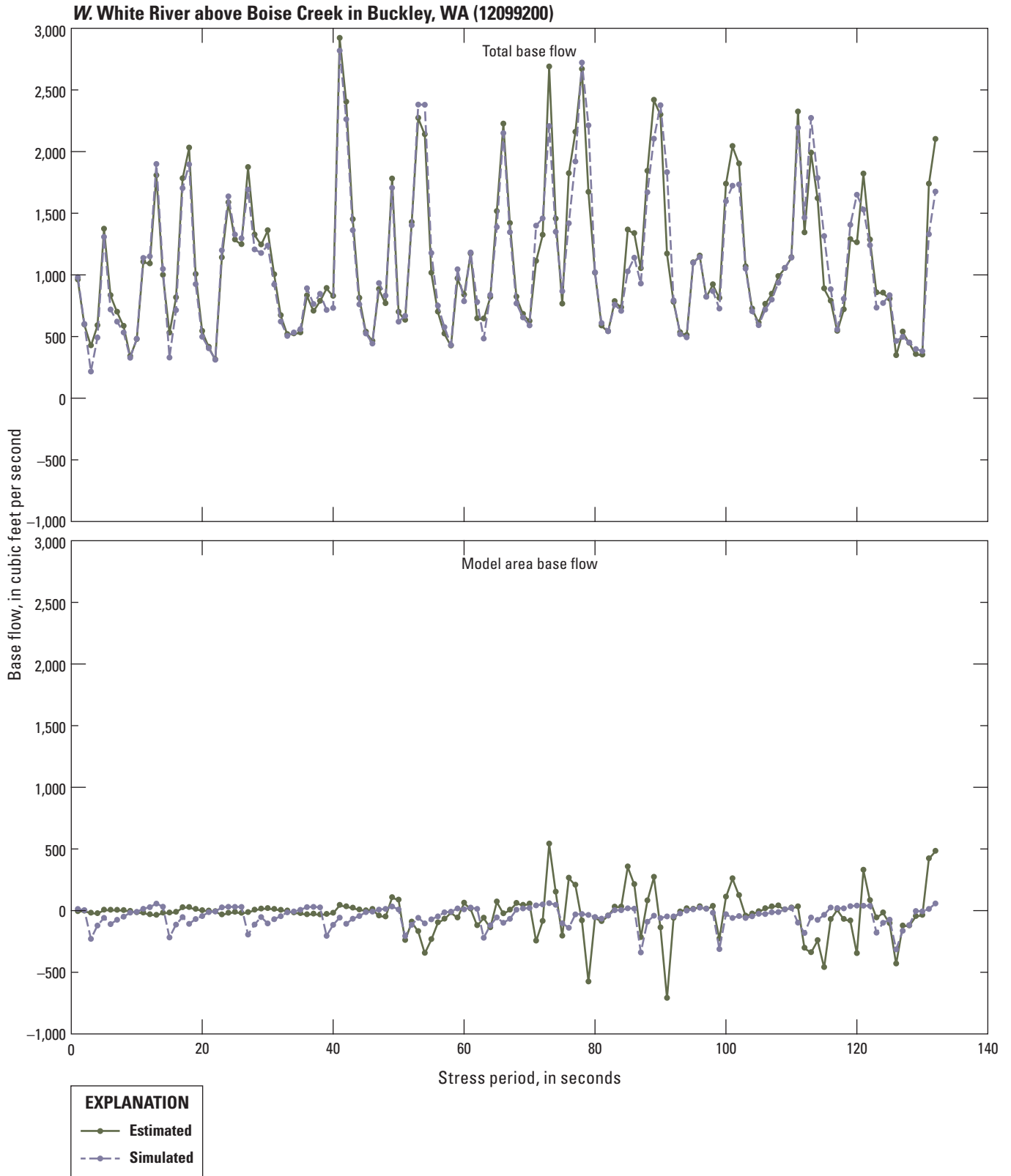


Figure 3.2.—Continued

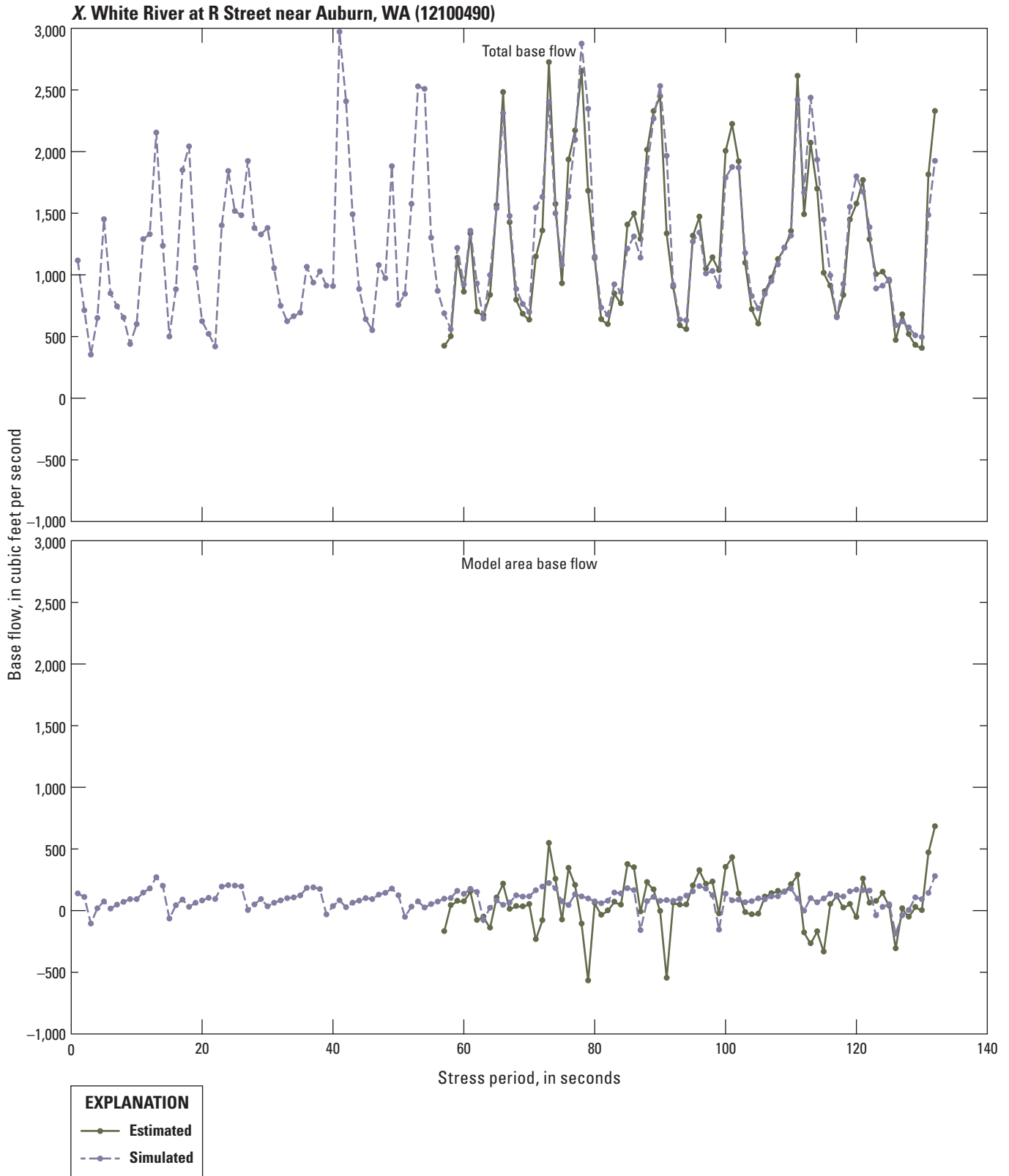


Figure 3.2.—Continued

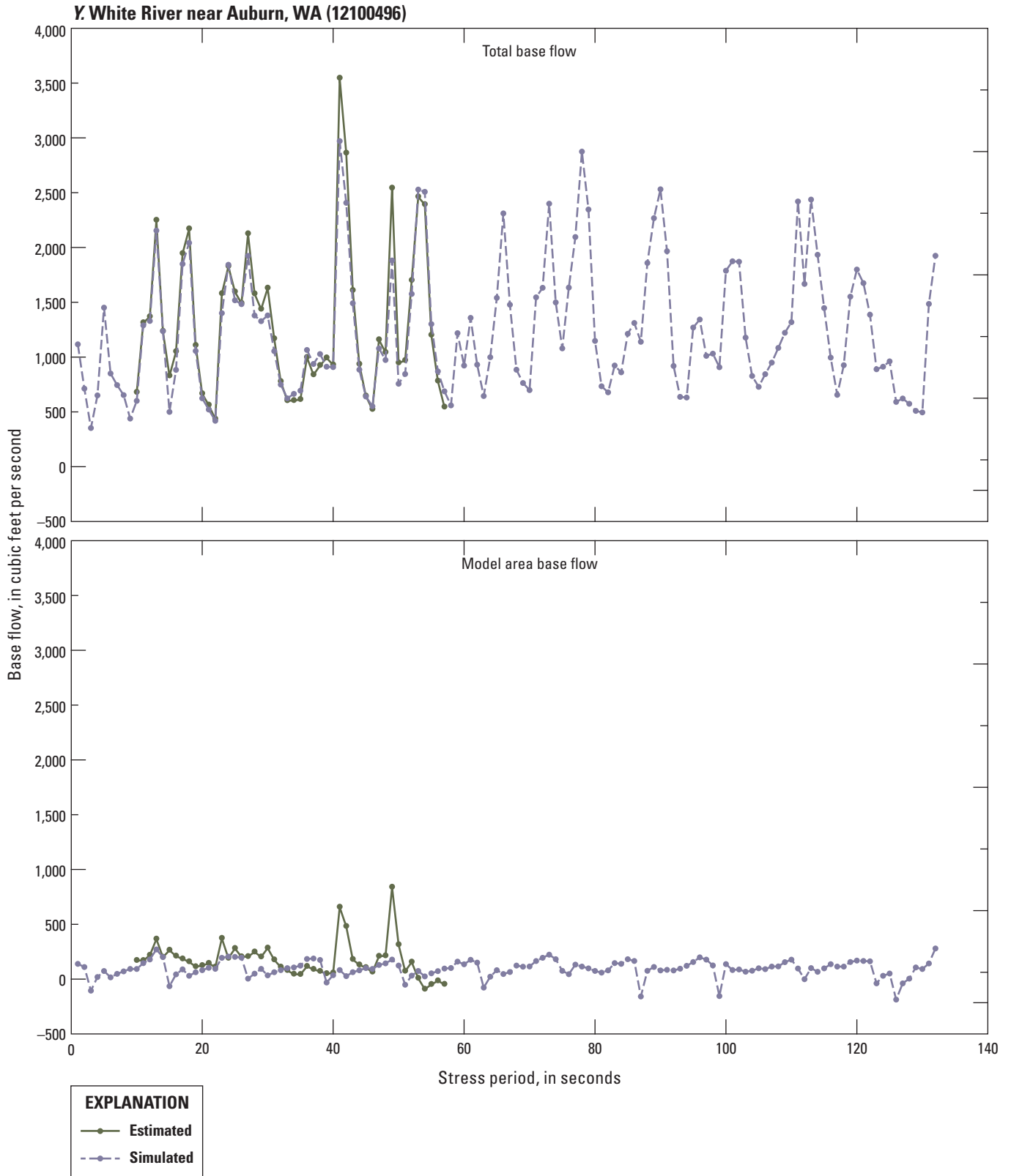


Figure 3.2.—Continued

For information about the research in this report, contact the
Director, Washington Water Science Center
U.S. Geological Survey
934 Broadway, Suite 300
Tacoma, Washington 98402
<https://www.usgs.gov/centers/washington-water-science-center>

Manuscript approved on April 21, 2024

Publishing support provided by U.S. Geological Survey
Science Publishing Network, Tacoma Publishing Service Center
Edited by John Osias and Nathan Severance
Layout and design by Luis Menoyo
Illustration support by Teresa Lewis

